A Study on the efficiency enhancement of automatic radar tracking and analyses of marine traffic in Tokyo Bay

Master Course Graduation Thesis

A STUDY ON THE EFFICIENCY ENHANCEMENT OF AUTOMATIC RADAR TRACKING AND ANALYSES OF MARINE TRAFFIC IN TOKYO BAY

March, 2009

Tokyo University of Marine Science and Technology
Graduate School of Marine Science and Technology
Course of Maritime Technology and Logistics

NGUYEN MINH DUC

Table of Contents

Acknowledgements

This Master Thesis is to be submitted to the Tokyo University of Marine Science and Technology to fulfill the requirements for the degree of Master of Engineering in the field of Maritime Technology and Logistics.

First and foremost, I would like to express my sincere gratitude to my supervisor, Associate Professor TAMARU Hitoi at the Route Planning Laboratory, Tokyo University of Marine Science and Technology (TUMSAT) for his continual support and encouragement, both in research work and daily life in Japan.

My further thanks should also go to my tutor, Ms Takashima, PhD Candidate at TUMSAT, who has always been willing to provide a helping hand whenever I am in trouble.

It could have been extremely hard for me to complete the thesis without the close cooperation and generous sympathy of my friends, especially those in Route Planning Lab. Their invaluable advices have always been an additional thrust force for me to overpass difficulties.

It is impossible for me not to mention here the Japan Ministry of Education, Science, Culture, and Sport (Monbusho) for their financial support during my course, as well as those in TUMSAT Student Office. My life in Japan would not have been so enjoyable without their attentions.

I cannot end without expressing my thanks and dearest love to my family, on whose constant encouragement and love I have relied throughout my time taking the Master Course and forever. Their love will always be the motivation inspiring me on my way to the land of hope and achievements.

Abstract

This master thesis is a study on the efficiency enhancement of automatic radar tracking target motion in Tokyo Bay. Focus of the study is on the radar and AIS based traffic observing system having been applied for real time visualizing of marine traffic in the Bay. Using the observing results, some aspects of marine traffic flows are analyzed with the aim of figuring out critically congested areas of navigation and producing suggestions for traffic route designing as well as traffic management.

In the first part of the study, an approach to automatic radar tracking would be introduced and applied to process actual radar images of Tokyo Bay. The approach was implemented for 2 different cases, ships without AIS and those equipped with AIS.

- For ships without AIS, a Relating-Function is introduced to evaluate the relation among 3 image position on 3 consecutive Radar images. Resulting Relating-Value would be utilized as a criterion on making decision on if the 3 points are images on a target. Basing on observation of real radar targets, value of factors in Relating-Function and threshold of relating-Value for decision making have been decided. The threshold values have been chosen to be -0.85 for target acquisition and -0.6 for target following, with factor value to be 0.3.

- For ships equipped with AIS, NMEA sentences of AIS message were decoded for the information. To take the advantage of this information, Relating-Function has been slightly modified, taking into account the speed and course over ground provided by AIS. Then, from observation of target motion on the radar screen and respective AIS information, threshold value for decision making (matching) was defined. In this section, a matching algorithm was used to match targets extracted from radar screen with AIS data in the database to define the Radar-AIS target.

Movement of targets tracked from radar images, however, considerably degraded by noise, especially targets course and velocity deduced from their positions. Therefore, inaccuracy and danger may arise if these data directly used in traffic analyses or calculation of own ship route. To reduce the effect of noise, Kalman Filter has proved to be efficient. In the study, a Kalman Filter has been designed and values of designing parameters have been determined from simulation experiments. The Filter, with some modification, can also be applied for motion tracking purpose.

Targets movement after tracking and filtering can then be used for analyzing characteristics of marine traffic in Tokyo Bay. In this study, conventional DCPA, TCPA criteria, as well as criteria of Bumper Model or Subjective Judgment (SJ) value have been applied for collision risk assessment. Some other characteristics of the bay marine traffic were also concerned in the study.

Chapter 1. Introduction

1.1 Geographic and Marine Traffic Conditions of Tokyo Bay

Located on the east coast of Japan in Kanto region, Tokyo bay and the port system inside the bay have long been the main gate for domestic trading of the most populous and prosperous region of Japan as well as the nation's foreign trade.

Geographically speaking, the bay is surrounded by the Boso Peninsula (Chiba prefecture) to the east and the Miura Peninsula (Kanagawa Prefecture) to the west. In narrow sense, Tokyo Bay is limited on the south by the straight line defined by the Cape Kannon (Miura Peninsula) on one end and Cape Futtsu (Boso Peninsula) on the other end. For a broad sense the bay area is that limited by a line connecting the two peninsulas out of Uraga Suido traffic route.

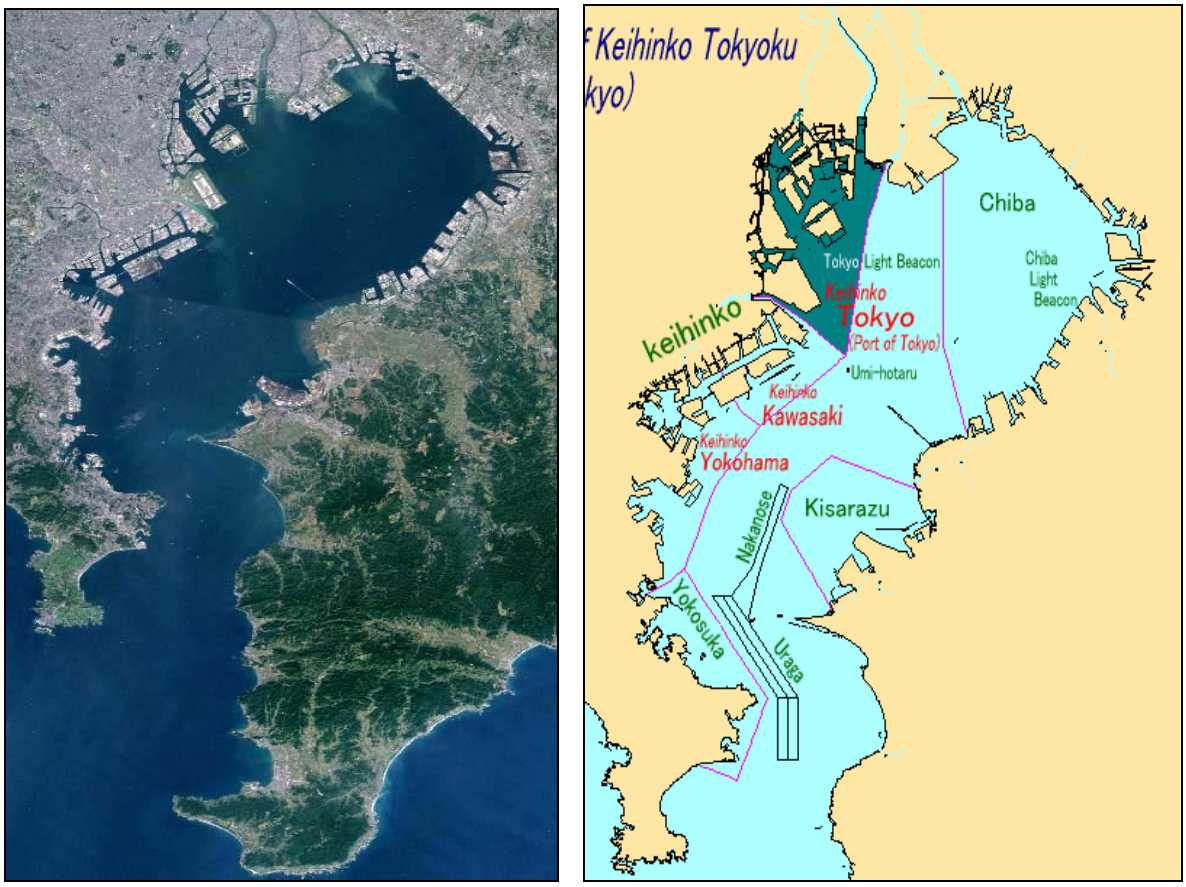

Fig. 1.1 Space view of Tokyo Bay and bay port system

Apart from the port of Yokosuka, which is mainly used for military purposes, other ports have been founded along the bay coast, including the Port of Tokyo, Port of Kawasaki, Port of Yokohama on the west and Port of Chiba, Kisarazu on the east. For the Port of Tokyo alone, the number of incoming vessel in 2006 was 31,653 ships with total gross tonnage of 176,064,000 GT. Number of ships entering Chiba wharves in the same year was 15,070 (23,369,328 GT) and that

for Yokohama port was 42,622 ships with 253,562,433 GT, including both coastal and sea going vessels.

With these statistic data as examples, keeping in mind the existence in the bay of a large number of service ships as well as fishing vessels, it is of no doubt that Tokyo bay is one of the most congested marine traffic areas around the world. On average, there are more than 1000 turns of ship navigating in, out or inside the bay in a day. In “rush hour”, the number of ship navigating in the bay may be well over 100 ships simultaneously. This can be seen in Fig. 1.2, where tracks are plotted for all ships navigating in the bay in one day.

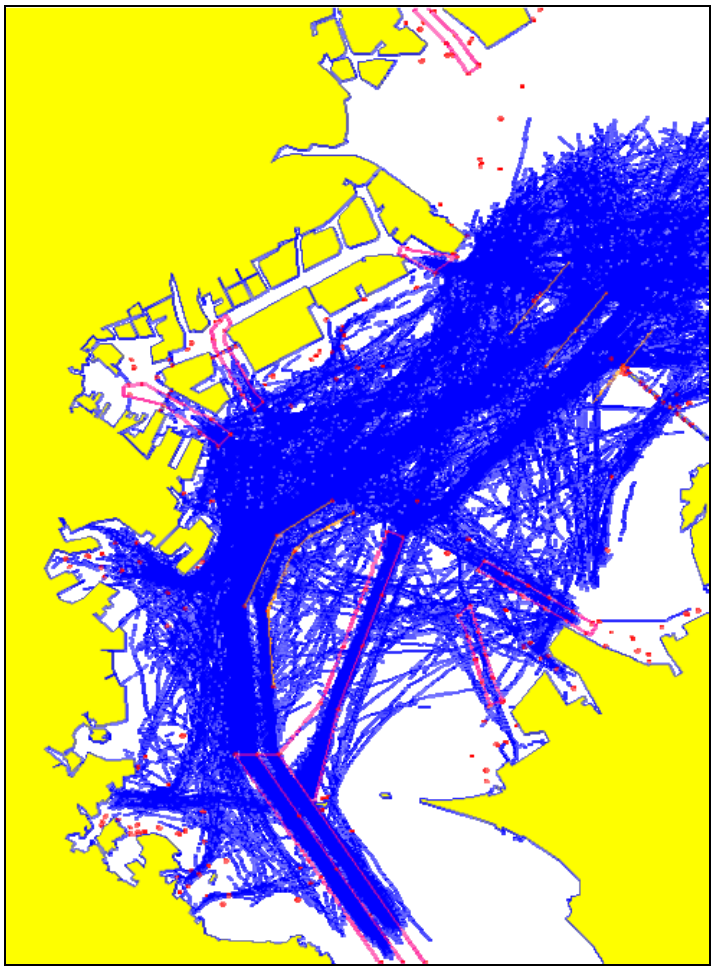

Fig. 1.2 Tracks of all ships in 1 day

The number of ships passing through Uraga Suido traffic route alone is from 600 to 800 ships per day. Further contributing to difficulty of navigation is the narrow traffic route condition. Width of the exit of Nakano traffic route is approximately 0.42 miles. That of Uraga Suido is around 0.5 miles, resulting in the highest ship density in the area to be more than 3.12 ships per square kilometer.

The concentration of busy ports in the region is also a challenging problem to the safety of marine traffic in the aspect that a number of ships have to be navigated across the main traffic flow while entering or leaving a port.

So far, more than 250 ships have involved in marine incident in the bay. In 2004 alone, 5 marine traffic accidents occurred inside Uraga Suido and Nakano traffic routes.

With the tendency of increasing of the ship's size and speed, damages resulting from marine traffic accident are becoming more and more severe, economically and environmentally. Therefore, the necessity of ensuring safety of navigation is, proportionally, more and more critical.

1.2 Marine Traffic Observation Facilities and Purposes

For the existing marine traffic condition of the bay, an efficient and accurate traffic observing system is indispensable as far as safety, efficiency of navigation and environment protection are concerned. These are, as a matter of fact, the utmost aims of traffic management and the motivation for applying available technologies in the construction of an advanced traffic observing system.

Thence, a synthesized observation system of the marine traffic in Tokyo Bay has been established, consisting of a radar network system of 2 radar stations located at Kawasaki and Yokosuka and an AIS receiver installed at Kawasaki station.

Each of the radars is used on 6 nautical miles range. Thus, watching region of the two radars covers almost all the important traffic routes and other important traffic waters in the bay.

AIS, which is working on VHF radio band, has a nominal working range of approximately 45 miles. The system, therefore, is able to receive AIS data of all ships even when the ships are out of gate line of Tokyo Bay or inside a port in the region, except for some internal limitations of AIS or signal blockage phenomenon.

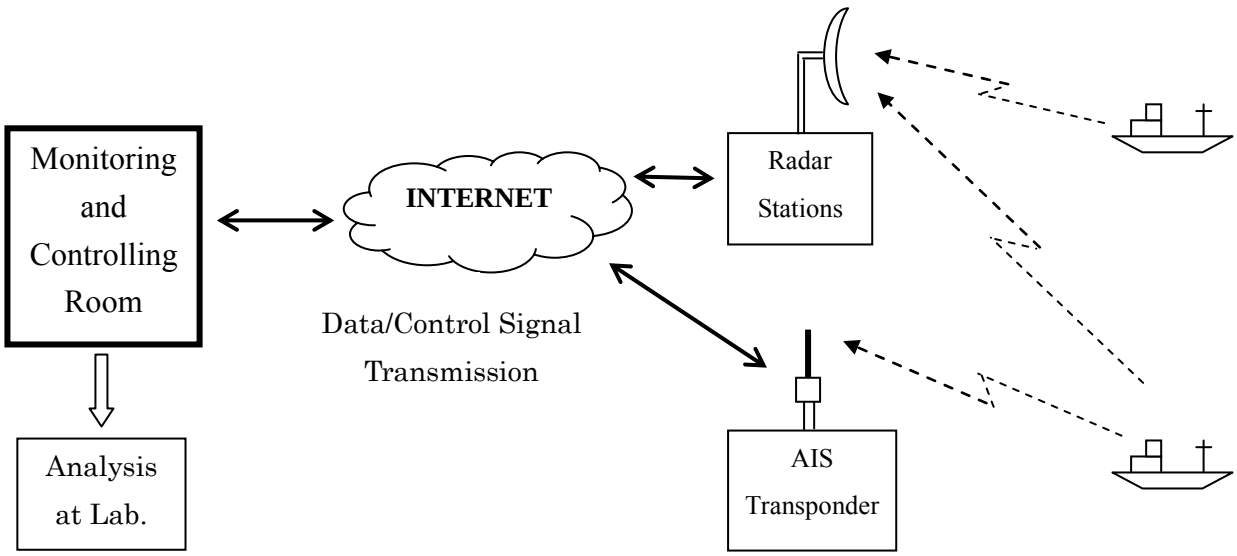

Fig. 1.3 Outline of observing system

Then, a media for transmitting control signal from central monitoring and controlling room to observing stations and data backward, using Optical Communication or ADSL protocols was set to operation.

The system, operated in a remote control manner, has the capability of automatically collecting and transferring data to the system control room (Marine Transport Joint Research Center) at Tokyo University of Marine Science and Technology (TUMSAT) through Internet.

After being transmitted to the monitoring and controlling center, data can be saved into the database for later traffic analyzing, or be decoded and re-uploaded for real time visualization of the bay traffic online.

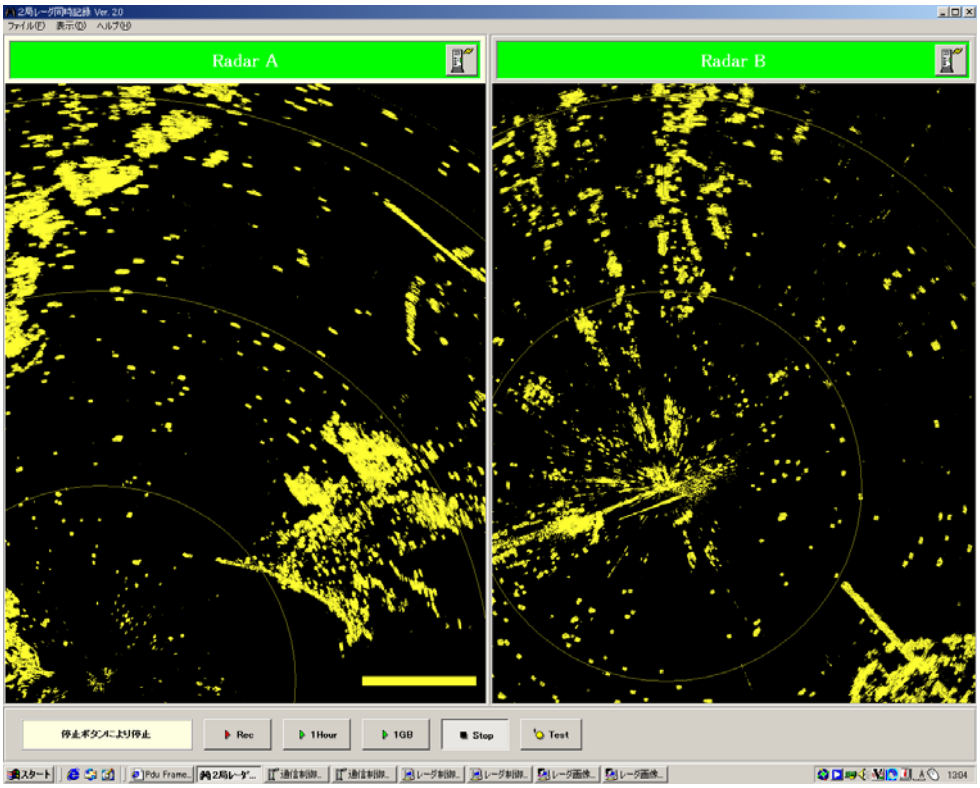

Fig. 1.4 Radar images of two radar stations viewed at TUMSAT

```
2006-03-28 23:14:39 !AIVDM,1,1,,B,19NS0Fh000:1F?hDG4KIOmC>0D1u,0*5E
2006-03-28 23:14:40 !AIVDM,1,1,,A,15AAA20002b05pND@QQL`oC>05hp,0*2D
2006-03-28 23:14:40 !AIVDM,1,1,,A,A04757QAv0agH2Jd;Vp`1Or3sRT6wdCdKQsvs>pN,0*0B
2006-03-28 23:14:40 !AIVDM,1,1,,A,369ffh50019wvldDC0NWP`3@0000,0*2B
2006-03-28 23:14:40 !AIVDM,1,1,,A,33:gEp1001b05J0D@vmB0J?>0000,0*75
```

Fig. 1.5 NMEA sentences of AIS data

Shown in the Fig. 1.4 and 1.5 are real time radar images of the network's two radar stations (Kawasaki station on the left and Yokosuka station on the right) and AIS data in the form of NMEA (National Marine Electronics Association) sentences received at monitoring room in

TUMSAT. Details of the system as well as data transmission method would be discussed in the next chapter in details.

From these data, a clear picture of marine traffic in the bay is at hand, enabling the accumulation of long time, continuous traffic observations with little human effort. The resulting traffic database, therefore, provides a stable base for traffic analysis, including but not limited to the following applications:

- Determining the ship density in a certain area inside the bay, changes of density with time in a day, time in a year. The information is necessary for traffic route design and application.

- Defining a safety boundary for ship maneuvering in the bay. Different criteria such as SJ value, Bumper model etc. are commonly applied for assessing risk of collision. Basing on long term observation of behavior of ship navigating inside the bay, some threshold value of SJ or suitable size of bumper model may be deduced and used as a recommendation for ship's officers while taking maneuver.

The traffic observing system, if operated in a real time basic, is able to supply a marine traffic service, with different services such as:

- Optimal route. From real time information of marine traffic, a route for a ship to enter or to leave a port can be calculated and transmitted to the ship in concern.

- Warning of possible risk of collision or possible human mistake in maneuvering. Statistically, human mistakes and equipment failure contribute a large part in marine accidents which result in loss of not only lives but also properties and long time effect to environment. If the situation is noticed from monitoring center, an in time warning to be provided would be invaluable.

However, for these real time applications, a suitable method of communicating between ships and system operators on shore must be established, together with regulations on the liability of parties involved.

1.3 Previous Researches on Observation System and Traffic Analysis in Tokyo Bay

Basing on the available facilities, several researches have been taken on the observation system itself and on marine traffic in Tokyo Bay.

Hagiwara, Shioji, Ohtsu, Tamaru, et al [3,4] (2003, 2004, 2005 and 2006) carried out several researches on the traffic management system, for which AIS and Planned Route information is used.

Liu et al [12,13,14,15] (2004, 2005 and 2006) carried out observations for several days in 2004. From the observing data, Liu calculated ship distribution density for some important marine traffic areas of the bay. Visual observations of the ship lengths were also taken to give reference data for considering the relation between the sizes of ship images on radar screen with ship's length for some certain ranges from the two radar stations (4 miles from Kawasaki station and 5 miles from Yokosuka station).

Next, AIS data were used for automatic tracking of ships. AIS track of the training ship Shioji Maru was compared to track of its images on radar screen to investigate the compatibility of Radar system and AIS.

Then, from position, course and speed of radar targets, several characteristics of marine traffic has been deduced, including relation between sizes of ships and their speeds, random distribution of the number of ships at gates of main traffic routes.

Okano et al [25] (2006, 2007), in their researches on Radar system have introduced an approach for automatic radar tracking and then applying the approach to process several days of radar data in 2006. Using this method, 40 to 50 percents of targets could be tracked automatically.

Other targets were tracked manually to provide the full target information data. From these data, Okano analyzed the movement of radar targets to sketch out a suitable size of bumper while using bumper model for adjusting risk of collision in the bay.

Apart from that, subjective judgment (SJ) value and DCPA/TCPA criteria were also used for risk assessments. From the distribution of dangerous encounters, Okano has deduced several conclusions on the bay's marine traffic conditions.

Basing also on the data received from the observing system, V.H. TRAN et al [22] (2006, 2007) suggested the application an Autonomous Traffic Management System. With the assumption that all ships in the area are equipped with AIS and strictly follow the instruction of traffic management center, the system takes into consideration the movement information of all existing vessels to calculate the recommended route for a new ship entering the bay for leaving port.

1.4 Purposes and Outline of the Study

With the aim of better efficiency and accuracy of autonomous traffic observing and extracting targets' motion data, purposes concentrated in this study are the followings:

- Introduce a method of automatic tracking to improve the efficiency and accuracy of targets motion tracking from the radar images, especially in noisy condition.
- Introduce an approach of using available AIS data to improve the efficiency and reliability of automatic tracking of ships equipped with AIS from radar images.
- Apply the Kalman Filter to rebuild the motion of targets tracked from radar data.
- Use the newly calculated target motions to analyze marine traffic in Tokyo Bay.

Contents of the study are arranged into the following chapters:

Chapter 2 Traffic Observing System and Fundamentals of Motion Tracking: The chapter deals in details with techniques aspect and designing parameters of the traffic observing system. General knowledge that will be used later for tracking target from radar images is also included. After that, several results of previous related researches will be briefly mentioned.

Chapter 3 An Approach of Automatic Radar Tracking: In this chapter, an approach of automatic tracking, using a Relating-Function as the base for matching. To determine the value of factors in Relating-Function, as well as Threshold of Relating-Value for decision making, observation has been carried out for targets navigating in Tokyo Bay. The approach was then applied with actual radar data to verify the efficiency and applicability.

Chapter 4 An approach of Automatic Radar Tracking with Supplementing AIS data: AIS data is quite accurate and easy to use. However, there are a large number of ships not yet equipped with AIS, and data provided by AIS is not always reliable if it is not cross-checked with data received by other means. Therefore, in this chapter, a method of taking advantage of AIS data to facilitate automatic Radar tracking of ships equipped with AIS is introduced. To take the advantage of data provided by AIS, Relating-Function is slightly modified and a threshold value for matching would be defined.

Chapter 5 Application of Kalman Filter to Rebuild Target Movement and Track Motion: The accuracy of target positions tracked from radar pictures is generally degraded by white noise. Effect of noise is even more serious to the target's course and speed calculated from one minute interval positions, making them inadequate for traffic analyzing. Thus, in this chapter, a Kalman Filter is designed to rebuild target movement, especially its speed and course from noisy position measurements. A model of target movement is used and designing parameters of the Kalman Filter are determined from simulation experiments.

Chapter 6 Analysis of Marine Traffic in Tokyo Bay: Basing on the movement of targets tracked from radar pictures, different risk assessment criteria such as Subjective Judgment (SJ) value, Bumper model or conventional DCPA/TCPA are used for adjusting the marine traffic condition in Tokyo Bay. Route use ratio is calculated for important traffic routes (Uraga Suido and Nakano). After that, the times and regions where care should be taken to ensure safe navigation would be Fig.d out for traffic route planning or traffic guidance purposes.

Chapter 7 Conclusion and Future Study: Summarizing results of the study and mentioning subjects for later study.

Chapter 2. Traffic Observing System and Fundamentals of Motion Tracking

2.1 Radar and AIS Traffic Observing System of Tokyo Bay

2.1.1 System Overview

Under the supervision of Tokyo University of Marine Science and Technology and funded by Nippon Foundation, the project of constructing a traffic observing system in Tokyo Bay was kicked of in 2000.

For trial, a radar station was first installed in the Sea Training Center (TUMSAT) in 2001. From the station, radar images were transmitted to the research room via Integrated Services Digital Network (ISDN lines) and were used for developing necessary software for system controlling and images processing.

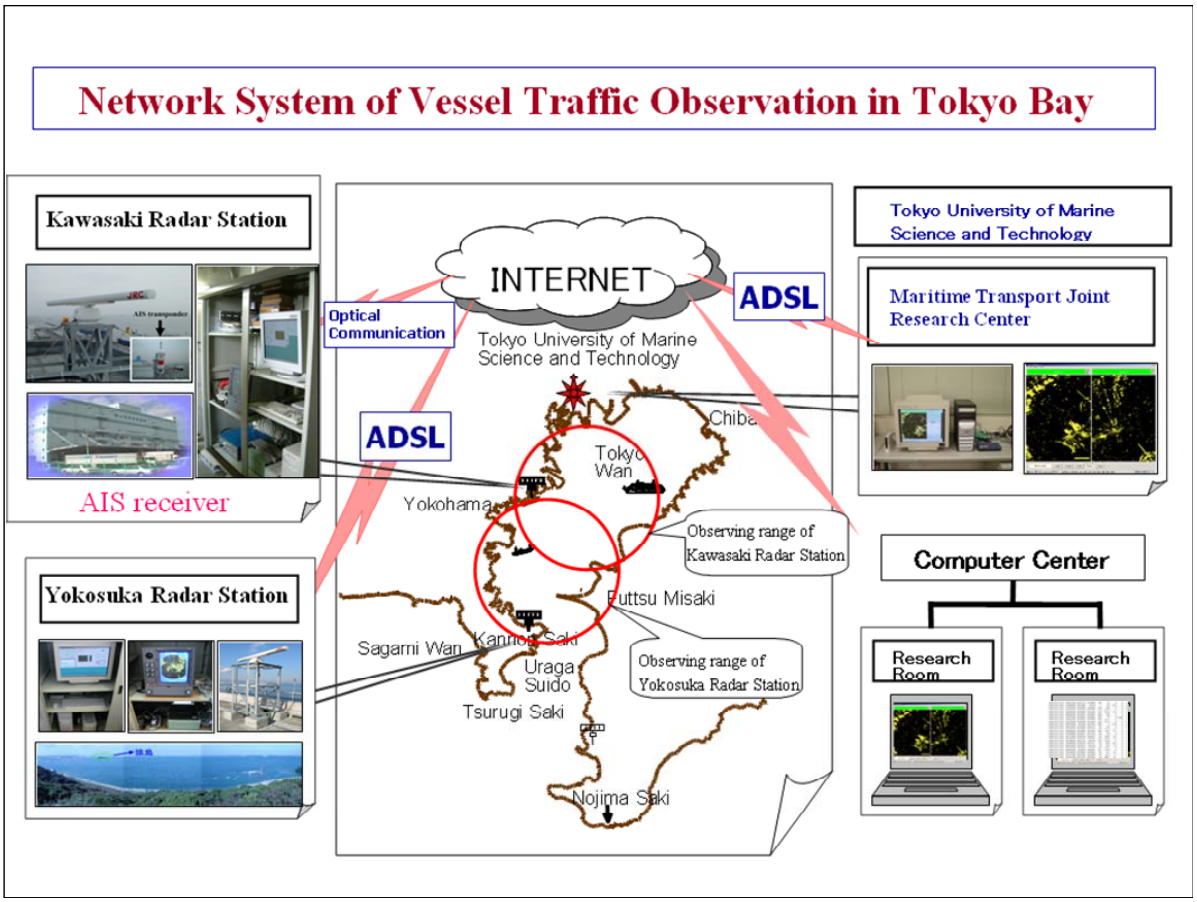

Fig. 2.1 Overall structure of traffic observing system of Tokyo Bay

Yokosuka Radar Station

In 2002, the system's first traffic observing radar station was installed at the National Defense Academy in Yokosuka (and therefore bearing the name Yokosuka radar station) and put into operation.

The radar antenna is located at:

Latitude: $35^0$15'66 N

Longitude: $139^0$43’41 E

For data transmission back and forth from the network, Asymmetric Digital Subscribe Line (ADSL) is applied for Yokosuka radar station. Via ADSL, radar images can be sent to the internet, from which they are forwarded to the control and monitoring station. Conversely, signal from monitoring station can be sent to radar station to control the station operation.

Kawasaki Radar Station

In a later phase of the project, another radar station was constructed in Higashi Ogishima (Kawasaki) in 2003. Position of this radar antenna is:

Latitude: $35^0$29’67 N

Longitude: $139^0$46’54 E

For simple and accurate identifying and following vessels equipped with AIS, an AIS transponder has also been installed in Kawasaki station, with the antenna located at:

Latitude: $35^0$29’67 N

Longitude: $139^0$46’54 E

Optical Communication Line is used for data transmission from and to Kawasaki station, including both radar images and AIS data.

Both of the stations are equipped with DGPS for position references.

With the two radar operated on 6 miles range, radar coverage area of the system includes almost all of the difficult and/or marine traffic congested areas of the bay, especially Uraga Suido (Fig. 2.2) and Nakano traffic routes.

Fig. 2.2 Uraga Suido traffic route viewed from Yokosuka Station

Base Station

Base station (or monitoring station) is located at Marine Transport Joint Research Center (TUMSAT) and connected to the Internet via ADSL. The main functions of the monitoring station are to remotely control operation of the whole system, collect and combine data from radar stations, AIS transponder to produce the best possible composite picture of real time marine traffic condition in Tokyo Bay. The picture can then be uploaded back to the internet as reference for interested personnel.

All the stations are connected to the Virtual Private Network (VPN) via IP-based network and modem router. The more detailed structure and communication method of the observing system is shown in Fig. 2.3.

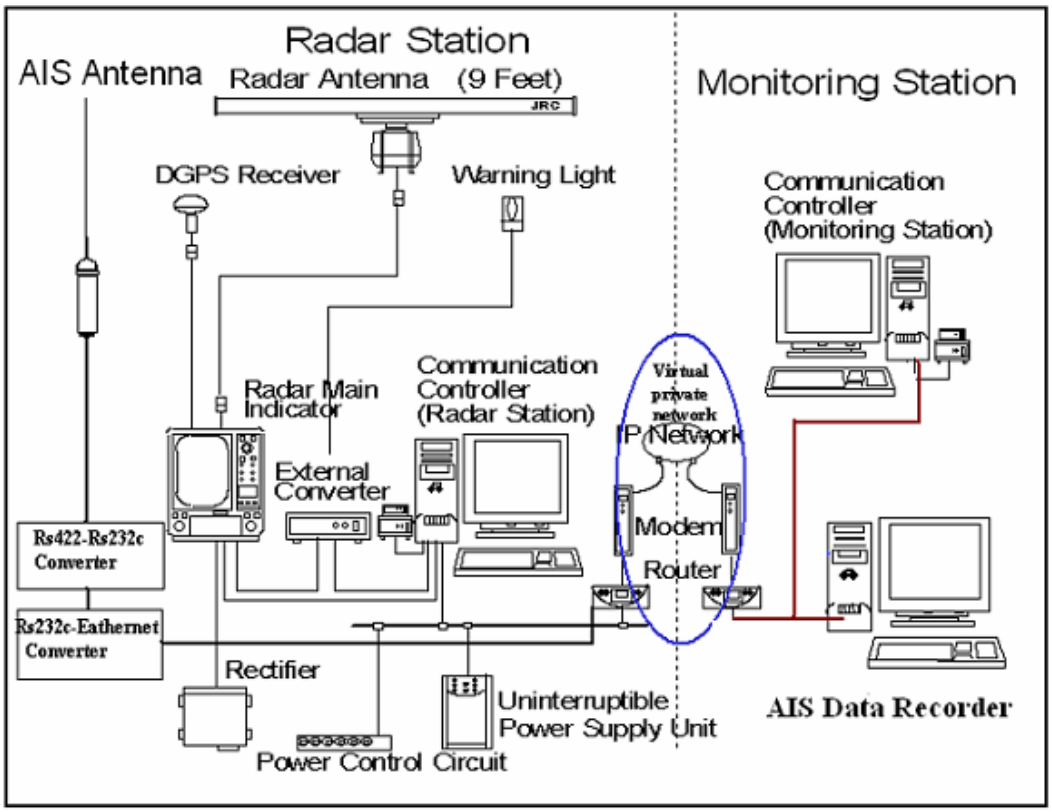

Fig. 2.3 Observing system structure and data transmitting principle

2.1.2 Radar Station Configuration

To fulfill the intended functionalities, a radar station contains 3 important parts:

- Marine radar
- Radar indicator
- Communication control unit and a means of communication

Used in the observing system of Tokyo Bay are JRC NKE-1056-9 radars with working characteristics listed below:

Table 2.1 General parameters

Antenna type	Slot antenna
Antenna size	519mm x 2850mm
Antenna weight	49 kg
Antenna Rotating Speed	app. 20 rpm
Transmitting Power	25kW ± 50%
Working frequency	9410 ± 30 MHz
Signal Generator	Magnetron M1437 (A)
Mixer	MIC Front End
Wind resistant	51.5 m/s (100 kts)
Carrier wave bandwidth	60MHZ
Pulse bandwidth	20 MHz (pulse width 0.08μs) 6 MHz (pulse width 0.2μs, 0.4μs) 3 MHz (pulse width 0.8μs, 1.2μs)
Sensitivity	7.5dB

Fig. 2.4 Radar structure

Table 2.2 Radar beam width

Horizontal Beam Width	0.8^0 ± 10%
Vertical Beam Width	25^0
Sizelobe level	Less than ±10^0: <=-26dB More than ±10^0: <= -30dB

Table 2.3 Radar Pulse Width and Repetition Frequency

	Short Pulse	***Medium Pulse***	***Long Pulse***
0.125 NM		0.08μs/2083Hz	
0.25 NM		0.08μs/2083Hz	
0.5 NM		0.08μs/2083Hz	
0.75 NM	0.08μs/2083Hz	0.2μs/2083Hz	
1.5 NM	0.08μs/2083Hz	0.2μs/2083Hz	0.4μs/1562Hz
3 NM	0.2μs/2083Hz	0.4μs/1562Hz	0.8μs/781Hz
6 NM	0.4μs/1562Hz	0.8μs/781Hz	1.2μs/521Hz
12 NM	0.4μs/1562Hz	0.8μs/781Hz	1.2μs/521Hz
16NM		0.8μs/781Hz	1.2μs/521Hz
24 NM		1.2μs/521Hz	
32 NM		1.2μs/521Hz	
48 NM		1.2μs/521Hz	
120 NM		1.2μs/521Hz	

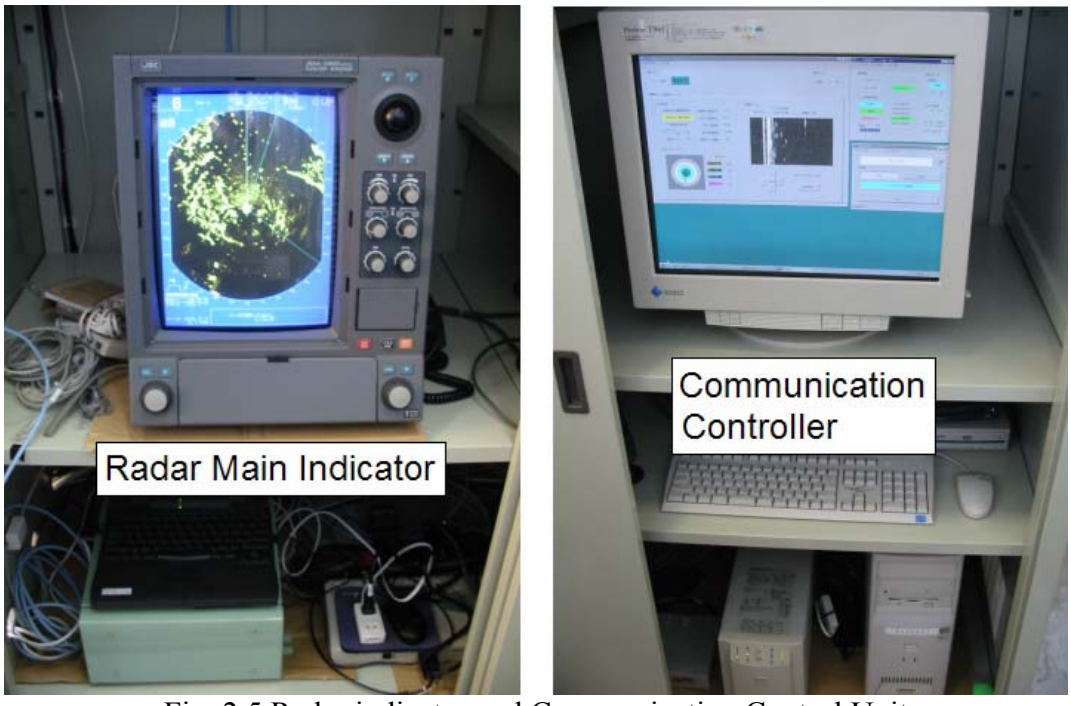

Fig. 2.5 Radar indicator and Communication Control Unit

The Indicator is of NCD-4096 type, having the main designing parameters:

Table 2.4 Indicator specifications

Size	370mm x 452mm x 555mm
Weight	34kg
Screen	CRT 15” Color
Resolution	1024x768 Pixels
Image Area	280mm x 210mm
VRM	2 (0.000~295.0NM)
EBL	2 (0.0^0~359.9^0)
Power Source	DC21V ~ 32V

Table 2.5 Communication Control Unit (in 2005)

Name			NCU-375A
Center Processing Unit	Name		DELL Precision Workstation
	OS		Windows NT4.0 Workstation
	CPU		Pentium III
	Processor Speed		866 MHz
	Drives		Hard Disk Drive 20 GB Floppy Disk Drive 01
	Memory		256 MB
	Expansion Slot	PCI1	Radar Signal Processing Board CDC-1064
		PCI2	Radar Signal Input Board CDD-665A
		PCI3	PIO Board
		PCI4	A/D Board
		PCI5/ISA2	SICI Adapter
		ISA1	Land Adapter
DVD-RAM drive	LF-D102JD		5.2 GB/ two-sides
Display Unit	Power Source		AC 100V, 50/60Hz
	Weight		18kg
	Name		T962
	CRT Size		21”
	Vertical scanning frequency		30Khz~130Khz
	Traverse scanning frequency		50Khz~160Khz
	Image Area Size		388mm x 291mm
	Power Source		AC100V, 50/60Hz

Other components of Radar station are listed in the following table (Refer to Fig. 2.3 and 2.3 for functions of each component in the system's operation)

Table 2.6 Other component specifications

Component	***Type***	***Number***	***Note***
DGPS receiver	JLR-4331E	1	
Alarm light	RLE-100	1	AC100V
Rectifier	NBA-3308	1	
Router	NZA-195	1	
Power supply control circuit	AP9211J	1	
Uninterruptible power supply	SU1000J	1	

Radar data from the station is transmitted to monitoring station through Virtual Private Network. Details of the data transmission is described in Fig. 2.3, in which radar images, after being converted to a suitable form, is transferred to VNP via modem router.

At the other end of transmission line, images are downloaded from VPN through modem router and recorded for later manipulating (displaying, analyzing, etc.).

2.1.3 Automatic Identification System [6,7,8,10]

2.1.3.1 AIS Overview and Guidelines

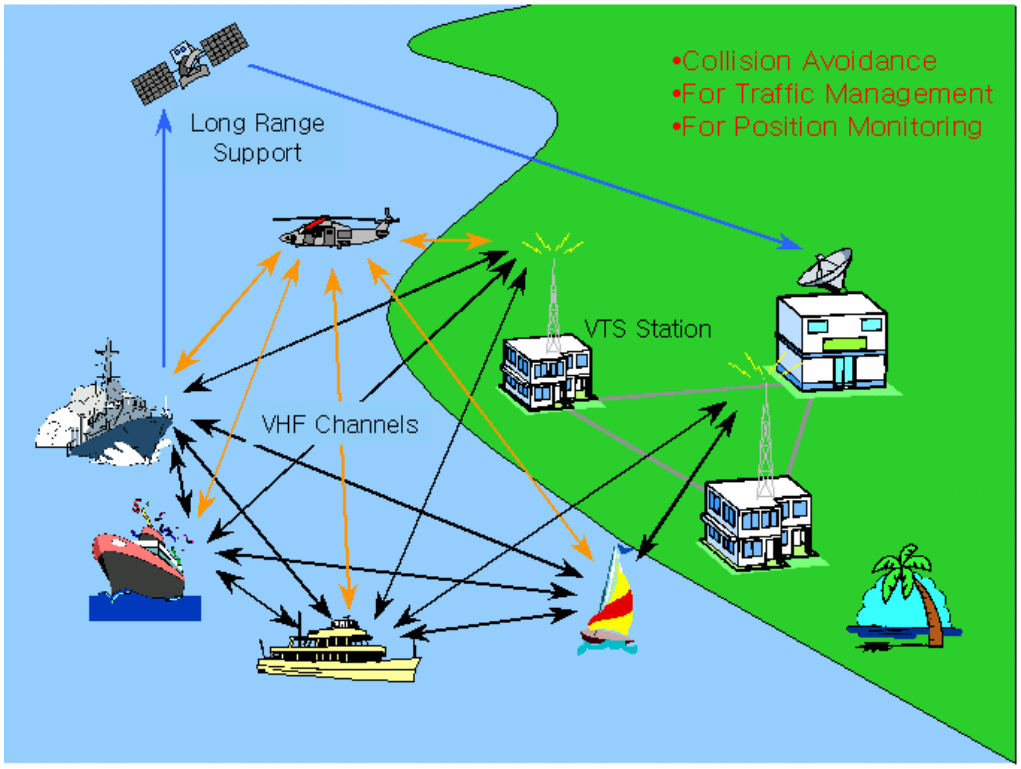

Fig. 2.6 Concept and Motivation of Introducing AIS

Initially called the “Ship-Ship, Ship-Shore (4S)” broadcast transponder, the technology formed the base of what eventually became known as “Universal Ship-borne Automatic Identification System (UAIS)”. For simplicity, it is often called “Automatic Identification System”, or AIS.

AIS technologies have been developed to make it an autonomous and continuous broadcast system operating in the Maritime mobile band to provide a means of sharing information between ship and ship, as well as ship and shore. According to IALA (International Association of Lighthouse Authority) guidelines, the principle functions of AIS are to facilitate:

- Information exchange between vessels within VHF range of each other, increasing situational awareness.

- Information exchange between a vessel and a shore station, such as a VTS, to improve traffic management in congested waterways.

- Automatic reporting in areas of mandatory and voluntary reporting.

- Exchange of safety related information between vessels, and between vessels and shore station(s).

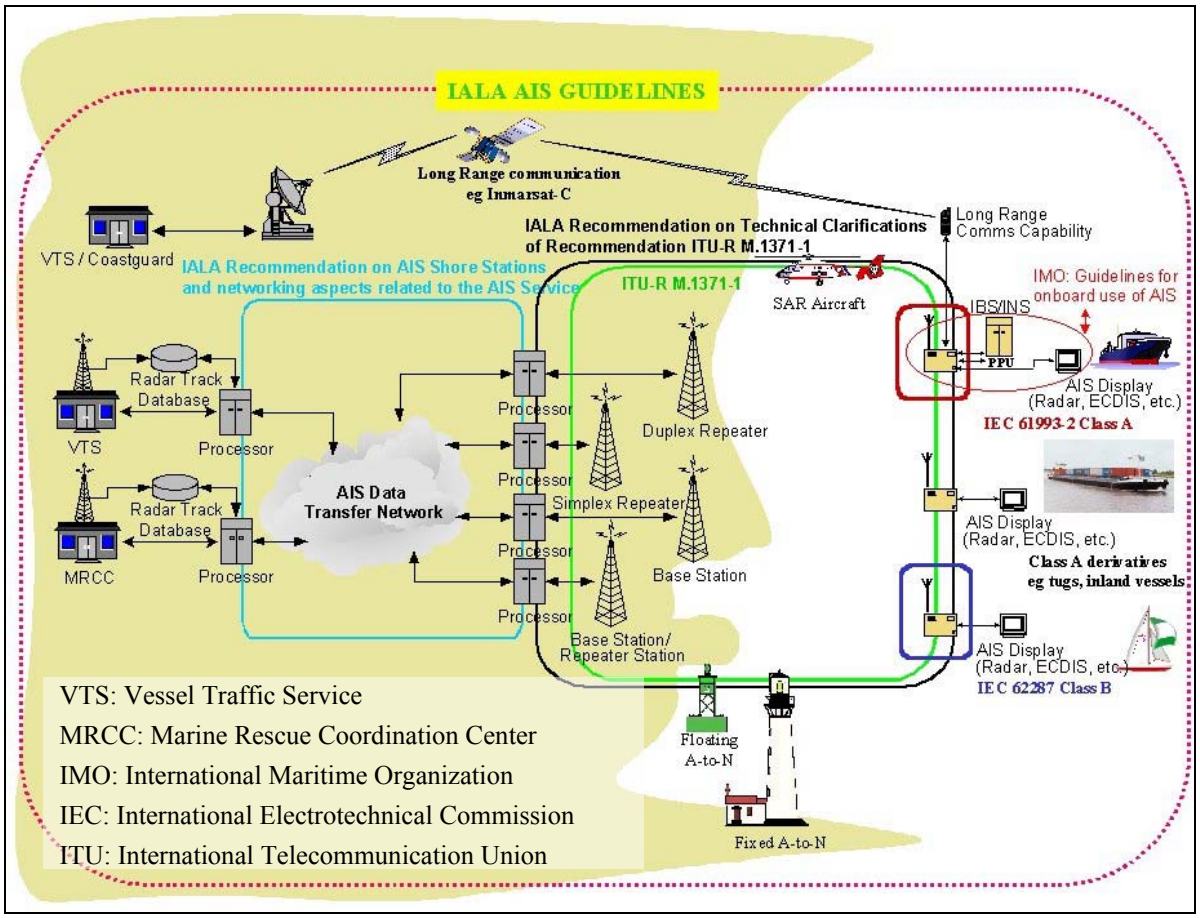

Fig. 2.7 IALA Guidelines on overview and reference document for parts of the system

Then, IALA has promulgated guidelines on the structure of the system, in which technical requirements of different parts are dealt with independently in documents or recommendations of respective organizations in charge (Fig. 2.7).

As shown in Fig. 2.7, ship borne AIS is divided into 2 main categories:

- Class A ship-borne AIS, which is used for most commercial ships of more than 300 GT engaged in international voyage; and some Class A derivative used for tugs, inland vessels, etc. Requirements for them are documented in ITU-R M.1371-1 (now superseded by M.1371-3), IEC 61993-2 and IMO Guidelines for onboard use of AIS.

- Class B ship-borne AIS are intended for boat, yacht and other vessel not required carrying Class A AIS. Performance of Class B AIS is given in ITU-R M.1371-1 (now superseded by M.1371-3) and IEC 62287.

Performance Standard of AIS

In terms of system functionality, the performance standard for AIS (IMO Resolution MSC.74 (69) Annex 3), requires that the system should be capable of operating:

- In the ship-to-ship mode, to assist in collision avoidance
- As a means for littoral states to obtain information about a ship and its cargo.
- As a VTS tool, i.e. ship-to-shore (for purpose of traffic management).

To meet the functionality requirements, AIS shall have the capability of operating in a number of modes, including:

- An “autonomous and continuous” mode for operation in all areas. This mode is capable of being switched to/from other modes by competent authority.
- An “assigned” mode for operation in an area subject to a competent authority responsible for traffic monitoring such that the data transmission interval and/or time slots may be set remotely by that authority.
- A “polling” or controlled mode where the data transfer occurs in response to interrogation from a ship or competent authority.

Apart from that, AIS must be able to provide information automatically and continuously without involvement of ship’s personnel, receive and process information from other source.

The structure of a ship-borne Class A AIS is shown in Fig. 2.8.

In Fig. 2.8, own ship information is collected form respective sensors or navigation system (on the left). Then, AIS message is created, encoded and sent through VHF Antenna automatically or as controlled by competent authority via DSC channel.

On the vice-verse direction, information from other source can be received, processed and displayed on display unit.

For details, refer to ITU-R M.1371-3, IALA Guidelines or equivalent documents.

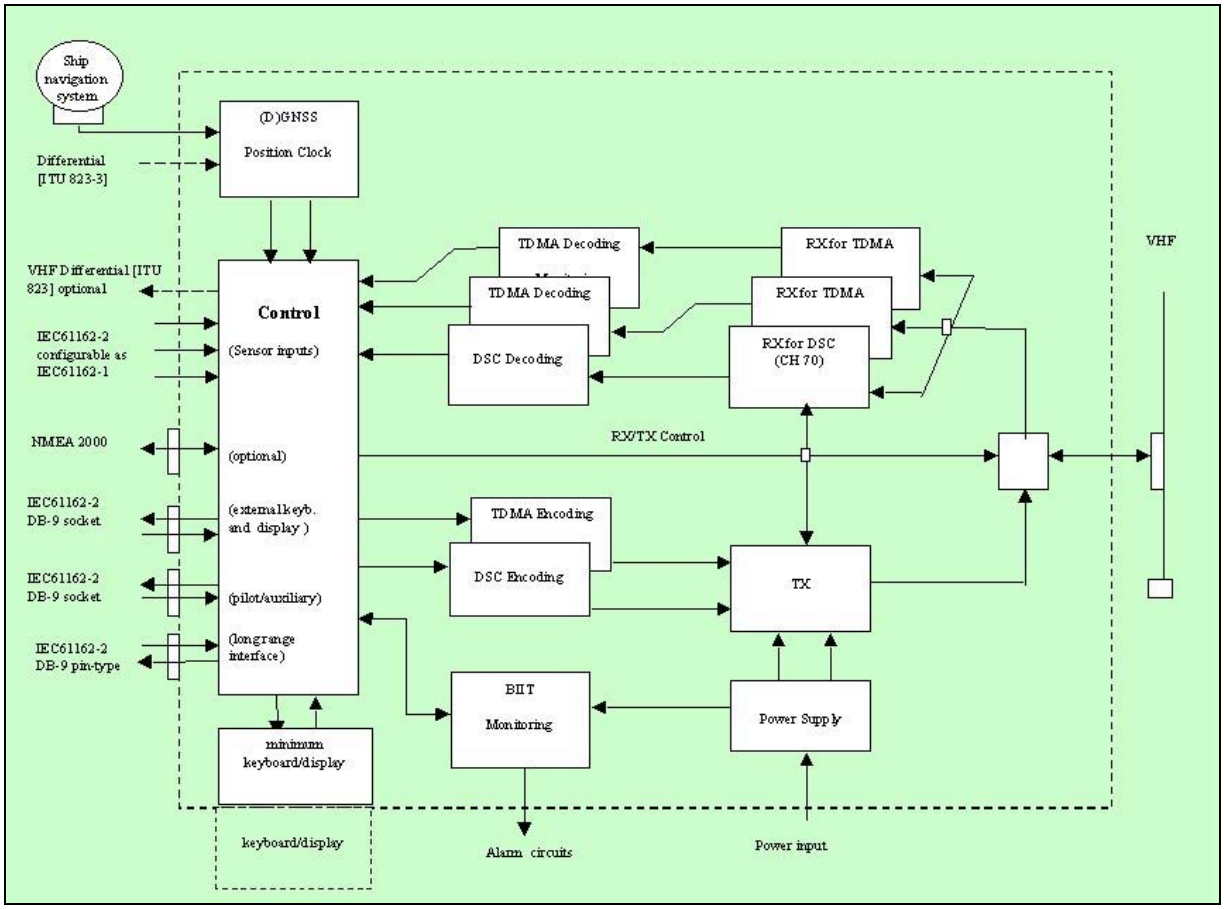

Fig. 2.8 IALA Guideline for Class A Mobile Station AIS structure

Frequency and Channel Access Scheme

AIS is assigned to work on 2 frequencies in maritime VHF channels:

- AIS 1: 161.975 MHz (Channel 87B)
- AIS 2: 162.025 MHz (Channel 88B)

Then, for sharing the 2 channels, Time Division Multiple Assess technique is used.

In TDMA, 1 minute interval of time is divided into 2,250 slots (1 slot = 26.7 ms). By self-organizing technique, each slot is assigned for 1 ship to transmit its message or part of the message if the message is divided into 2 or more sentences. In the later case, other slot (slots) will be reserved for the ship's AIS to transmit the other sentence (sentences) and all sentences of the same message have to be combined before decoding message for information. For details, refer to ITU-R M.1371-3, IALA Guidelines or equivalent documents.

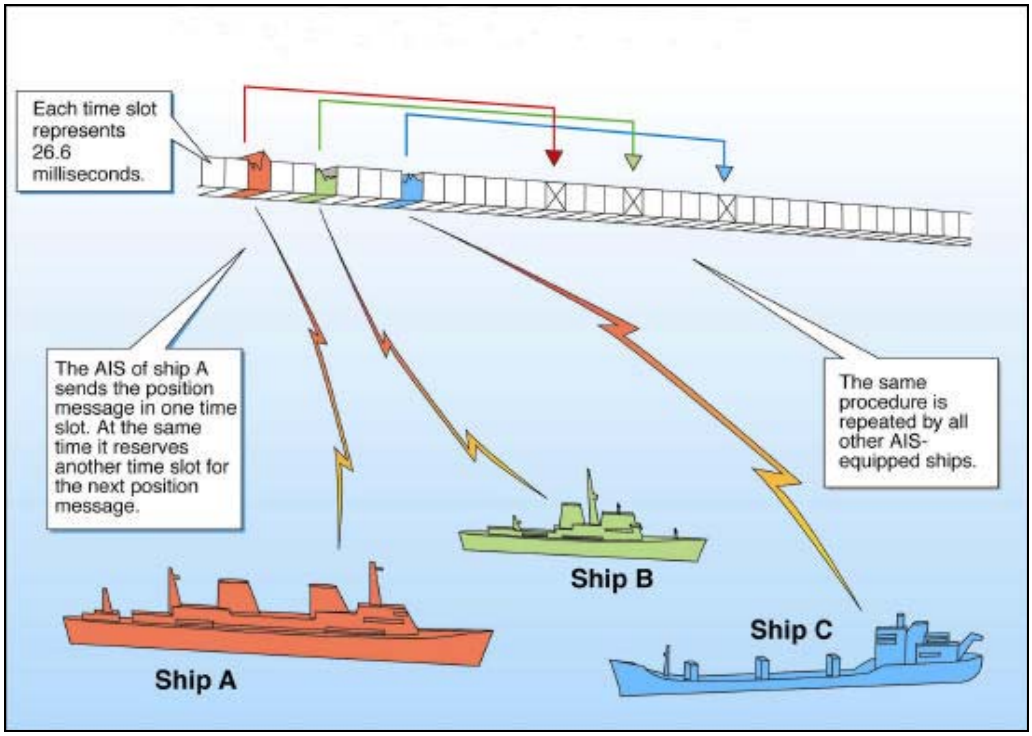

Fig. 2.9 TDMA technique used in AIS

AIS data and update rate

AIS data are classified into 4 following categories

Table 2.7 AIS data categories

Data Category	***Data Content***
Static	MMSI number, IMO number, Call sign Length and beam Type of Ship Location of position-fixing antenna
Dynamic	Time (UTC) Ship's position and position accuracy Heading, Course over ground (COG) Rate of turn (ROT) Speed over ground (SOG) Navigation status
Voyage related	Draught Cargo type Destination Estimated time of arrival (ETA)
Safety related messages	Broadcast message Addressed message

Reporting interval for the information is as followings:

Table 2.8 Data reporting interval

Ship's Dynamic Conditions	***Reporting Interval***
Ship at anchor or not moving faster than 3kts	3 min
Ship at anchor/moored and moving faster than 3kts	10 sec
Ship moving at speed from 0-14 kts	3 1/3 sec
Ship moving at speed from 0-14	6 sec
Ship moving at speed from 14-23 kts and changing course	2 sec
Ship moving faster than 23 kts	2 sec
Ship moving faster than 23 kts and changing course	2 sec
Static data	6 min or on request

2.1.3.2 AIS data transmission

Fig. 2.10 AIS transponder and radar antenna of Kawasaki station

With AIS transponder located in Kawasaki station, the system is enabled to collect AIS data from ships equipped with AIS navigating in the bay or nearby regions. Communication between AIS unit and monitoring station can also be remotely controlled.

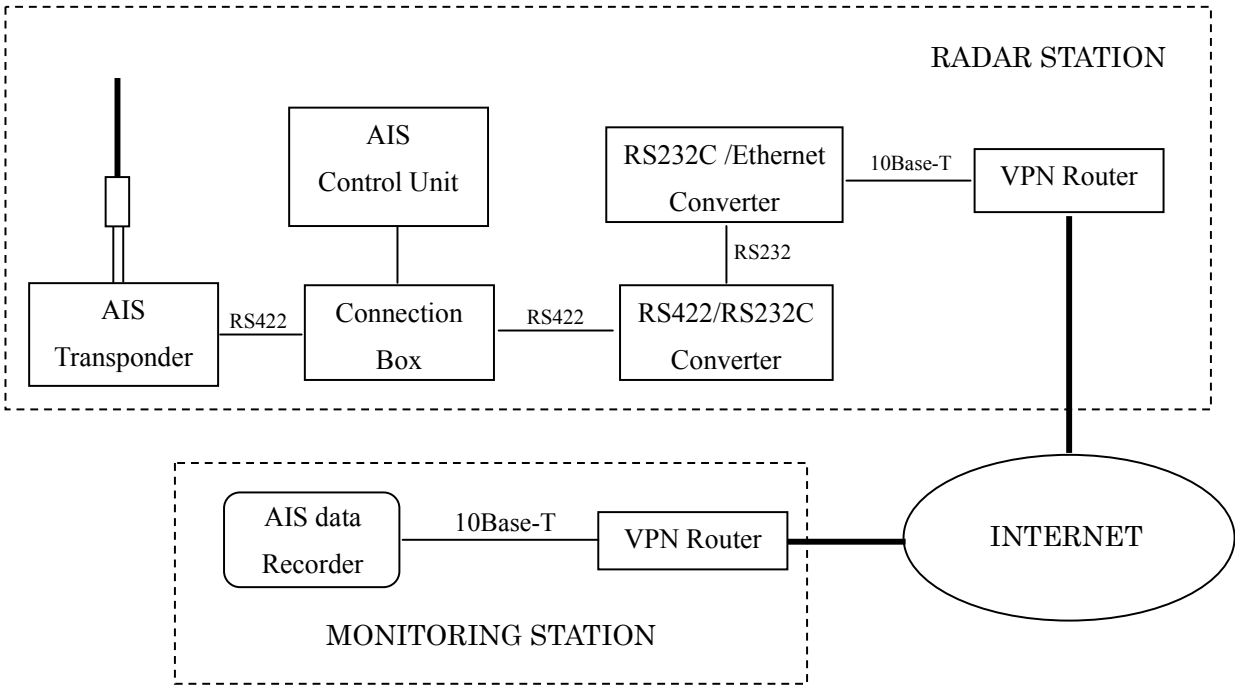

Fig. 2.11 Transmitting AIS data to monitoring station

AIS data from the station is transmitted to monitoring station through Virtual Private Network. Details of the transmission flow is described in Fig. 2.11, in which AIS data, after converted to a suitable form, is transferred to the Internet via VNP router.

At the other end of transmission line, data is downloaded through VPN router and saved into the AIS database.

2.1.4 Monitoring Station

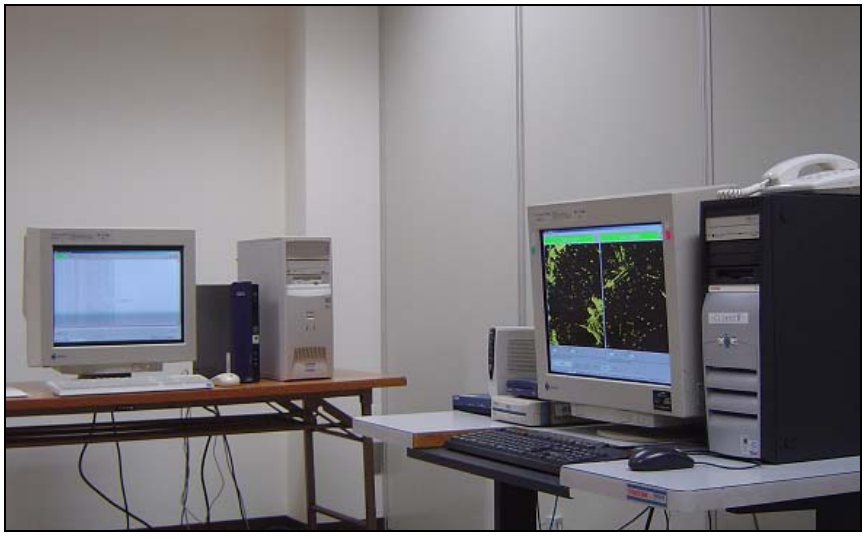

Fig. 2.12 Monitoring station

If radar systems and AIS receiver are to be compared with “Eyes” and “Ear” of the system, monitoring station takes the part of system’s “Brain”.

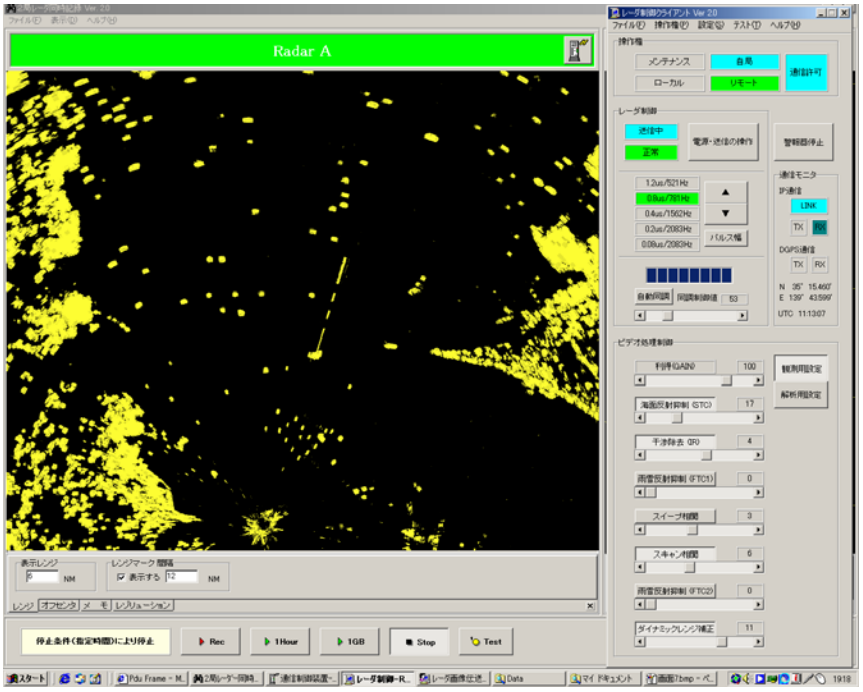

Fig. 2.13 Radar station operation control interface

In the monitoring room, necessary software has been installed to allow the remote controlling of the radar stations operation. Shown in Fig. 2.13 is the control interface for radar station, including the following radar control functions:

- Radar gain/tuning control
- Radar range and/or pulse width selection
- Radar sea clutter control (STC)
- Radar rain clutter control (RTC)
- Interval/speed of radar image transmission
- Radar image quality selection etc.

The second function of monitoring station is to process and display data. An available motion tracking algorithm can be applied to track targets navigating in the bay. Then, radar targets data, together with AIS data are imposed on an electronic chart to be uploaded to the Internet through VNP router.

The other function of monitoring is to record radar images and AIS data for traffic analyzing and managing purposes. AIS data is saved continuously and automatically into AIS database whenever AIS data of ships are received by the AIS transponder and transferred to monitoring station. For radar images, due to limitation in the storage space, images are saved at the interval of 1 minute. Basing on these radar images and AIS data, the study is conducted.

2.2 Radar Images and Fundamentals of Radar Tracking [11,17,25]

2.2.1 Radar Bitmap Image [25]

A bitmap (or raster) image is one of the two major graphic types (the other is vector image). Bitmap based images are comprised of pixels in a grid. Pixels are picture elements; tiny dots of individual color that make up what one sees on computer screen. All these tiny dots of color come together to form the images we see. Most computer monitors display approximately 70 to 100 pixels per inch. The actual number depends on the monitor and screen settings. Each pixel or "bit" in the image contains information about the color to be displayed.

Bitmaps are restricted to rectangle. All scanned images are bitmaps, all images from digital cameras are bitmaps and radar images are not an exception.

Bitmap images have a fixed resolution and can not be resized without losing image quality. When the size of a bitmap picture is increased, additional pixels have to be created and imposed on the pictures to fill the gaps between original pixels. Color for these added pixels must be estimated through interpolation process. On the other hand, when the size is decreased, some pixels of the images must be thrown away.

Common bitmap based formats are JPEG, GIF, TIFF, PNG, PICT, and BMP. Most bitmap images can be converted to other bitmap-based formats very easily. Although many graphics formats are bitmap-based, bitmap (BMP) is also a graphic format.

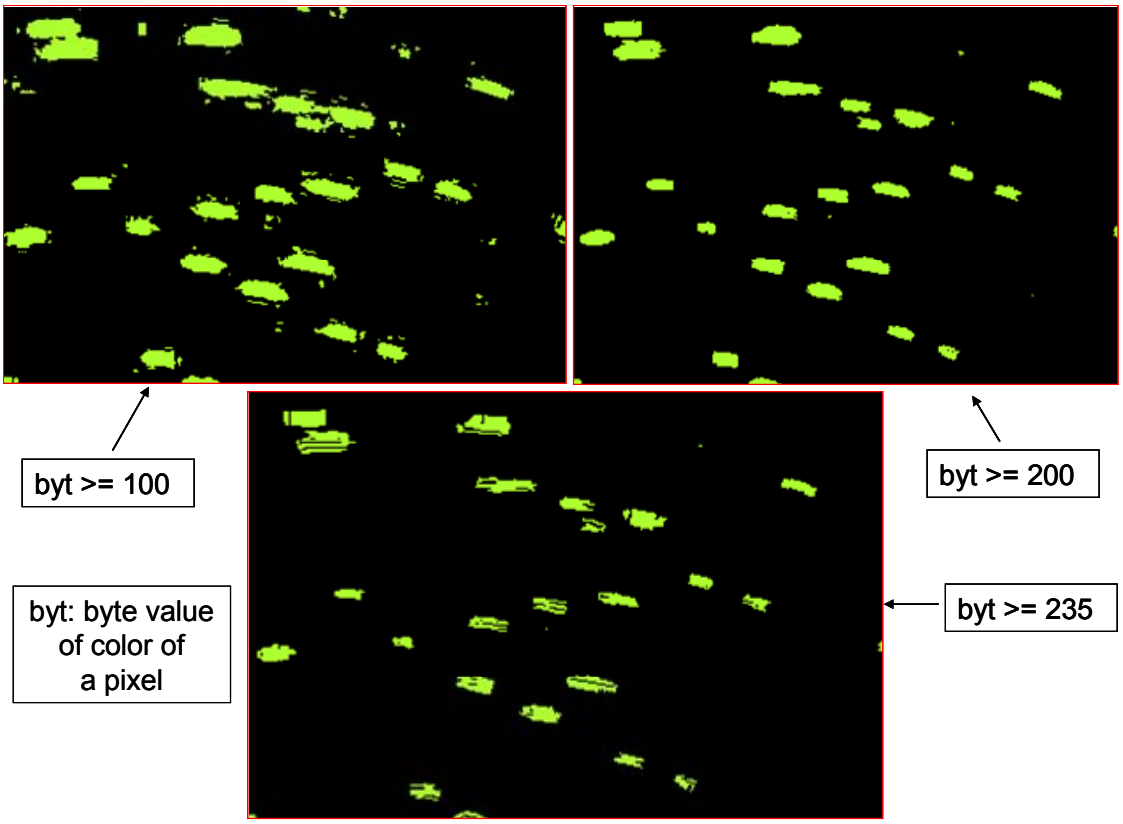

Fig. 2.14 Radar image for different cut-off value of color

In recording radar images of marine traffic Tokyo Bay, BMP graphic format is used. For BMP format, the image is expressed by a grid starting from the down, left most pixel. Information of color to be displayed for one pixel on the image is expressed by 1 byte (8 bits).

Therefore, color of a pixel is a value in the range from 0 to 255, where:

0: Completely black

255: The brightest color of the range

Commonly, power of signal reflected from targets with highly reflective surfaces and/or target in proximity of radar antenna is stronger and the brightness of the equivalent pixel, as a result, is higher than those of weak reflecting signal. Noise from different sources such as rain clutter, sea clutter or system internal noise is, usually, weaker than signal and the value of color of noise pixels on the screen, therefore, is rather small. Hence, it is reasonable to set a noise/signal separating value (cut-off value) to reduce the existence of unwanted noise on radar images. If value of the pixel color is larger than the cut-off value, the pixel color will be taken. Otherwise, the color will be removed and value 0 (completely black) is set to that pixel.

However, targets may disappear (or be lost) from radar screen if the cut-off value is set too high. Effects of the choice of the cut-off value are shown in Fig. 2.14.

It can clearly be seen in Fig. 2.14 that the larger cut-off value for color of image pixels actually sharpens the image with the price of erasing possible data signal. Basing on observation, Okano et al have suggested erasing all pixels that have byte value color being less than 200 [(22)].

Size of radar images has been set to be 1024 by 1024 (pixels).As just the bay-ward direction needs watching, radar screens should be switched to the OFF-CENTER mode to give priority of image resolution and coverage to the bay ward direction. Hence, positions of radar stations on its equivalent images are as followings (from left, down corner of radar images):

Yokosuka Station:

X (East ward) = 500 (pixels)

Y (North ward) = 30 (pixels)

Kawasaki Station:

X = 450 (pixels)

Y = 350 (pixels)

These values have to be taken into account when it is necessary to rotate the image to compensate for radar North Mark error or radar images deformity if any.

2.2.2 Fundamentals of Motion Tracking from Radar Images [(11,17)]

2.2.2.1 Motion Tracking Fundamentals

In the field of image processing, the term “motion tracking” refers to the process of finding how objects have moved in an image sequence. Movement of target may be that in space or just in image plane.

The process comprises of 2 operations: Acquiring and Following Targets.

Target acquisition

Acquisition is the act of determining the existence of a target. Solving this task, several techniques are commonly used, including:

- Image differencing: Defining the object by the difference between consecutive images. The differences may be results of a moving object overlying static background, moving object overlying another moving object, etc.

- Moving edge detector: Defining the object from detected edge

Target following

Following the target is to observe the positions of an object or objects in a time sequence of images. Techniques normally used for the operation are those listed below

- Object matching: The objects in each image are located. Then, objects are matched between images.

- Minimum path curvature: The core of this technique is to minimize the curvature of the path connecting candidate objects.

- Model based methods: The approach is applied with the assumption that there is a mathematic model of objects motion (e.g. position, speed, course, acceleration). Model is used for object's position prediction.

Then, object is searched by scanning from the predicted position and using an algorithm of matching.

The search for object is not always successful due to uncertainties or changes in the model or simply because of noise that cause shifting or deformation of target. In this case, necessary change or updating must be made to the model. Kalman filter may be a solution to fill this gap.

- Kalman filter: The art of Kalman Filter is to estimate the most possible object position from noisy measurement of its position, using knowledge of past positions, under the assumption that a mathematic model of object motion is available and the noise is white.

Procedure of target following is similar to that used in model based method, except that the mathematic model is continuously updated whenever the search for object has been successful.

Due to the system uncertainty in modeling as well as noise, the object is searched for by scanning a searching area around the predicted position.

- Condensation: The above mentioned methods are insufficient if complex movement (i.e. the movements change) is concerned. In this case, a set of different models (multi models) must be used. Then, a mechanism for model selection shall be constructed.

- Hidden Markov Model: Hidden Markov Model comprises sets of equations describing the system, including:

States occupied by a system

Possible transitions between states

Probabilities of transitions

Then, an algorithm for transition recognizing is used for prediction of system state. The object is searched from predicted state.

- Optic flow: The method is applied with the assumption that each pixel moves but does not change in intensity. Optic flow associates displacement with each pixel.

- Area based methods: The principle of these methods is to match small region in image 1 with small region in image 2, with the assumption that objects move but does not deform.

For details of the image processing techniques, refer to appropriate materials dedicated for the field.

2.2.2.2 Tracking Motion from Radar Images

Tracking motion from radar images (from hereon referred to as Radar Tracking) is the process of acquiring and following radar targets (ships, buoys etc.) from radar images sequence.

Motions of radar targets are those in the plane of radar pictures.

Each pixels or combination of pixels on radar images is an object overlying the pure black background. However, those objects may be a moving vessel, a fixed target or simply a noise arising from many sources of radar noise.

Therefore, the task of automatic radar tracking is to distinguish moving targets (ships) from noise and follow these targets continuously.

In this study, methods of automatic tracking would be discussed in details in chapter 3 and 4.

Chapter 3. An Approach to Automatic Radar Tracking of Targets Motion in Tokyo Bay

3.1 Reading Radar Picture for Objects

As mentioned in chapter 2, radar images are saved in the form of 1024 x 1024 pixels bitmap (BMP). For this format, image pixel's color is a value in the range from 0 to 255, expressed by a byte, started from the byte number 1078 in the image file. Value of this byte is color of image's pixel at the left, down corner, the first picture point. From this point, color values of following pixels rightward (consecutive) and upward are coded consecutively, using 1 byte 1 pixel principle.

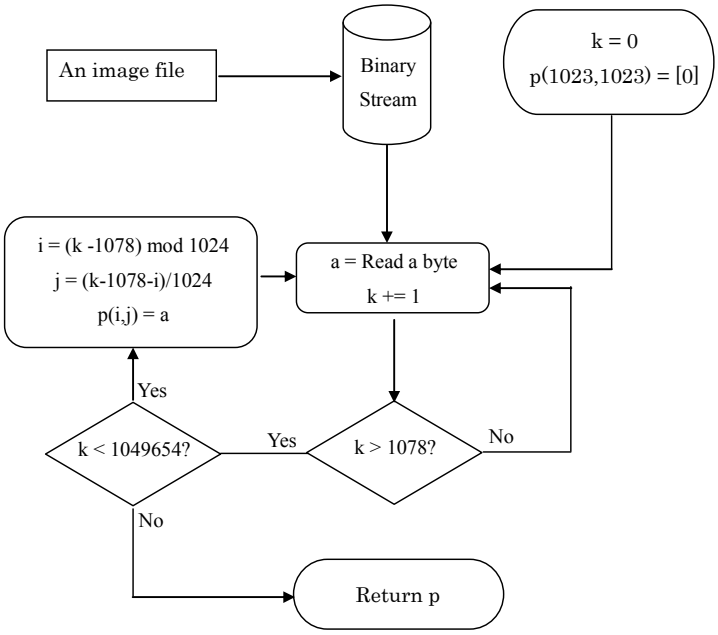

Fig. 3.1 Reading color value from radar picture

Then, using the flow chart in Fig. 3.1, a picture file can be read into a matrix (or 2 dimensions array) of color value (matrix p in the Fig.).

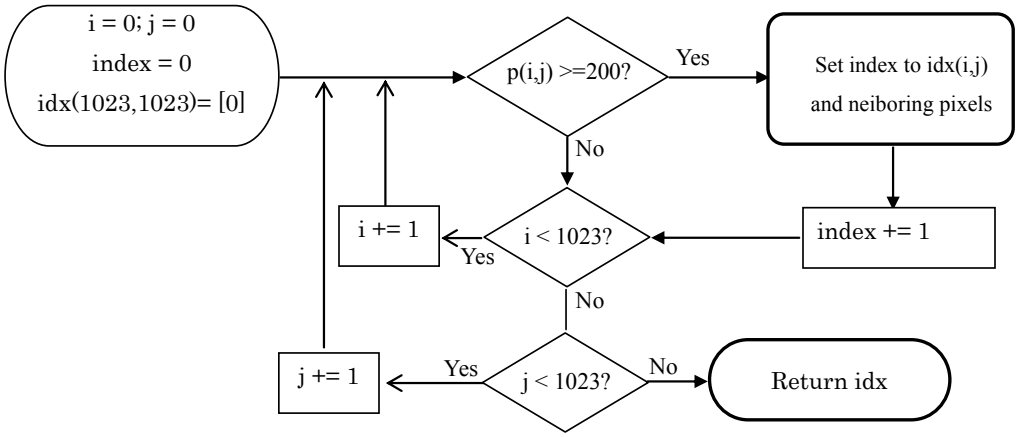

Fig. 3.2a Setting index to the illuminated pixels

An object on radar picture is a combination of illuminated pixels having connection, i.e. every pixel in the combination lies next to at least one other combination's pixel.

To define the objects on the screen, every pixel is given an index in a way that all pixels that should be in the same combination will be given the same index. This can be realized using the flow chart shown in Fig. 3.2a and 3.2b, where a 1024x1024 matrix (or 2 dimensions array) is used to record the indices of all image pixels. It should be noticed that the "Setting Index to Pixel" procedure is a repeating process that call itself inside the loop as shown in Fig. 3.2b.

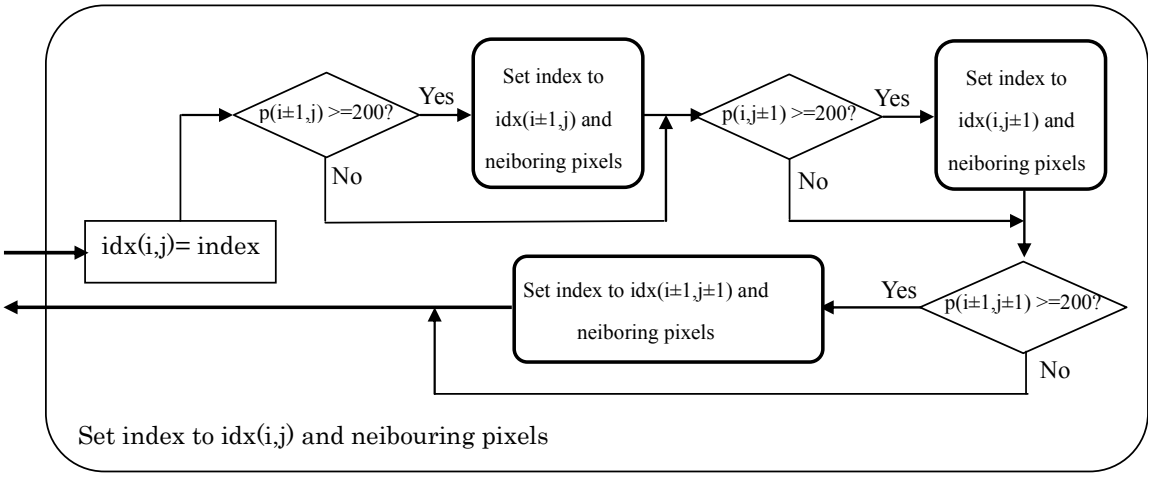

Fig. 3.2b Repeatedly setting index to the illuminated pixels

From the matrix of indices (idx matrix in Fig. 3.2a, 3.2b), it is an easy task to extract objects.

In this study, the objects are called Image Position. Therefore, an "Image Position" is defined by its coordinators (x, y), number of brink pixels and a matrix containing color values of each pixel in that Position. These parameters can be calculated easily from color values and indices matrices.

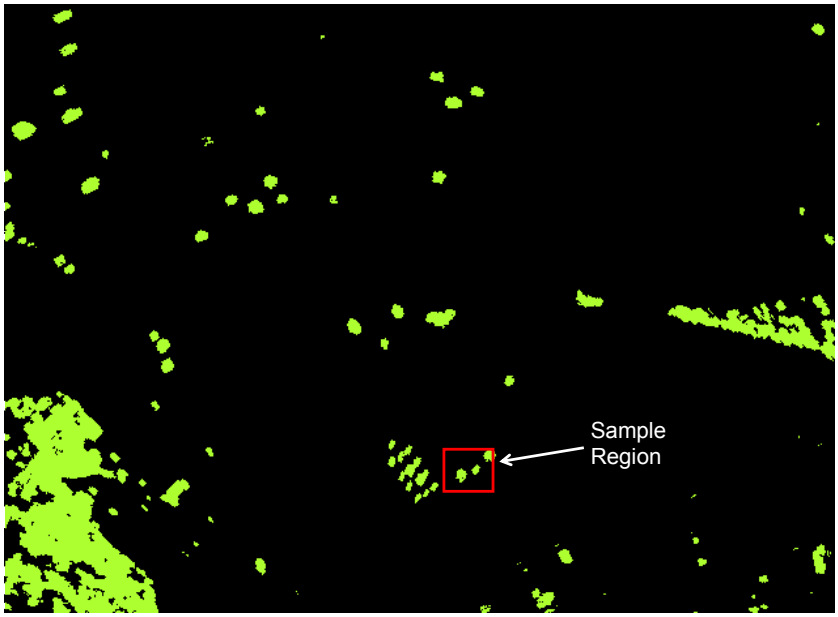

Fig.3.3a Part of a radar picture

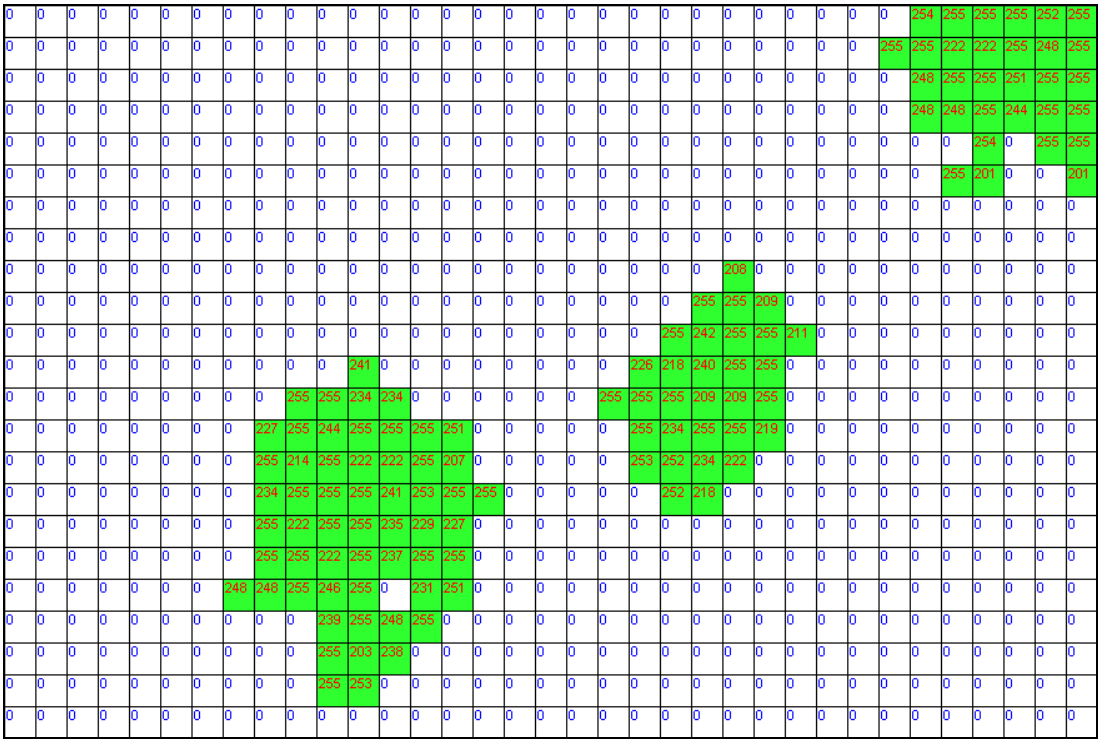

Fig. 3.3b Equivalent values of color for each pixel (p matrix)

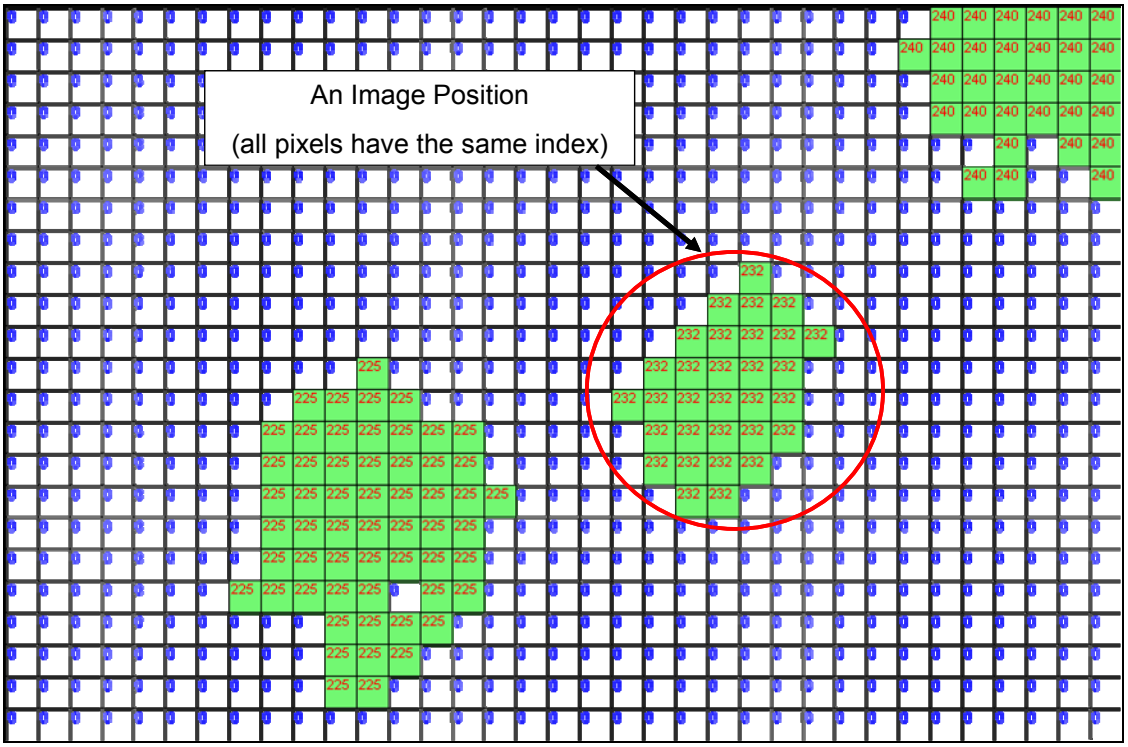

Fig.3.3c Indices of pixels on the radar picture (idx matrix)

An illustration is shown in Figures 3.3a, 3.3b, and 3.3c for the picture reading process. Sampling region is marked in Fig. 3.3a; values of elements of color matrix (p) are shown in Fig.

3.3b and elements of indices matrix (idx) are expressed in 3.3c for each pixels of the sampling region. From this, Image Position shall be extracted.

3.2 General Radar Tracking Principle Used in the Study

Radar pictures of the stations are transferred to and saved at the server with the interval of 1 minute. Then pictures of the two stations are imposed on each other to produce the composite radar pictures of Tokyo Bay. Basing on the quality of the pictures of the 2 stations and taking into account the region of concern, suitable boundaries have been set for pictures of each radar.

Because of the error in setting North direction (North Mark) at radar station, bearings of radar pictures are also deviated. Therefore, pictures of each station have to be slightly rotated around their radar station position a suitable angle before imposing.

To define the suitable deviating angles for each radar station respectively, it is necessary to fit the buoys positions on radar pictures to their absolute positions in latitude and longitude as extracted from navigation chart.

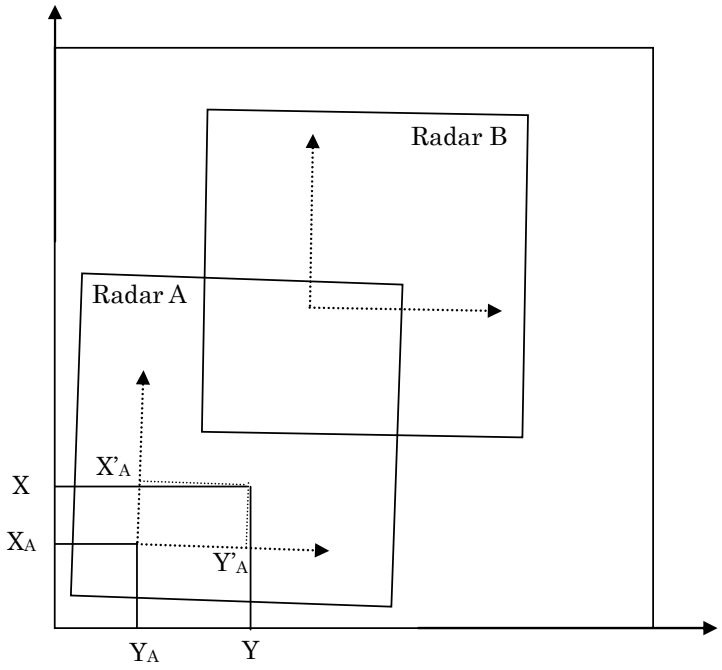

Fig. 3.4 Combine Two Radar Pictures

Formulae for the coordination shifting and rotating used in the study are:

$X = X_A + X'_A \times \text{Cos}(\theta_A) - Y'_A \times \text{Sin}(\theta_A)$ (3.1)

$Y = X_A + X'_A \times \text{Sin}(\theta_A) + Y'_A \times \text{Cos}(\theta_A)$ (3.2)

or

$X = X_B + X'_B \times \text{Cos}(\theta_B) - Y'_B \times \text{Sin}(\theta_B)$ (3.3)

$Y = X_B + X'_B \times \text{Sin}(\theta_B) + Y'_B \times \text{Cos}(\theta_B)$ (3.4)

Where θ_A, θ_B are rotating angles for radar A pictures and radar B pictures respectively.

In this study, $\theta_A = 0.5^0$ and $\theta_B = 0.5^0$ have been chosen and checked for fitting.

From the picture, a set of "Image Positions" can be extracted.

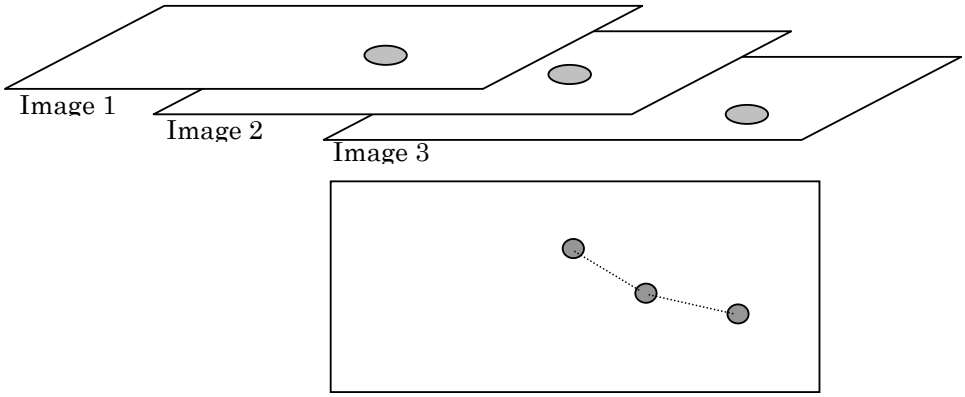

Fig. 3.5 Track a target from 3 consecutive radar pictures

Assuming that 3 Image Positions Sets of 3 sequential radar pictures have been extracted, 3 positions in close proximity on the 3 pictures respectively are put into a Relating-Function (defined in following section) to define their Relating-Value (an evaluation of relationship). Then, Relating-Value of these 3 positions is used to decide if these 3 positions are images of a target on the 3 pictures (Matched).

In the study, a simple model is used for modeling target motion, in which target speed, course over ground and image size are assumed to be constant.

From this model, position of the target on the following picture can be predicted.

Searching area is defined from predicted position and target matching is performed by applying Relating-Function.

After position for target has been found, the model of target motion (target's speed, course and size) will be updated.

The process is repeatedly applied to follow the target in concern.

3.3 Automatic Tracking of Target Motion on Radar Pictures

3.3.1 Relating-Function

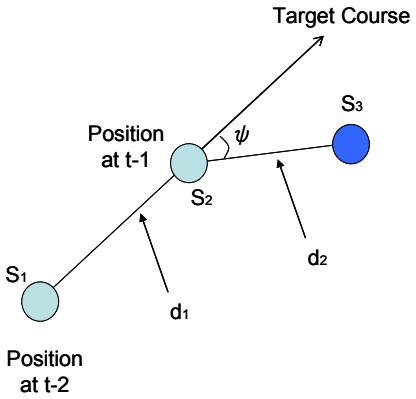

Fig.3.6 Three positions Relationship

To evaluate the possibility for 3 positions to be the track of a target, in this study, a "Relating-Value" is defined and used from here on.

Considering 3 positions extracted from 3 consecutive images at time t-2, t-1 and t respectively, a Relating-Function will be used to calculate these 3 positions Relating-Value as followings

$$R = d_{mdf} + f \times S_{mdf} - \cos(\psi)$$

$$d_2 \le d_1 \Rightarrow d_{mdf} = \frac{d_1}{d_2} - 1$$

$$d_2 > d_1 \Rightarrow d_{mdf} = \frac{d_2}{d_1} - 1 \qquad (3.5)$$

$$2 \times S_2 > S_1 + S_3 \Rightarrow S_{mdf} = \frac{2 \times S_2}{S_1 + S_3} - 1$$

$$2 \times S_2 \le S_1 + S_3 \Rightarrow S_{mdf} = \frac{S_1 + S_3}{2 \times S_2} - 1$$

Where:

- R: the Relating-Value to be calculated
- d_1, d_2: the distances between the positions (Fig. 3.6)
- d_{mdf}: modified distance ratio
- S_i: number of pixel in i^{th} position (i = 1, 2, 3)
- S_{mdf}: modified pixel ratio
- ψ: difference between relative bearing from positions at (t-2) to (t-1), and bearing from positions at (t-1) to t, respectively.

In Relating-Function (3.5), d_{mdf} values the distance relationship of the 3 positions. By this definition, d_{mdf} is always larger than or equal to 0 and equality just occurs when $d_1 = d_2$. If the difference between the 2 distances becomes larger, d_{mdf} is larger accordingly.

S_i (i = 1, 2, 3) represents the size of each position. Then, S_{mdf} evaluates relationship between 3 positions in size. Like d_{mdf},, value of S_{mdf} is always larger than or equals to zero for all cases. The equality is when the size of position at (t-1) is equal to half the sum of those at (t-2) and t.

From (3.5) and common knowledge of navigator, it can be seen that the most possible case for these 3 positions to be 3 consecutive images on radar screen of a target is when:

$d_1 = d_2$, $S_1 = S_2 = S_3$, $\psi = 0$ $\Rightarrow$ Relating-Value = -1.

The larger this value becomes, the less possible these 3 positions are consecutive images of a single target.

Factor f is added to express the difference in distribution of d_{mdf} and S_{mdf}. Value of f would be chosen from observation of radar target motion in Tokyo Bay.

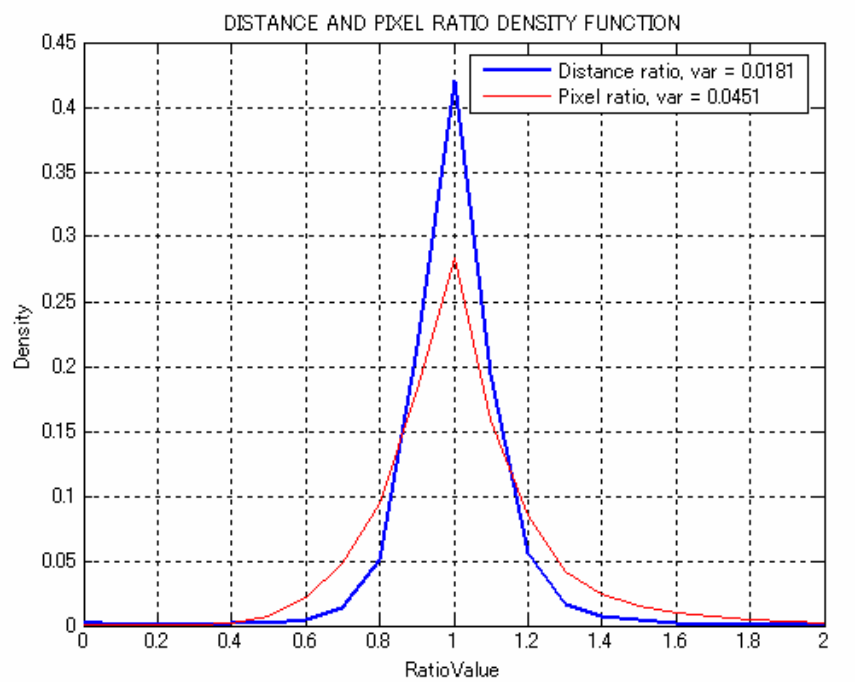

Fig. 3.7 Distance and Pixel Ratio density function

Distance-Ratio = d_1/d_2 (see Fig. 3.6)

Pixel-Ratio = $2xS_3 / (S_1+S_2)$

As seen clearly in Fig. 3.7, variance of the distance ratio is much less than that of pixel ratio. Therefore, value of f should be chosen to be less than 1. Experiments have shown that choice of this factor to be from 0.2 to 0.5 is acceptable.

Relating-Value for different choices of f has been calculated and shown in Fig. 3.8.

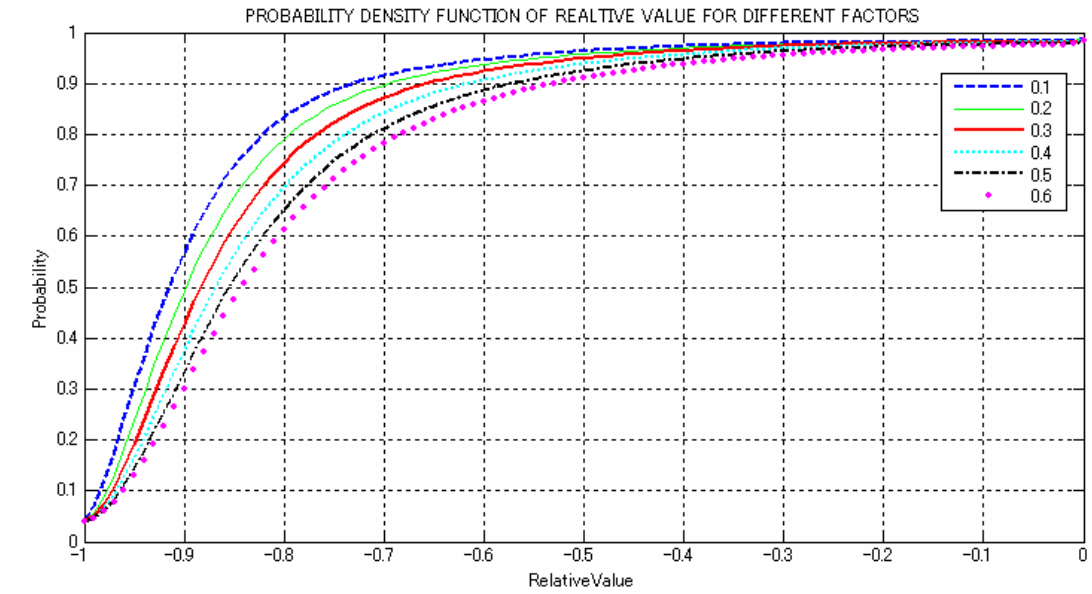

Fig. 3.8 Relating-Value distribution

In Fig.3.8, distribution functions of the Relating-Functions have been drawn for various f values from 0.1 to 0.6.

For larger value of f, Relating-Value becomes larger. Then, there may be cases when 3 noise positions of similar sizes can have Relating-Value as small as Relating-Value of 3 images of a real target.

On contrary, if f is too small, Relating-Value of 3 noises positions with similar distances between them, may also be smaller than that of 3 real images of a target. Thus, it is difficult to distinguish target from noise.

This can be illustrated in Fig. 3.9. For image positions (both noises and target images) distributed as those in this Fig., only the first case is a real target, the other 2 cases are just random distribution of noise. If f is too large, 3 positions forming the actual target (a) will have the similar Relating-Value with the 3 random noise positions in (b). On the other hand, if value of f is too small, case (a) and (b) will give similar value of Relating-Function. Those are motivations for the choice of a suitable value of f.

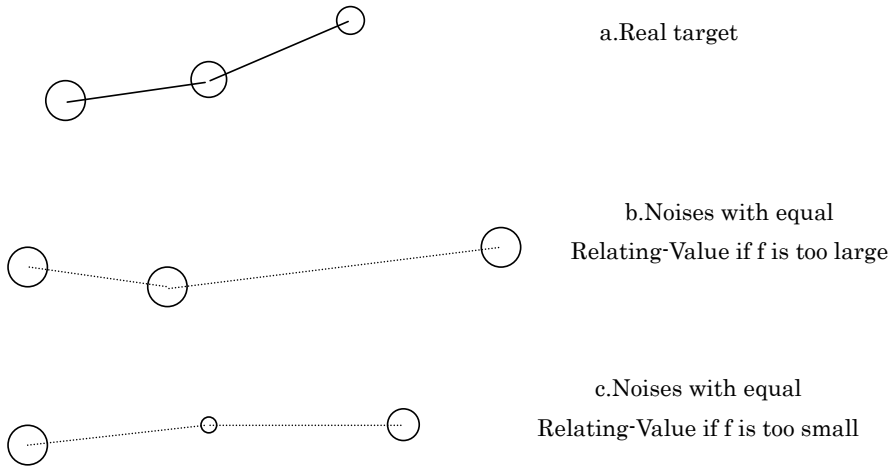

Fig. 3.9 Effect of f value to Relating-Value

In this study, value of f to be 0.3 has been used.

From Fig. 3.8, it can be seen that for this value, Relating-Value in more than 90% of observations is less than -0.60. This value is used as threshold value for following a moving target, i.e. if Relating-Value of previous position, current position of a target and a new position is less than -0.6 then this position can be taken as the new position of target.

To avoid taking noise as target, the Threshold value for taking 3 free image positions as a possible target (target acquisition) is -0.85. Another method for avoiding the risk is to use another form of Relating-Function as following:

$$R = d_{mdf} + f \times (S_{mdf1} + S_{mdf2})/2 - \cos(\psi)$$

$$S_3 \le S_1 \Rightarrow S_{mdf1} = \frac{S_1}{S_3} - 1$$

$$S_3 > S_1 \Rightarrow S_{mdf1} = \frac{S_3}{S_1} - 1 \qquad (3.6)$$

$$S_3 \le S_2 \Rightarrow S_{mdf1} = \frac{S_2}{S_3} - 1$$

$$S_3 > S_2 \Rightarrow S_{mdf1} = \frac{S_3}{S_2} - 1$$

The aim of form in 3.6 is to avoid cases as that in Fig. 3.10, where Relating-Function 3.5, if applied, will produce the same Relating-Value for real target (b) and noises (a). Formula 3.6 is, on the other hand, able to distinguish noise and real target because of the different form of modified pixel ratio (image size relation).

However, as targets have been acquired, formula 3.5 is more suitable, taking into consideration the possible low rate change of image size as targets are moving toward or away from radar stations.

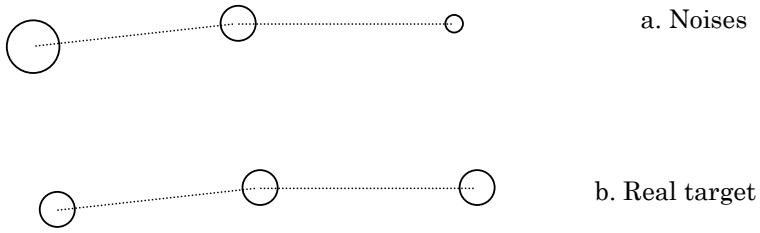

Fig. 3.10 Limitation of Relating-Function 3.5

3.3.2 Moving Target Acquisition

As mentioned earlier, target acquisition is the act of determining the existence of a target on radar screen. In automatic tracking, the acquisition is realized by considering the relationship (or the match) between 3 image positions on 3 consecutive radar pictures.

For a position (position 1) on the radar picture at time (t-2), the positions (position 2) that may combine with this position 1 to form a target can be found from radar picture at (t-1). Then, from position 1 and possible position 2 above, a third position (position 3) is searched from radar picture at time t.

The principle is clearly described in Fig. 3.11 and the flow chart in Fig. 3.12.

Taking into account the speed of ship moving in the bay, searching area for position 2 is the area inside a circle centered at position 1 and the radius is chosen to be 45 pixels (or equivalent to the speed of 15m/s).

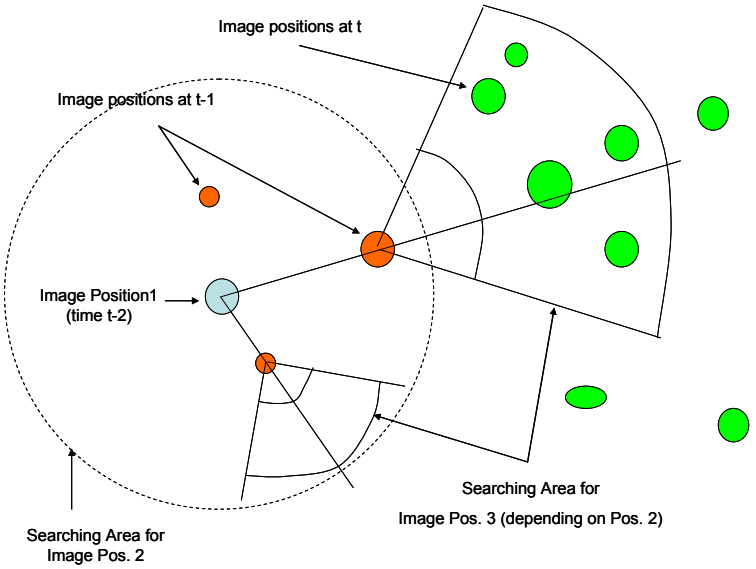

Fig. 3.11 Searching Area for Target Acquisition

Searching area for position 3 is defined from position 1 and position 2. It should be borne in mind that for each possible position 2, an individual searching area is found for position 3 and a set of candidate positions can be formed. The shape of searching area of position 3 is the same with that defined for target following (section 3.3.3).

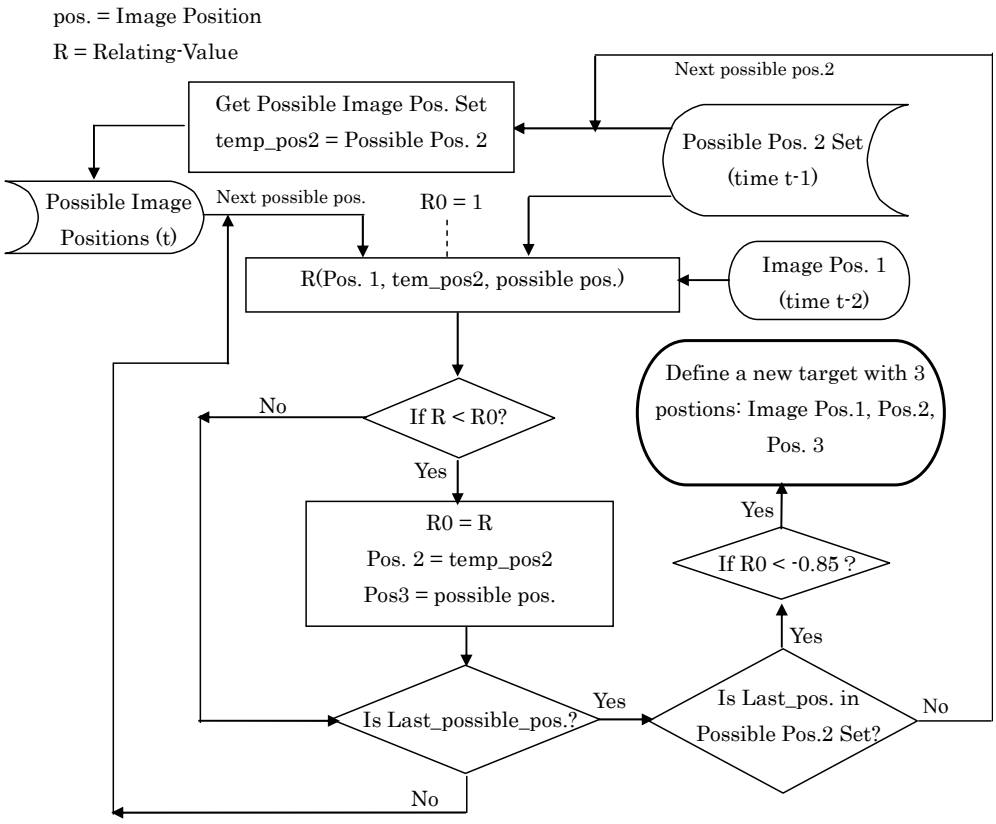

Fig. 3.12 Moving target acquisition flow chart

To evaluate the "Match" of 3 positions, Relating-Function is used. Flow chart in diagram 3.12 gives details of the target acquisition process. In 3.12, the "Possible Position 2 Set" consists of image positions on radar picture at (t-2) and lying inside the searching area for position 2. Possible Image Position at (t) consists of those on radar picture at (t) and lying inside the searching area defined from position 1 and position 2. It should be noticed that not every image position is image of a ship (moving target). Therefore, the acquisition is not always successful.

Threshold value for target acquisition is -0.85, which has the meaning that: If Relating-Value of "the 3 best matched image positions" is less than -0.85, the 3 image positions are three consecutive images of a moving target. Otherwise, the 3 images positions have No-Relation.

3.3.3 Moving Target Following

Procedure to search for the following position of a moving target is shown in Fig. 3.13. In this procedure, using target's previous position and current position, its new position is specified from the new positions set (consisting of image positions from the newest radar picture).

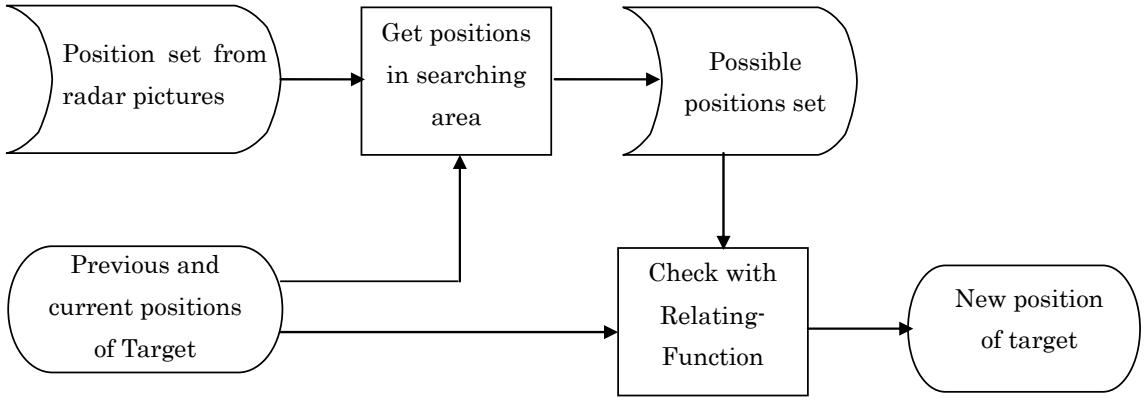

Fig. 3.13 Flow chart of moving target following

The principle is illustrated more details in Fig. 3.14.

In Fig. 3.14, previous and current positions of a moving target (target 1) are imposed on radar picture at time t. Then, a searching area is defined with the bold boundary. In this study, searching area is determined to be the area limited by 2 circles centered at current position of the target and 2 bearings crossing at this position.

Considering the normal speed of ships and possible speed changes (as target speed may change but just slowly), radiuses (r1, r2) of limiting circles can be chosen as followings:

$r1 = 0.5 \times d$

$r2 = 2.0 \times d$

where d is the distance between target previous and current positions.

Similarly, taking into consideration normal change in target course in 1 minute, limiting angle is set:

$\theta = 60^0$

These choices of values for limiting angle are, however, rather randomly and do not affect the tracking results very much.

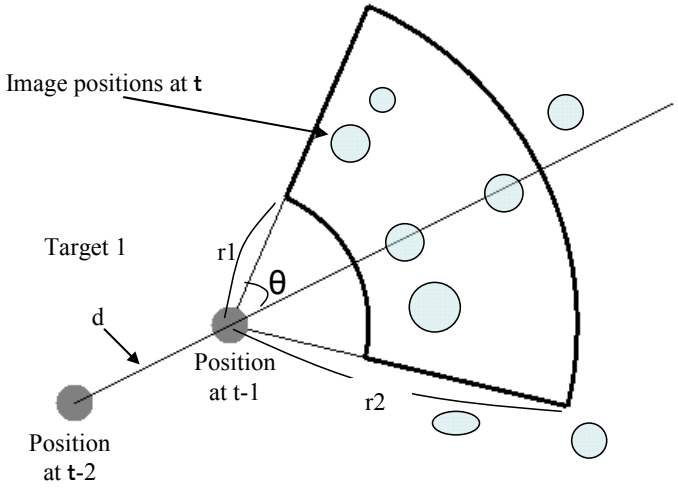

Fig.3.14 Moving target following principle

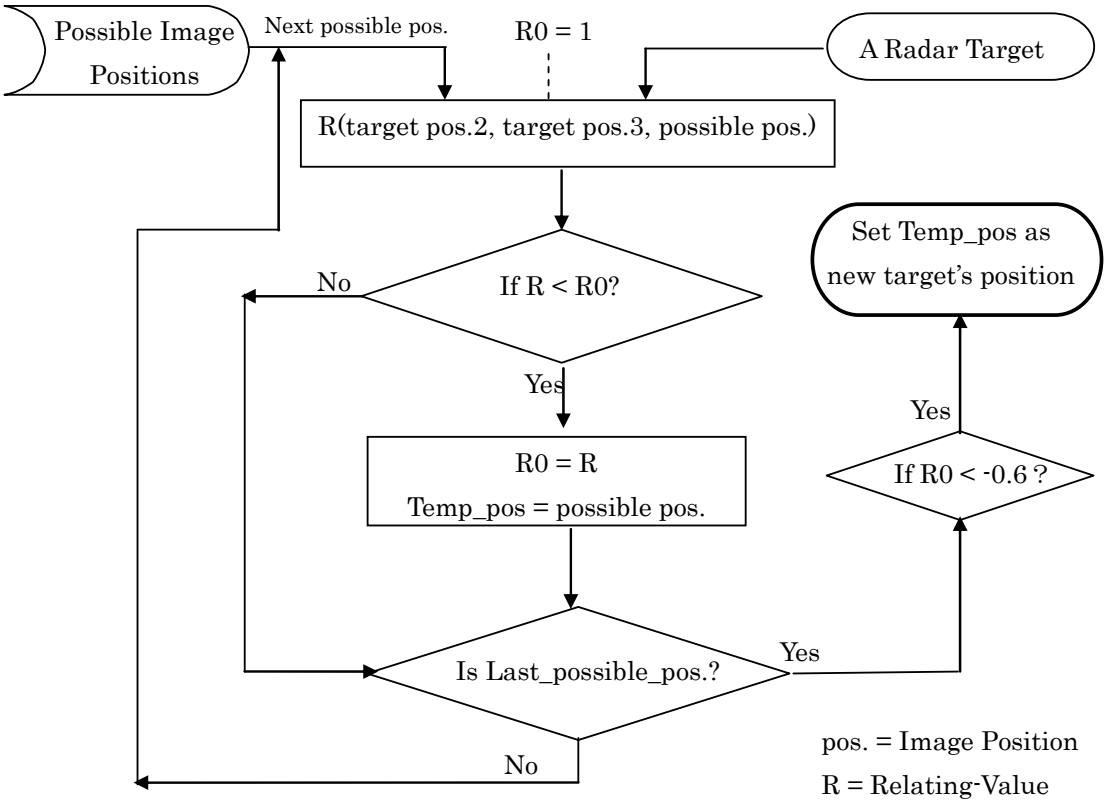

Fig. 3.15 Search for following position from possible position set (Matching)

Target following procedure is summarized in 3 following steps:

- Step 1: Define the possible position set for that target. The possible positions are those lying in the searched area as shown in Fig.3.14.

- Step 2: Use formula (3.5) with target's positions at t-2, t-1 and every one position in the set found in step 1 to determine the most possible position (the position with smallest Relating-Value).

- Step 3: If Relating-Value is less than the defined threshold value, this position is taken as target new position.

In some cases, due to noise, overlapping or reflection characteristic of the target, position of target in an image can not be found. We refer to this case as a lost target.

Tracking of a lost target can be done in a similar way as the above procedure and is illustrated in Fig. 3.16.

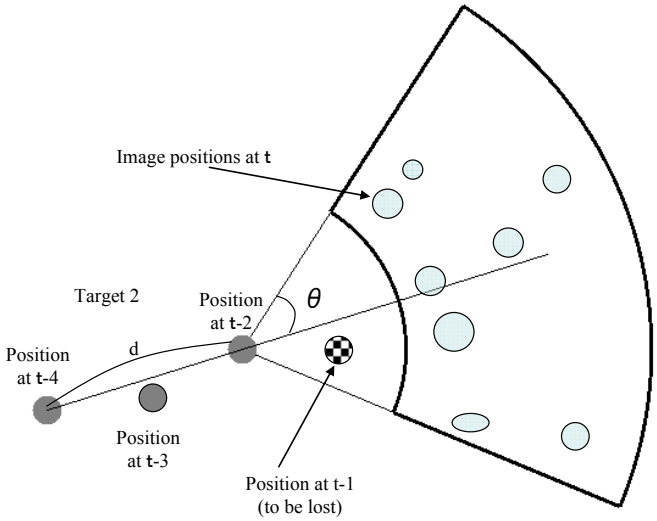

Fig.3.16 Track a Lost Target

Suppose position of target at t-1 was not found, its position at t is searched from the positions set, using its position at (t-4) and position at (t-2).

First, the search area is defined from bearing and distance of these 2 positions. Positions inside this area are extracted.

Then, Relating-Function is used to check Relating-Value of target's two positions mentioned above with every position in the set to find the most possible position and decide if this one can be taken as new position of target.

Matching procedure is exactly the same with that in flow chart in Fig. 3.15, with the notice that target's positions at (t-4) and at (t-2) are used in Relating-Function together with candidate image position from possible position set.

3.3.4 Possible Overlapping Couple Tracking

Due to the limitation of picture resolution and distance from radar station to targets, there are cases where images of two or more targets overlap or may overlap each others. In this study, just the case of two targets overlapping each other was taken into consideration. These two targets are hereafter referred to as Possible Overlapping Couple.

The problem of 3 or more targets overlapping is rather rare and very complicated to solve, therefore not to be included.

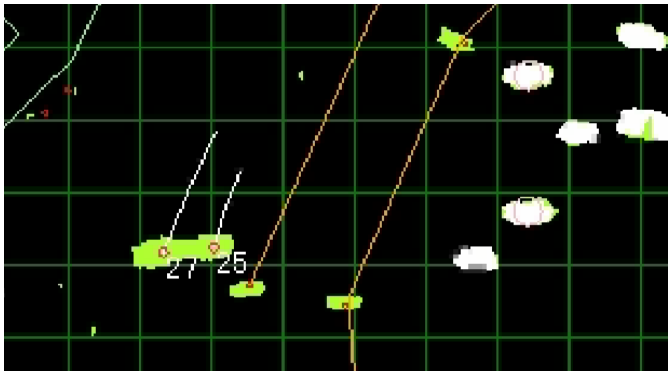

Fig. 3.17 Target Overlapping Situation

A case of targets overlapping is shown in Fig. 3.17, where 2 targets with ID 25 and 27 overlap each other to form a common larger position.

In this study, an algorithm is suggested for simple cases of overlapping. This can be described in diagram in Fig. 3.18.

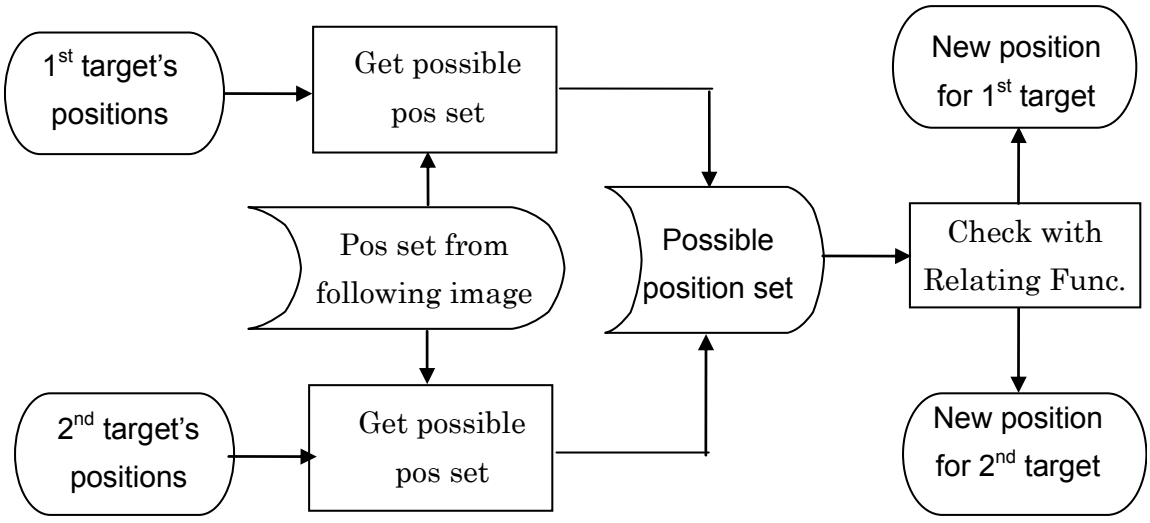

Fig. 3.18 Following Possible Overlapping Couples Flow Chart

Principle of the method is to take into consideration candidate positions for both targets simultaneously. If the images of 2 targets actually overlap to form a larger image position, then,

this position is divided among the 2 targets. In this case, image position is divided into 2 parts by a line perpendicular to the line connecting the Dead-Reckoning positions of 2 targets at the time when the new radar picture is saved.

For position matching, Relating-Function is used for the positions of each target with its equivalent part of the image position to decide if it is suitable to take this part to be new position of the target. For this purpose, in the Relating-Function, image size relation should be omitted as position size is no longer reliable.

$$R = d_{mdf} - \cos(\psi) \qquad (3.7)$$

Procedure for solving this case is as followings:

- Step1: Define the possible positions set for each target in the couple. The searching area and possible positions are defined the same way as descried in 3.3.3 for moving target.

- Step 2: Consider the combined set to confirm the overlapping case.

It is considered the case when there are no suitable positions for each target and/or two targets have the same most suitable position. Here, the Relating-Function with f = 0 is used. Then, the case is affirmed if the common position is larger than current positions of both targets.

- Step 3: If the overlapping case is confirmed, the overlapping position will be divided into 2 positions by a line perpendicular to the relative bearing to two dead reckoning positions of the two targets (Fig.3.19).

- Step 4: Apply the Relating-Function for each position in the combined position set to determine the most possible position for each target.

- Step 5: Decide if this position can be taken as position of the target.

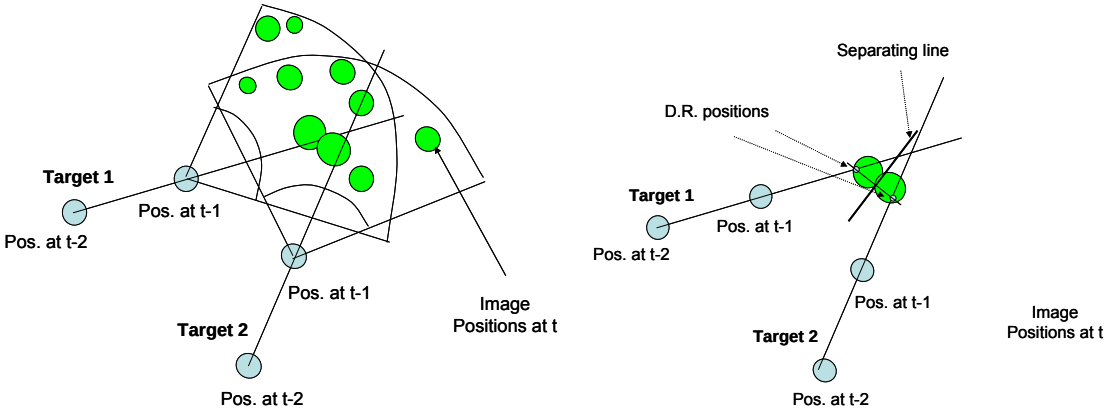

Fig. 3.19 Overlap Couples Following Illustration

3.3.5 Non-Moving Target Acquisition

Very slowly moving or non-moving targets (ships at anchor, buoys, etc.) can be tracked in a rather simple way in this study.

First, non-moving target's current position is placed on the new image. All the positions of the new image that overlaps with it are take into consideration.

The new position of this target is the one that most deeply overlap with its current position.

3.3.6. Overall Target Tracking Procedure

To achieve the best possible results, tracking program should follow a certain procedure as listed below:

3.3.6.1 Start Tracking

- Step1: Read 3 first pictures into 3 image position sets respectively.
- Step 2: Define the non-moving targets from image positions sets (3.3.5).
- Step 3: Define moving targets (3.3.4).
- Step 4: Classify moving targets into normal moving targets set and set of possible overlapping couples. The moving targets are coupled if the distance between them is decreasing below a certain value.

In this study, when the distance between 2 targets falls below 30 (pixels), the two targets are considered a possible overlapping couple.

- Step 5: Shift the position sets backward. In this step, the image positions, which are not yet determined to be the position of any target is saved for later defining the existence of a moving target with it to be one of the position when following radar pictures are available.

3.3.6.2 Continue Tracking

- Step 1: Read a new radar picture into the newest positions set.
- Step 2: Determine image positions of existing non-moving targets.
- Step 3: Define new non-moving targets.
- Step 4: Determine positions of existing moving targets not in possible overlapping couples.
- Step 5: Solve the possible overlapping couples.
- Step 6: Define new moving targets.
- Step 7: Classify moving targets into normal moving targets set and possible overlapping couples set.
- Step 8: Shift the position sets backward.

3.4 Automatic Tracking Results

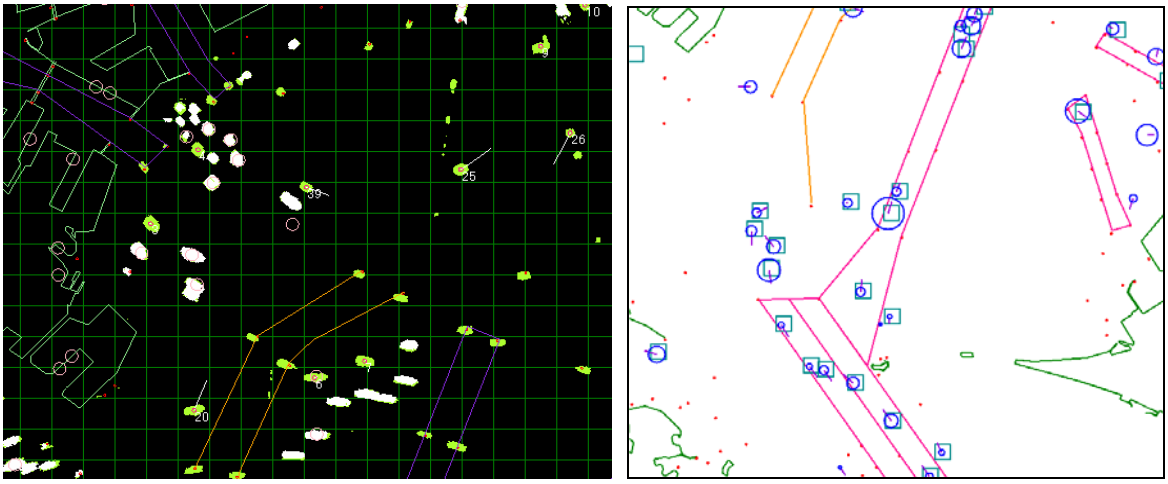

– □: manually tracked targets
- ○ with velocity vector: targets automatically tracked by this approach.

Fig. 3.20 Tracking and Result Checking Screens

Tracking approach mentioned above has been applied to process radar pictures of Tokyo Bay for several days in 2006. To ensure the accuracy, tracking process was continuously checked using automatic tracking interface. Checking screen was shown in the left part of Fig. 3.20, where moving targets were marked with red circle and their track was shown by white line, non-moving targets pixels were changed into white for classification.

In Fig. 3.21, number of ship tracked against time (in minute) of this automatic tracking approach was compared with the results of previous approach (used in the works of Okano et al, Liu et al). The bold line in blue represents results of this approach while thin, red one is that of previous approach.

In comparison with previous approach, the number of targets tracked automatically has been increased drastically, and, as shown in Fig.3.20, many targets have been tracked automatically before they are recognized by manual observation.

Apart from that, there are cases where it is difficult to affirm the existence of a moving target, especially for those with small and weak radar reflection. The auto-tracking program can detect these at the price of possibility of taking noise as targets.

The other problem that needs further studying is target swapping. It is the case where a target is lost for several minutes. When it is acquired again on the radar pictures, it is considered a new target, without any relation with the lost one. AIS data, if used together with radar images for tracking, can solve the problem. The MMSI of ship, received from AIS, can be used for two target matching.

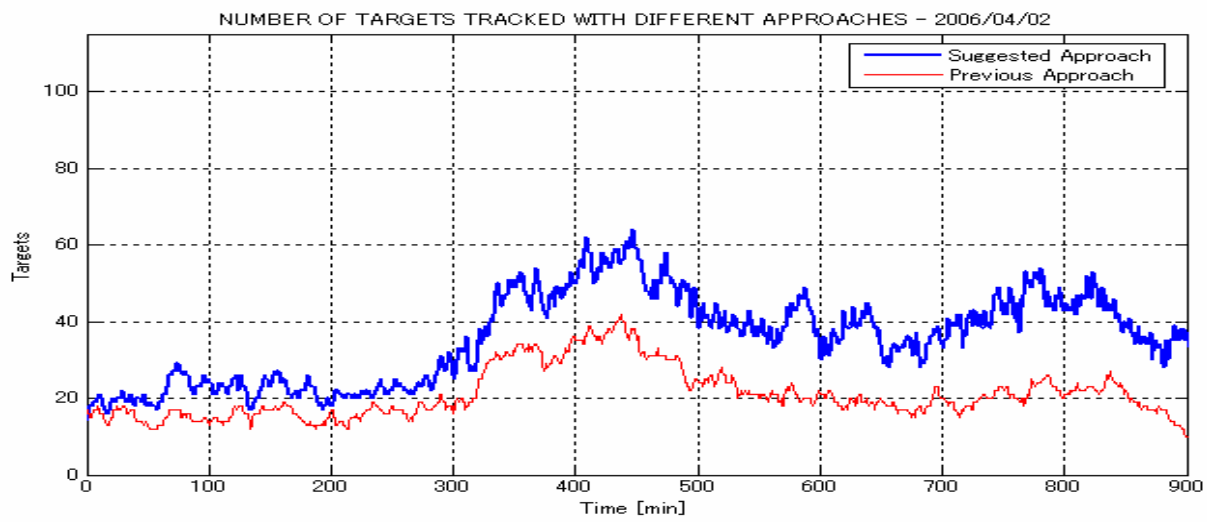

Fig. 3.21a Automatic Tracking Results

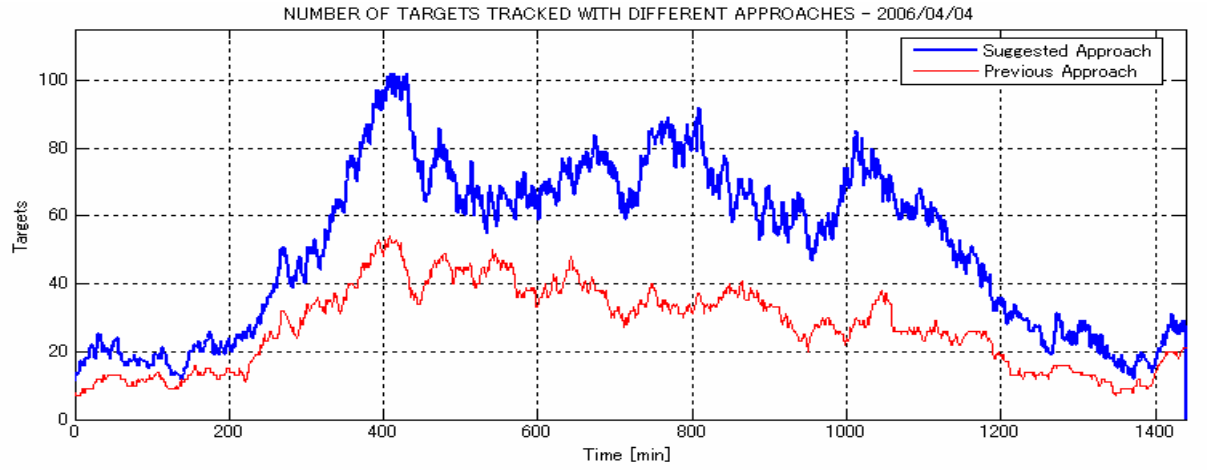

Fig. 3.21b Automatic Tracking Results

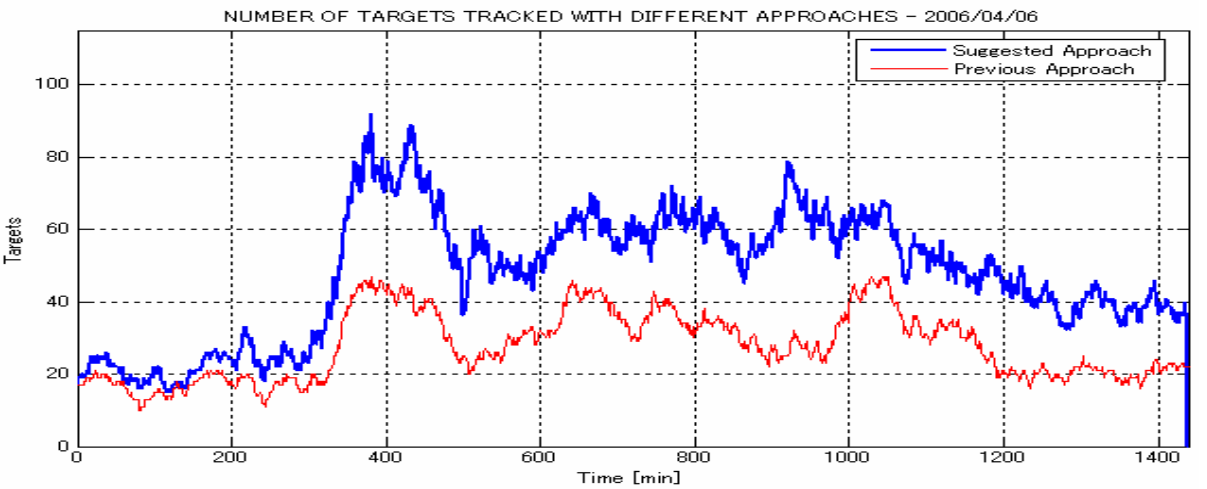

Fig. 3.21c Automatic Tracking Results

3.5 Conclusion

In this chapter, an approach for automatic tracking of targets motion from the radar pictures. Using the approach, searching area is defined basing on common knowledge of ship's movements, including the normal speed and course changing in the time interval between radar pictures.

Then, for matching, the Relating-Function is used as a fuzzy reasoning. This function takes into account the heading difference, size ratio and distance ratio of image positions in concern. From observation, threshold values of the Relating-Function have been decided as followings:

- For target acquisition: -0.85
- For target following: -0.6

In order to track targets in overlapping, a simple algorithm is used, in which the overlapping position is shared between 2 targets if overlapping case has been confirmed.

Chapter 4. Automatic Tracking of Targets on Radar Pictures with Supplementing AIS Data

4.1 AIS Data Format and Data Decoding

SOLAS Regulation V/19 requires that: All ships of 300 gross tonnage and upwards engaged in international voyages and passenger ships irrespective of size shall be fitted with Automatic Identification System (AIS) as follows:

- Ships constructed on or after 1 July 2002;
- Ships engaged on international voyages constructed before 1 July 2002;

+ In the case of passenger ships, not later than 1 July 2003;

+ In the case of tankers, not later than the first survey for safety equipment after 1 July 2003;

+ In the case of ships, other than passenger ships and tankers, of 50,000 gross tonnage and upward, not later than 1 July 2004;

+ In the case of ships, other than passenger ships and tankers, of 300 gross tonnage and upwards but less than 50,000 gross tonnage, not later than the first survey for safety equipment after 1 July 2004 or by 31 December 2004, whichever occurs earlier;

+ Ships not engaged on international voyages constructed before 1 July 2002, not later than 1 July 2008.

For ships not included in the above regulation, the International Electro-technical Commission has completed the Class B certification standard, in which compatibility is ensured for the most importance information at, however, lower update frequency.

As already mentioned in 2.2.4, information provided by AIS can be classified into dynamic and static ones. Dynamic information, mostly transmitted in Position Message (Message 1, 2, 3, or Message 18, 19 of Class B AIS) can be used as supplement for automatic radar tracking.

In exchanging information between marine electric and electronic equipments, NMEA (National Marine Electronics Association) 0183 has been adopted as the standard protocol. NMEA output is EIA-422A but for most purposes, it can be considered RS-232 compatible. Typically, a standard AIS message is in the form of following NMEA sentences:

!AIVDM,1,1,,A,14eG;o@034o8sd<L9i:a;WF>062D,0*7D (4.1)

Where, in order:

!AIVDM	The NMEA message type
1	Number of sentences (some messages need more than one)
1	Sentence number
	The blank is the sequential Message ID

A	The AIS Channel (A or B)
14eG…	The encoded AIS Data
0*	End of data
7D	NMEA Checksum

Unlike normal ASCII (8 bits), in the NMEA encoding for AIS, each ASCII character corresponds to 6 binary bits, using the following mapping scheme:

Table 4.1 NMEA's ASCII characters and correspondent binary representations

ASCII data	***Binary data***		***ASCII data***	***Binary data***		***ASCII data***	***Binary data***
0	000000		E	010101		c	101011
1	000001		F	010110		d	101100
2	000010		G	010111		e	101101
3	000011		H	011000		f	101110
4	000100		I	011001		g	101111
5	000101		J	011010		h	110000
6	000110		K	011011		i	110001
7	000111		L	011100		j	110010
8	001000		M	011101		k	110011
9	001001		N	011110		l	110100
:	001010		P	100000		m	110101
;	001011		Q	100001		n	110110
<	001100		R	100010		o	110111
=	001101		S	100011		p	111000
>	001110		T	100100		q	111001
?	001111		U	100101		r	111010
@	010000		V	100110		s	111011
A	010001		W	100111		t	111100
B	010010		’	101000		u	111101
C	010011		a	101001		v	111110
D	010100		b	101010			

Using the converting scheme, encoded AIS data is transformed into string of binary data. An illustration is given here for encoded AIS data in (4.1):

000001 000100 101101 010111 011100 001010 010000 000000 000000 000000 110111 001000 110111 100001 101000 011100 011101 110010 011111 101011 110000 110101 010111 010000 000000 001000 011000 011011 (4.2)

From the data string, AIS data can be retrieved, using the un-packaging map below, with Position Report (Message 1, 2, 3), taken as example:

Table 4.2 AIS Class A position report message

Parameter	***Number of bits***	***Description***
Message ID	6	Identifier for this message
Repeat Indicator	2	Indicate how many times msg has been repeated
User ID	30	MMSI Number
Navigation Status	4	0 = underway using engine 1 = at anchor
Rate of turn	8	0...± 126 (turning right/left)
SOG	10	Speed over ground in 0.1 knot step
Position accuracy	1	1 = high; 0 = low
Longitude	28	Longitude in 1/10000 min (negative for West)
Latitude	27	Latitude in 1/10000 min (negative for South)
COG	12	Course over ground in 1/10 degrees
True Heading	9	Degree (0-359)
Time stamp	6	UTC second when the report was generated
Reserved for regional application	4	
Spare	1	Not used. Should be set to zero
RAIM_Flag	1	Receiver Autonomous Integrity Monitoring flag of Electronic Position Fixing Device
Communication State	19	
Total number of bits	**168**	

Other type of messages, including static information format is not used in the research and hence not mentioned here. A program for decoding AIS data can be found in the Annex 2.

4.2 AIS-Radar Target

AIS information, though very accurate, can not replace the functions of radar due to some reasons:

- Firstly, many vessels are not yet equipped with AIS and the existence of them can not be defined.

- Secondly, if there is an error in AIS dynamic information, this error is usually very large and difficult to be noticed.

- Thirdly, there are cases where the update rate of AIS data is low, especially when there is no or just small change in speed and course.

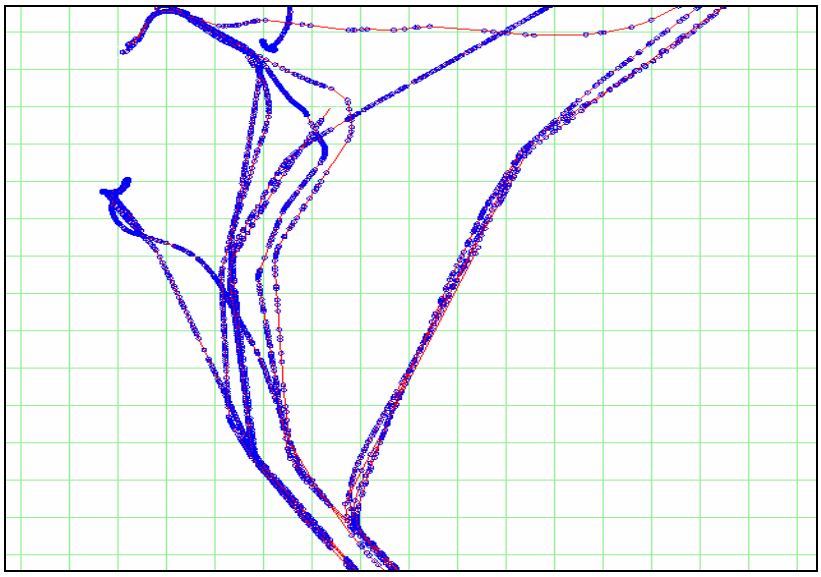

Fig. 4.1 AIS tracks in Tokyo Bay

An illustration is shown in Fig. 4.1, where the tracks of some AIS targets tracks are drawn by connecting positions received from their position messages whenever targets' positions are updated. On some part of the track, positions are distributed sparsely, representing the low update rate of AIS data.

Observing the AIS data of targets moving in Tokyo Bay, situations, in which ship's AIS information was not updated for up to 6 minutes, have been witnessed. For such cases and other reasons mentioned above, observation by radar is indispensable.

Once available, AIS targets from AIS database are matched with targets tracked from radar pictures to define AIS-Radar targets. In this paper, the term AIS-Radar Target is used to refer to the radar targets which have been confirmed to be the image on radar screen of ship equipped with AIS, for which, AIS data is available in AIS database.

Then, AIS data can be used to facilitate the respective target's following.

Matching algorithm is based on the estimated AIS position at time radar picture is saved, position tracked from radar picture, speed and course over ground from AIS message and those calculated from target's positions on radar pictures.

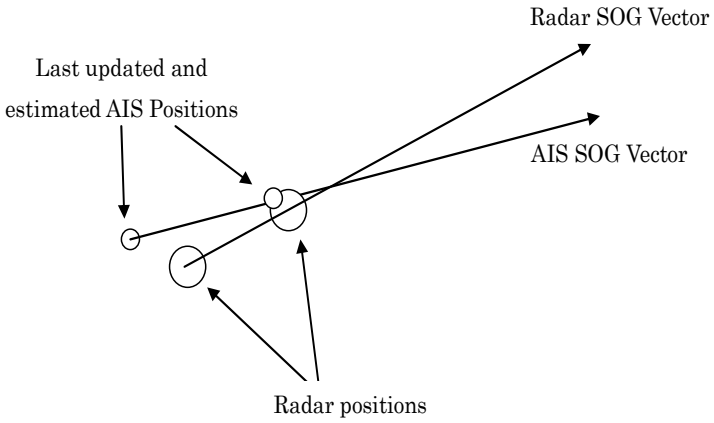

Fig. 4.2 Matching Radar and AIS

The following formula is used in this study for AIS, radar matching.

$$R\_M = \frac{d}{D} + \frac{\Delta v}{\Delta V} + \frac{\Delta \omega}{\Delta \psi} \qquad (4.3)$$

where

d: distance between radar position and estimated AIS position

$\Delta v = |SOG_{AIS} - SOG_{Radar}|$: Speed difference

$\Delta \omega = |COG_{AIS} - COG_{Radar}|$: Course difference

D: Limit distance

ΔV: Limit speed difference

$\Delta \psi$: Limit course difference

In (4.3), limiting values are chosen to reflect the errors of radar target movement on the screen, error in estimated AIS position, and errors in speed and course over ground calculated from radar positions. For radar pictures of Tokyo Bay, the limiting values are chosen to be:

D = 10 (pxls)

ΔV = 5 (pxls/min)

$\Delta \psi$ = 20 (deg)

Using Relating Function for radar and AIS targets (4.3), the matching procedure can be realized, using the flow chart shown in Fig. 4.3.

As shown in the diagram, for a radar target, formula (4.3) is used to scan through the AIS database to get the AIS target that most fits the radar target. Then, if Relating-Value is less than a

threshold (here chosen to be 1.5), the AIS data is considered to be AIS data of the target tracked from radar screen.

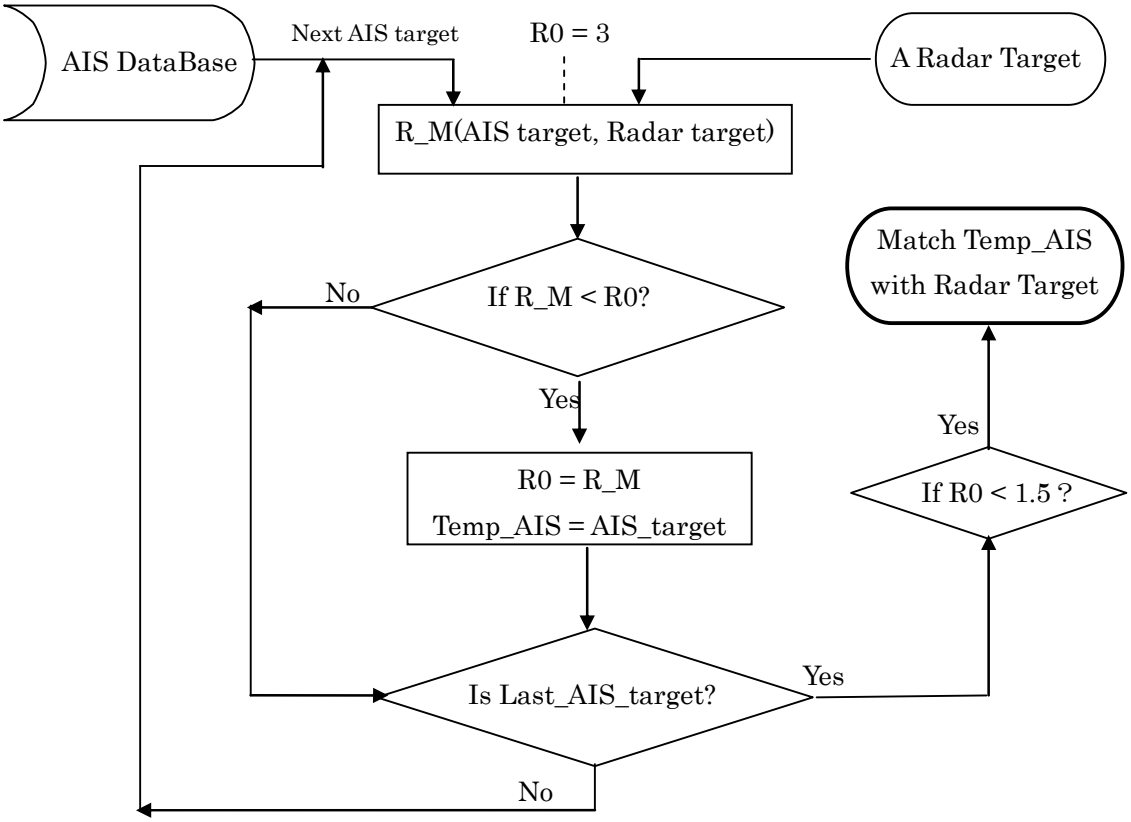

Fig. 4.3 Matching AIS with Radar Target Flow Chat

4.3 Modified Relating-Function for Following AIS-Radar Target

Suppose that a radar target has been matched with AIS data, then, AIS data can be applied to facilitate the automatic tracking. Illustrated in Fig. 4.4 is an AIS-Radar target with current position S2 (position at t-1) and previous position S1 (position at t-2). Its following position must be determined from the set of image positions extracted from radar picture at t. In this case, Course Over Ground (COG) and Speed Over Ground (SOG) provided by AIS are used as supplementing information.

To take the advantage of AIS data, Relating-Function (in formula 3.5) is slightly modified to the form:

$$R = d_{mdf} + f \times S_{mdf} - \cos(\psi)$$

$$d_2 \le d \Rightarrow d_{mdf} = \frac{d}{d_2} - 1 \qquad (4.4)$$

$$d_2 > d \Rightarrow d_{mdf} = \frac{d_2}{d} - 1$$

Where:

d = AIS_Sog[pxls/min] x 1[min]: the distance covered by AIS speed over ground in 1 minute.

Ψ: the difference between AIS_COG and direction from target's current position to the position that needs checking.

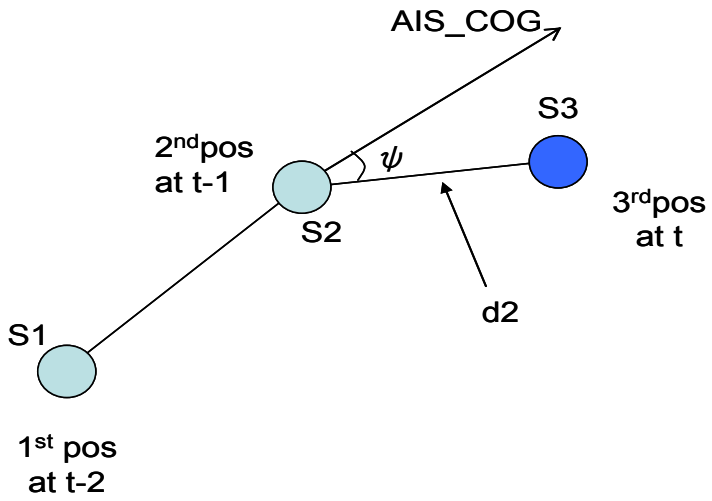

Fig. 4.4 AIS-Radar Target and an image position Relationship

In (4.4), d_{mdf}, which is not less than 0, represents the relation ship between the distance from target's current position to position in concern and AIS_SOG. S_{mdf} is the same as defined in 3.5; and Ψ is the bearing relation.

The best reliable case for taking a position as new position of AIS-Radar target is when this new position has the same size with target's positions, lies on the direction of COG from target's current position at a distance that equals to the distance run by target with SOG in 1 minute. In this case, R = -1.

The larger R becomes, the less possible the image position is the new position of the AIS-Radar target.

4.4 Observation Result

To prove the strong point of the modified Relating Function (4.4) over that in (3.5), observation has been conducted in Tokyo Bay for actual ships equipped with AIS and their equivalent radar images on radar screen. Distribution of course difference and distance ratio are shown in Fig. 4.5. For both course difference and distance ratio, distributions converge nicely.

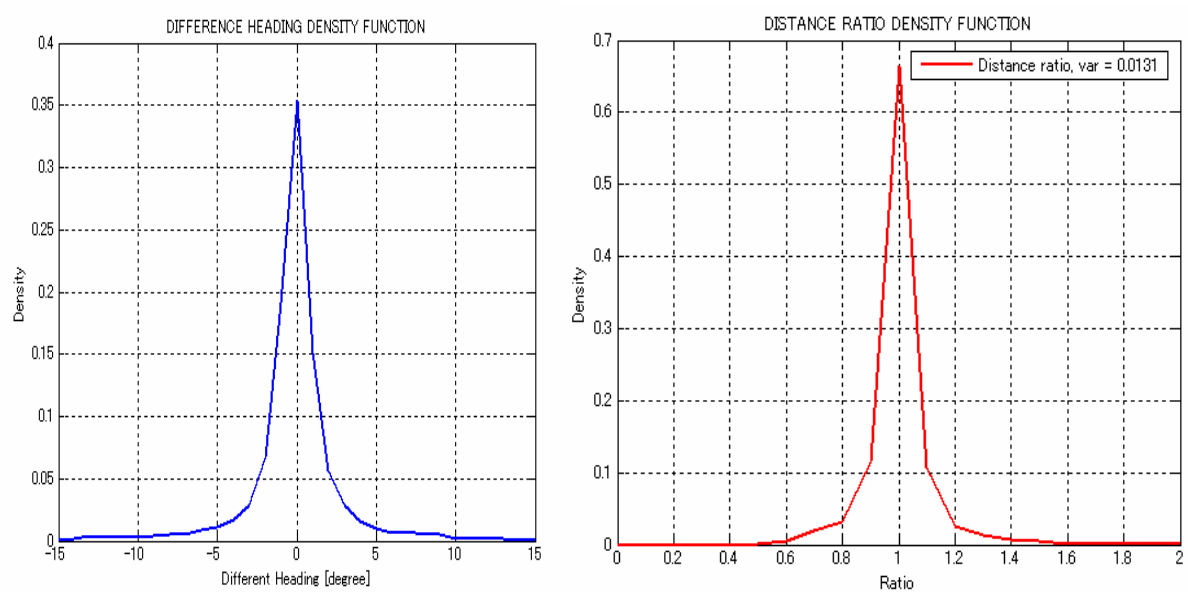

Fig. 4.5 Distribution function of Course Difference and Distance Ratio

Next, Relating-Value is calculated from the observation results, using different value of f factor. In comparison with probability density function in Fig. 3.8, convergence of Relating-Value is also much better here. The improvement makes it possible to better distinguish target position from noise on radar pictures.

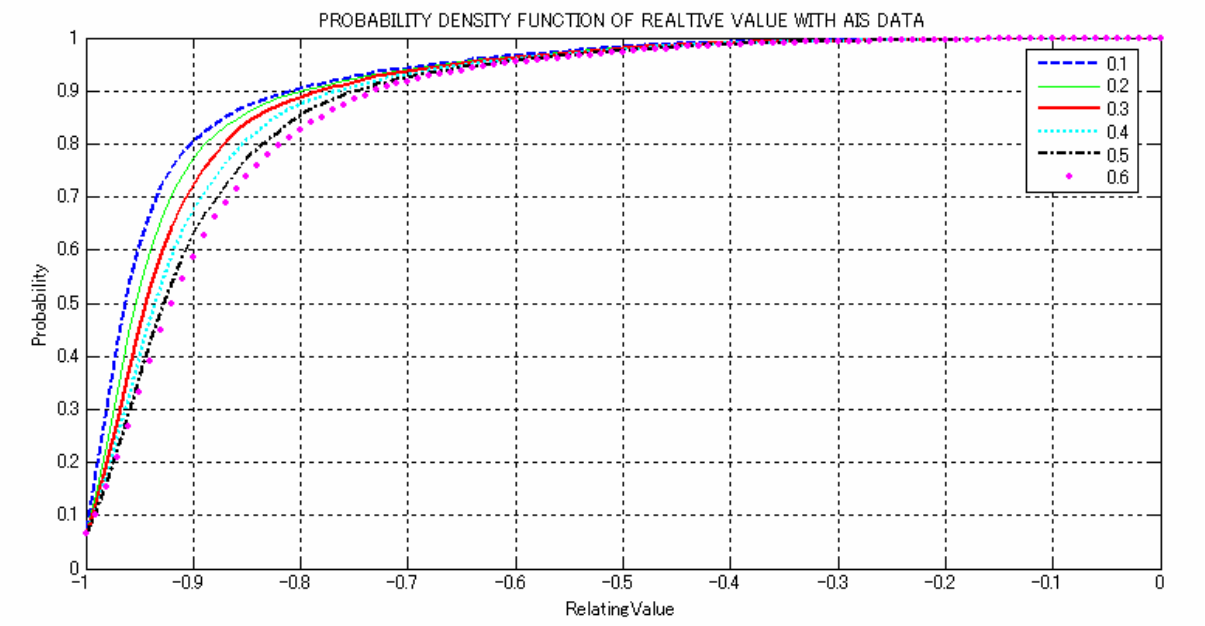

Fig. 4.6 Distribution Function of Relating-Value when AIS data is used

In this study, value of f to be 0.3 is chosen. Threshold value is chosen to be -0.8 for following a target.

4.5 Following AIS-Radar Target

4.5.1 Moving AIS-Radar Target Following

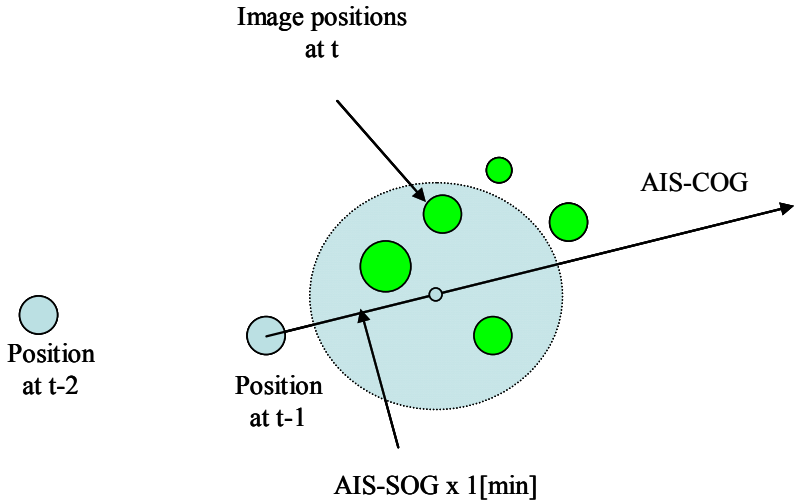

Fig. 4.7 Track AIS-Radar Target

In this target following approach, searching area is defined by a circle centered at a position lying on AIS_COG and at a distance equal to the distance run by target in 1 minutes from the current position.

Then, a matching algorithm similar to that used in section (3.3.4) is used to determine the target new position from the possible image position set. Differences of this algorithm, compared to the one mentioned above, are:

- A modified Relating-Function is used, that takes target's current position, possible position, AIS COG and SOG as parameters.

- Threshold value for setting the most possible position to be new position of the AIS-Radar target is -0.8.

The detailed flow chart of tracking (following) process is shown in Fig. 4.8.

It is clear from the flow chart that a set of possible image positions have be formed, consisting image positions lying inside the searching area. Then, Relating-Function is used for matching the AIS-Radar target with the candidate image positions. Repeating this process, the best matched image position is extracted from the possible position set. This best matched Relating-Value is compared to threshold value (-0.8) for decision to determine if the position is suitable to be taken as AIS-Radar target's following position.

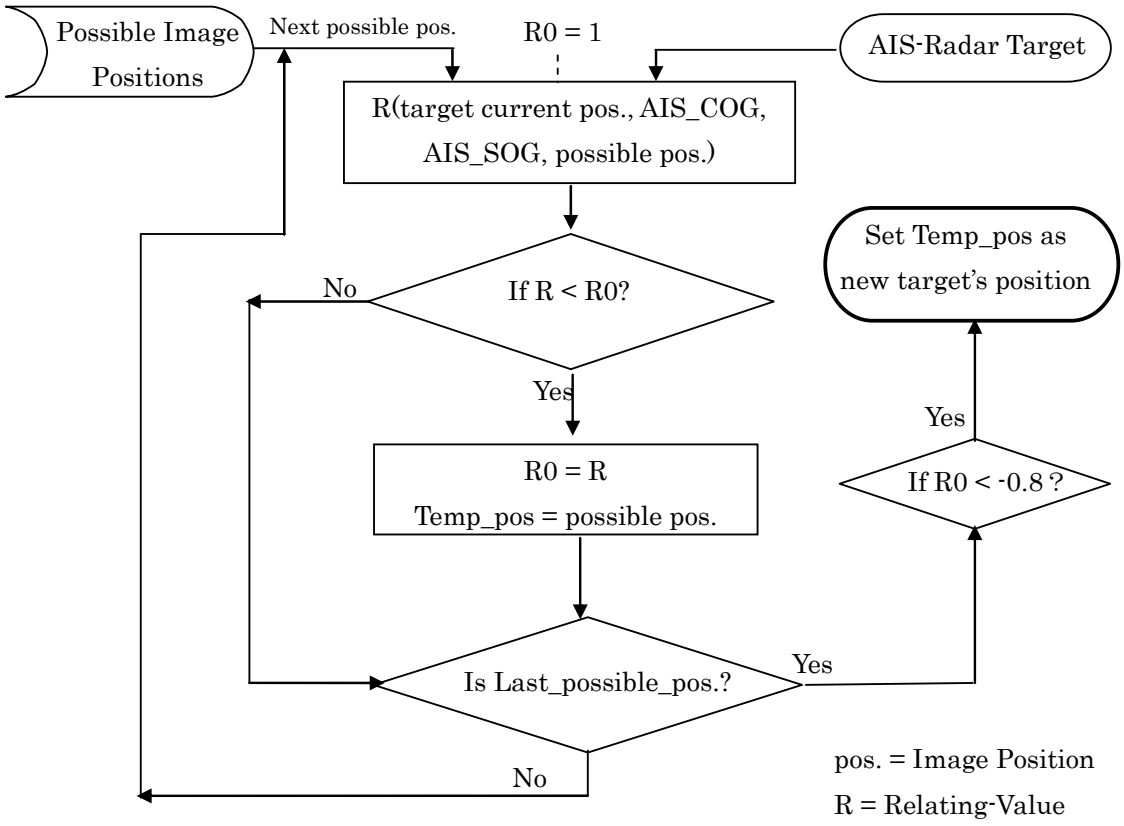

Fig. 4.8 Search for new position from possible position set

4.5.2 AIS-Radar Target in Overlapping Case

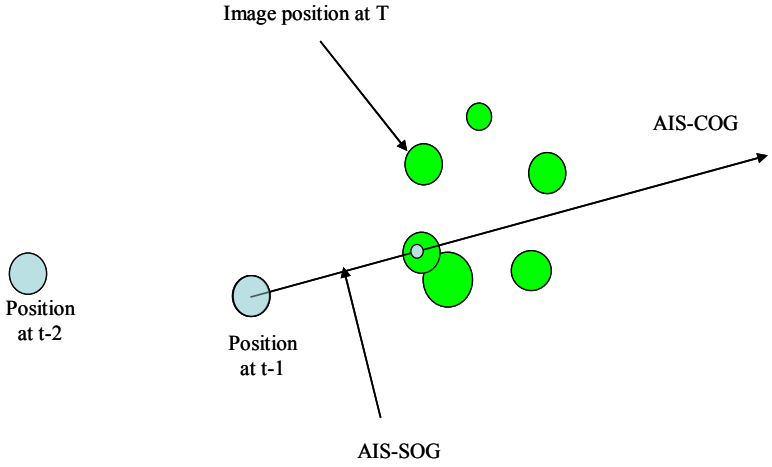

Fig. 4.9 Search for following target position in overlapping case

For an AIS-Radar target in overlap, current target's position is shifted along the AIS_COG a distance equal to that covered by AIS_SOG in 1 minute. Then, the possible overlapping position is considered to be the position that most deeply overlaps with this shifted position.

With the assumption that the shape of target's image on radar screen does not change, current image position of target can be shifted to best fit the outline of the combine position to determine the position of the target in the combined position.

4.6 AIS-Radar Target Tracking Results

4.6.1 Tracking Results

The approach is applied for several days of AIS and radar data in 2006. Number of ships tracked by this method is compared to number of those equipped with AIS data navigating in the region. Checking screen is used for ensuring the accuracy, as in Fig. 4.10.

For all days, more than 80% of AIS targets can be tracked. Success tracking ratios for the 3 days data used in the figures are:

- Apr 2nd: 85%
- Apr 4th: 83%
- Apr 6th: 84%

Here, the ratio is calculated by the following formula:

$$Ratio = \frac{\sum_{1}^{1440} N_i}{\sum_{1}^{1440} AIS_i}$$

Where i is the time (minutes) of the day, N_i and AIS_i are the number of AIS-Radar targets and AIS targets at the time i respectively.

Another advantage of this approach is that these targets can be followed continuously.

Other AIS targets can not be tracked by this approach due to the fact that their images on radar, due to some different reasons, abruptly increase or decrease in sizes to a level that they may cause the Relating-Value to be larger than the threshold value used for decision making. Therefore, to ensure the reliability of the tracking result, the position should not be taken as the target's image without any cautions.

Other targets, including ships not equipped with AIS and AIS targets which can not be matched with radar targets can still be followed using the approach described in chapter 3 of this study.

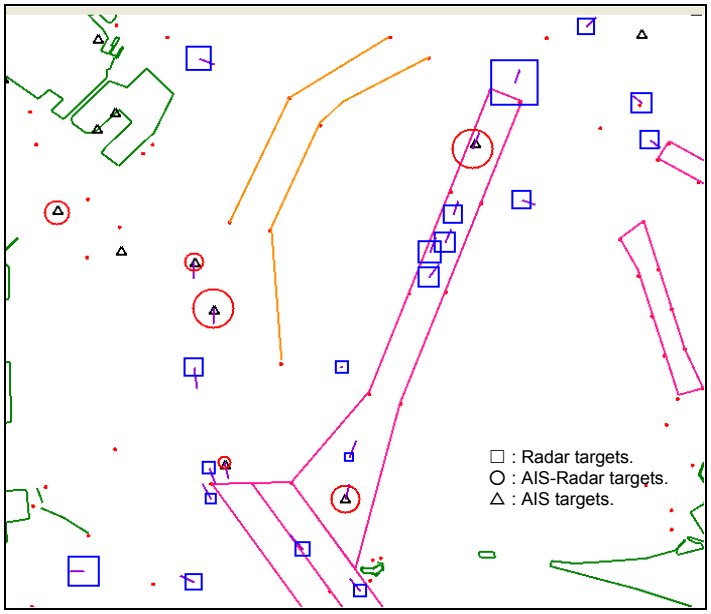

Fig.4.10 AIS-Radar target checking Screen

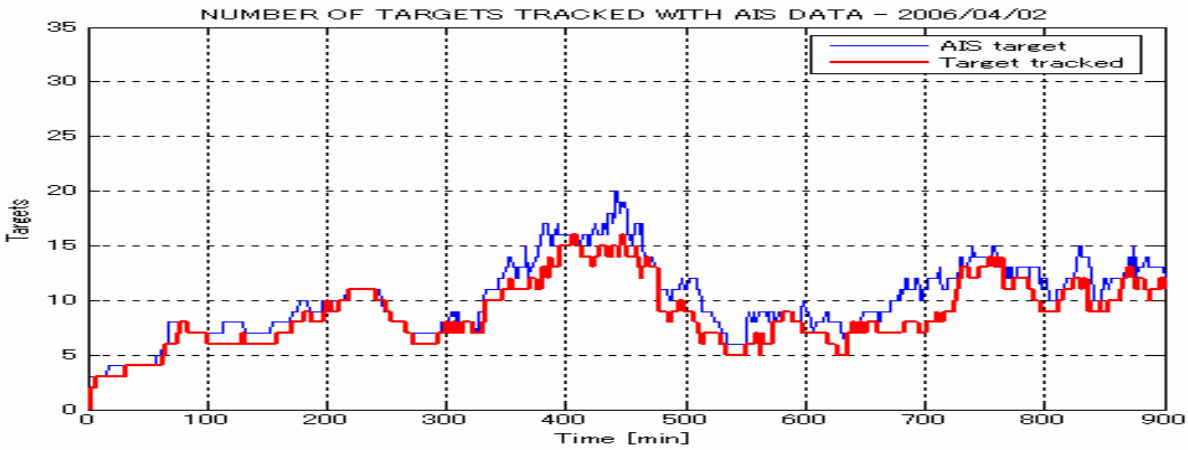

Fig. 4.11a Tracking AIS-Radar Target Result

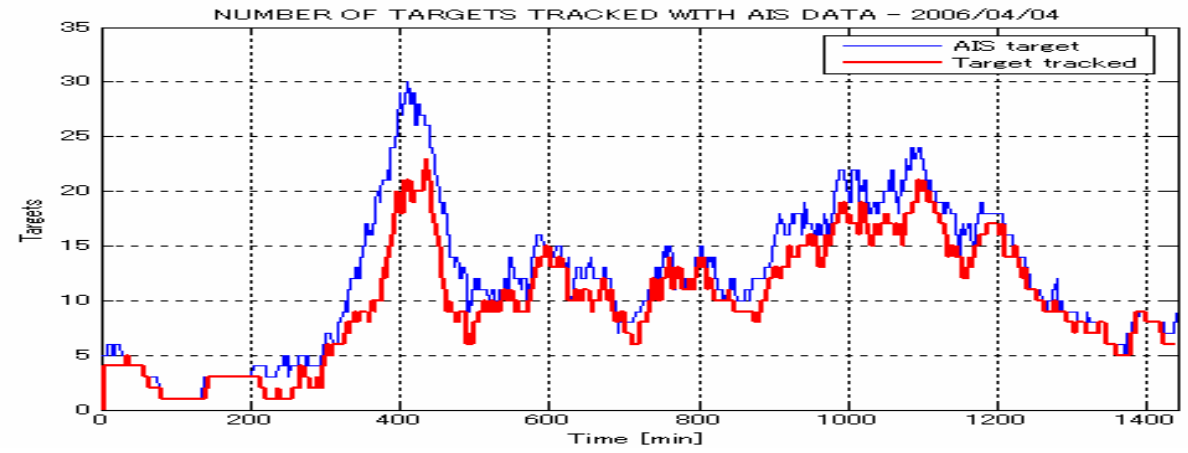

Fig. 4.11b Tracking AIS-Radar Target Result

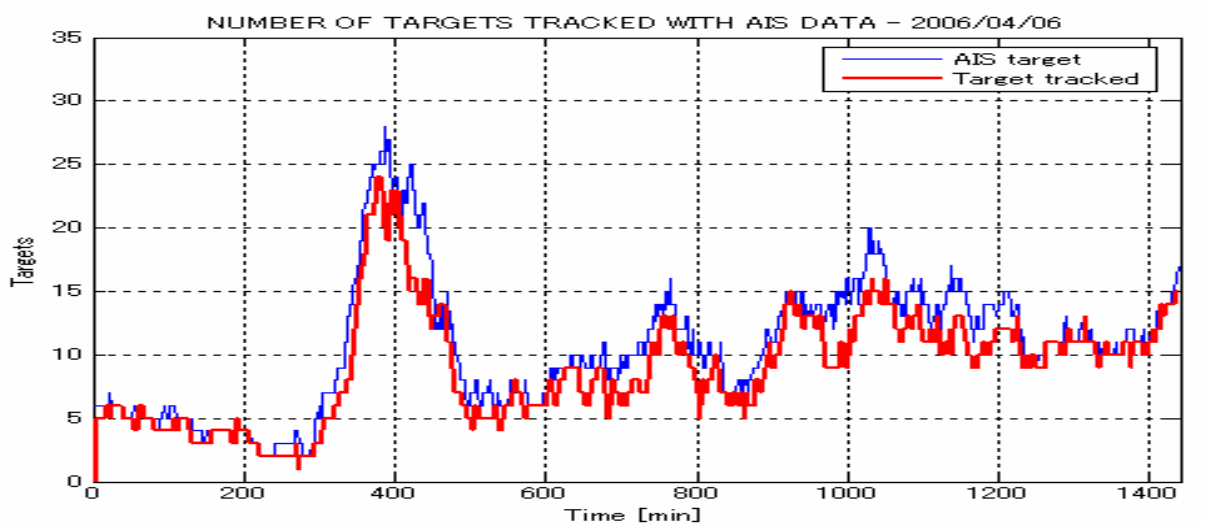

Fig. 4.11c Tracking AIS-Radar Target Result

4.6.2 Deviation of Ship Center as Indicated by AIS and on Radar Image

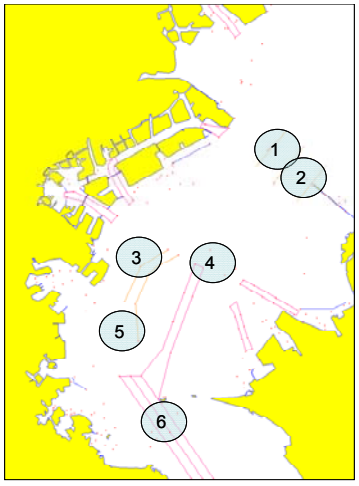

Fig.4.12 Watching Region

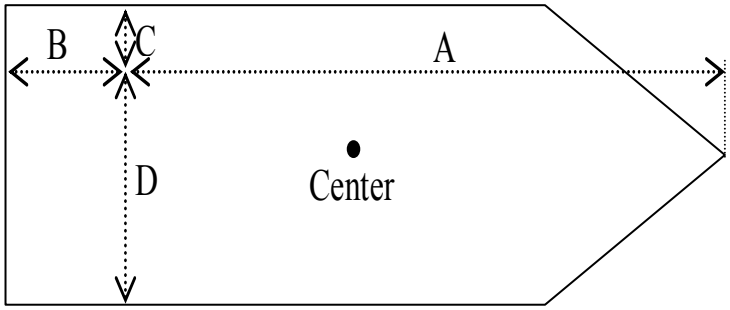

Fig.4.13 AIS Position and Ship Center

To check the consistency of AIS and Radar data, positions of targets on radar screen have been compared to those provided by AIS, for AIS-Radar targets. In order to have the same reference point, position provide by AIS is shifted to the ship center. This can be done with the data decoded from ship static data message (Message 5 of AIS Class A data), where position of GNSS antenna is encoded in the 4 values A, B, C, D as shown in Fig. 4.13.

Then, coordinators of the ship's center position provided by AIS can be calculated as followings:

$$Xc = Xais + (A-B)xSin(hdg)/2 + (D-C)xSin(hdg+90)/2$$
$$Yc = Yais + (A-B)xCos(hdg)/2 + (D-C)xCos(hdg+90)/2$$

Where

- Xc, Yc: coordinators of the ship' center in east and north directions
- Xais, Yais: AIS position coordinators
- hdg: heading (provided by AIS)

Observations have been taken for 6 different regions indicated in Fig. 4.12. These regions are all on the main traffic flow in the bay, from the bay mouth on the south to port of Tokyo and port of Chiba on the north. Distributions of deviation are shown in Fig. 4.14, with the mean deviations in X (East ward) and Y (North ward) axis for each region. It can be seen that normally, the total deviation is in the range of 7 pixels (app. 150 meters). The deviations follow the common tendency for each region, which is the combined result of deformity of radar pictures and aspects of ships passing through the region.

The aspect of ship (angle difference between ship's heading and bearing of radar station from ship) has a significant effect on the deviation of its image on radar screen. This can be seen in all the figures, specifically in the deviations of region 5 and region 6. In these two regions, due to the existence of bi-directional navigation, the distributions form 2 regions asymptotically over the origin, for the same condition of radar picture deformity. The fact should be taken into account while considering the collision risk in head-on encounter.

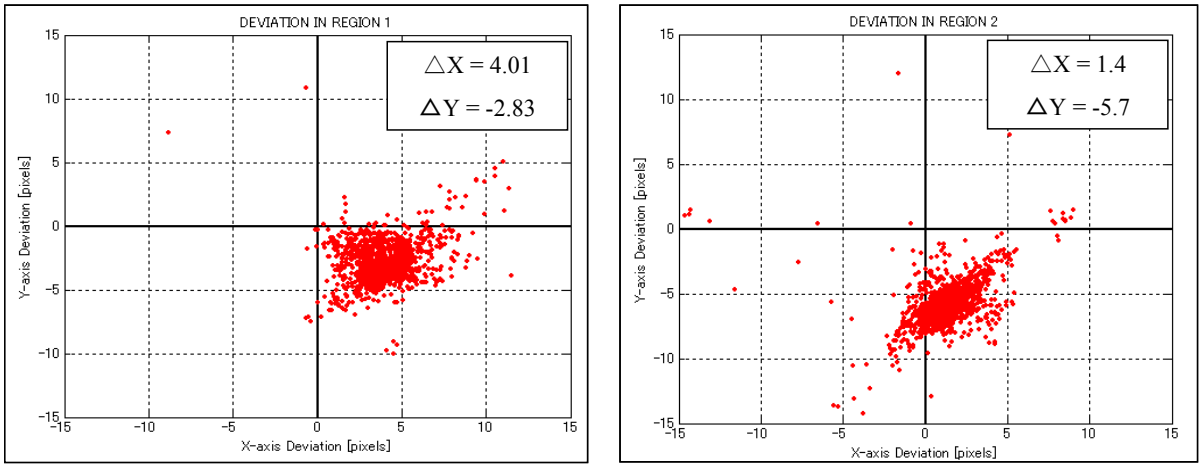

Fig.4.14a Radar and AIS position deviation for different areas in the bay

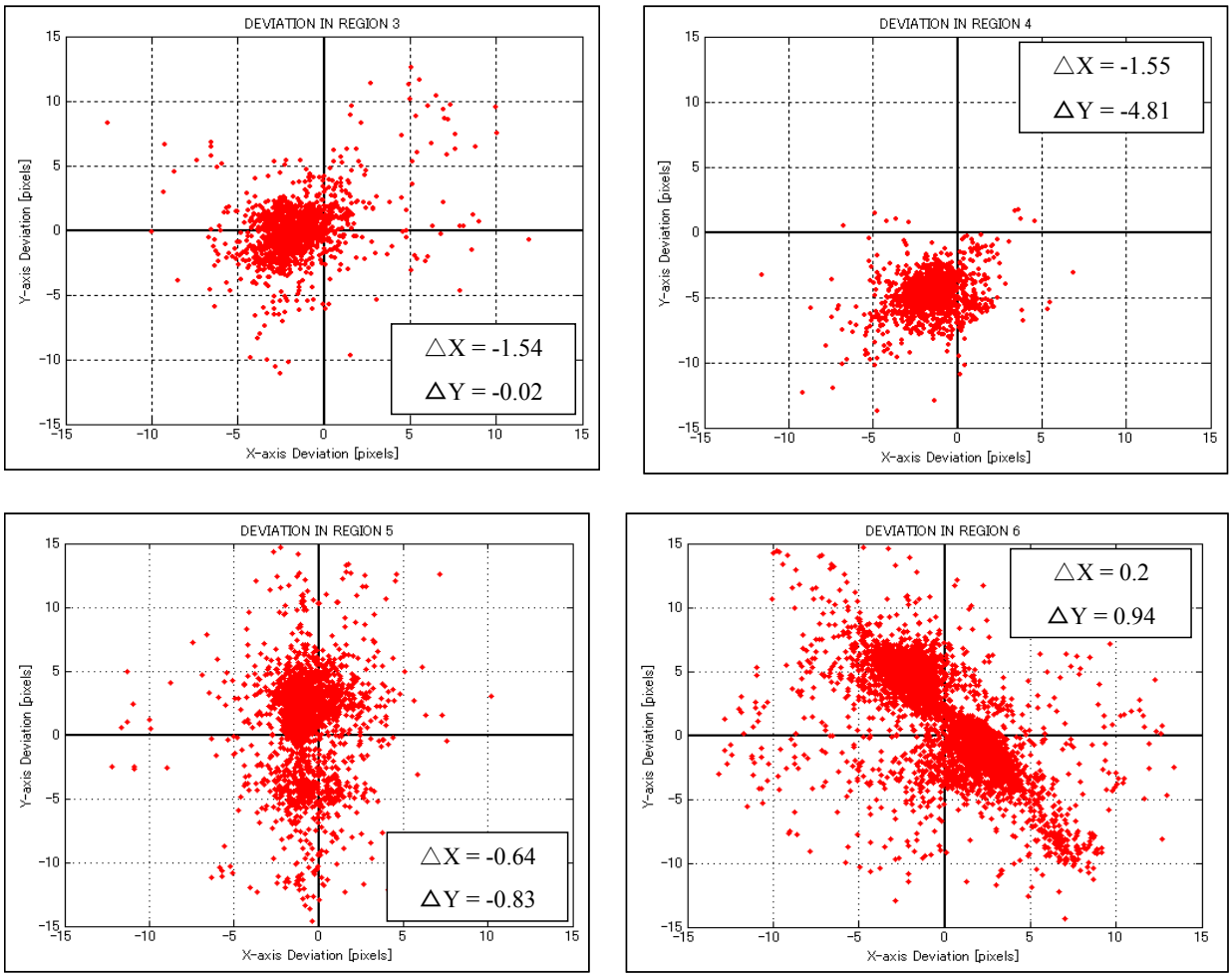

Fig.4.14b Radar and AIS position deviation for different Areas in the Bay

4.7 Conclusion

In this chapter, a method of using available AIS data to increase the automatic tracking efficiency for target equipped with AIS has been introduced.

Firstly, a matching algorithm is used to match AIS data to radar targets tracked from radar screen. A Relating-Function is used for this task with the threshold value decided to be 1.5.

Secondly, the Relating-Function for 3 image positions relationship is slightly modified to take the advantage of course and speed over ground as provided by AIS. Using this formula, Relating-Value becomes more converged, then, the threshold value to be -0.8 can be chosen for target following.

Using this approach, more than 80% of ships equipped with AIS can be tracked accurately.

Later, comparison is made between AIS provided position and position on radar image for AIS-Radar target to Fig. out the effect of ships' aspect to their deviation on the Radar screen.

Chapter 5. Application of Kalman Filter for Reconstruction of Target Motion and Motion Tracking

5.1 Introduction of Kalman Filer [2,16,20,21]

Kalman Filter has long been regarded as the optimal solution to many tracking and states predicting problems. It is a recursive filter that estimates the states of a dynamic system, basing on the linear model of the system and sequential measurements of system output.

Consider a dynamic system with the discrete state space model as followings

$$X_k = A \times X_{k-1} + B \times U_k + W_{k-1} \qquad (5.1)$$

$$Z_k = H \times X_{k-1} + V_k \qquad (5.2)$$

Where A, B, H are transition matrix, control matrix and observation matrix respectively. State variables and control input at time step k are expressed by vectors X_k and U_k.

Z_k is a vector containing output measurements of the system, called observation vector.

The random matrix variables W_k and V_k represent the process and measurement noise respectively and are assumed to be independent of each other, white, zero mean with normal probability distributions.

$$p(W) \cong N(0, Q), \qquad Q = E[W \times W^T] \qquad (5.3)$$

$$p(V) \cong N(0, R), \qquad R = E[V \times V^T] \qquad (5.4)$$

In (5.3) and (5.4), process noise covariance Q and measurement noise covariance R are assumed to be constant.

Then, the system's state variables can be estimated by operating the Kalman filter recursively through 2 steps, namely "Predict" and "Correction":

Time update equations ("Predict"):

$$\hat{X}_k^- = A \times \hat{X}_{k-1} + B \times U_k \qquad (5.6)$$

$$P_k^- = A \times P_{k-1} \times A^T + Q \qquad (5.7)$$

Measurements update equations ("Correction"):

$$K_k = P_k^- \times H^T \times (H \times P_k^- \times H^T + R)^{-1} \qquad (5.8)$$

$$\hat{X}_k = \hat{X}_k^- + K_k \times (Z_k - H \times \hat{X}_k^-) \qquad (5.9)$$

$$P_k = (I - K_k \times H) \times P_k^- \qquad (5.10)$$

K is called Kalman gain matrix and P is covariance of estimate errors.

$P_k = E[(X_k - \hat{X}_k) \times (X_k - \hat{X}_k)^T]$, and $\hat{X}$ is the estimated state vector.

5.2 Design a Kalman Filter for Target Motion

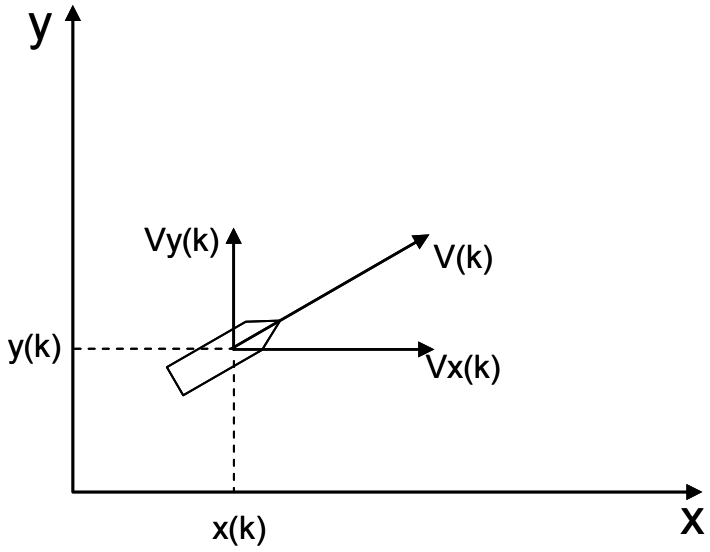

Fig. 5.1 Target motion coordination

For the movement of a target ship on Radar screen, state vector is taken in this study as following

$$X = \begin{bmatrix} x & y & v_x & v_y & a_x & a_y \end{bmatrix}^T$$

Where, x, y are coordinators of target's position on an earth fixed horizontal frame (normally North-East frame). v_x, v_y are speed components and a_x, a_y are acceleration components in x and y direction respectively.

While tracking target's motion on radar pictures, unfortunately, information about targets' maneuver is unknown, or, no clue is available for calculation or estimation of ship's acceleration. Therefore, these values can be assumed to be

$$\dot{a}_x = 0 \text{ and } \dot{a}_y = 0 \quad (20)$$

and changes in target's speed are considered to be biases.

In this case, ship's speeds in both x (Eastward) and y (Northward) directions are considered to be constants. The assumption is acceptable if sampling time is small enough. When Kalman filter is used for reconstructing target movement from its DGPS position, the sampling time is 1s, v_x and v_y will be almost constants because of the very small changes in ship's speed and course over ground in a period of 1 second.

However, for lower sampling frequency, v_x, v_y may actually change from one sampling to another. Therefore, to have the flexibility in applying Kalman Filter for system of different natures, kinematics equations of acceleration is taken as:

$$\dot{a}_x = -(1/T) \times a_x$$

$$\dot{a}_y = -(1/T) \times a_y$$

Here, scalar T plays the role of a Low-Pass Filter and the value for it is left as a designing parameter and the value of that will be chosen from simulation results.

Then, kinematics equations of the system are expressed in continuous and discrete forms as

$$\begin{cases} \dot{x} = v_x \\ \dot{y} = v_y \\ \dot{v}_x = a_x \\ \dot{v}_y = a_y \\ \dot{a}_x = -(1/T) \times a_x \\ \dot{a}_y = -(1/T) \times a_y \end{cases} \qquad (5.11)$$

The discrete form of 5.11 can be produced by discretizing those equations, using sampling time Δt. Then, following equations are readily got:

$$\begin{cases} x(k) = x(k-1) + v_x(k-1) \times \Delta t + a_x(k-1) \times \Delta t^2 / 2 \\ y(k) = y(k-1) + v_y(k-1) \times \Delta t + a_y(k-1) \times \Delta t^2 / 2 \\ v_x(k) = v_x(k-1) + a_x(k-1) \times \Delta t \\ v_y(k) = v_y(k-1) + a_y(k-1) \times \Delta t \\ a_x(k) = \left\{1 + (-1/T) + (-1/T)^2 / 2! + (-1/T)^3 / 3! + ...\right\} \times a_x(k-1) \\ a_y(k) = \left\{1 + (-1/T) + (-1/T)^2 / 2! + (-1/T)^3 / 3! + ...\right\} \times a_y(k-1) \end{cases} \qquad (5.12)$$

where x (k) = x (k x Δt), y (k) = y (k x Δt) and so on.

From (5.12), with sampling time Δt = 1 (min), ship's motion can be written in state space form (5.1), (5.2) by forming the matrices as:

$$A = \begin{bmatrix} 1 & 0 & 1 & 0 & 0.5 & 0 \\ 0 & 1 & 0 & 1 & 0 & 0.5 \\ 0 & 0 & 1 & 0 & 1 & 0 \\ 0 & 0 & 0 & 1 & 0 & 1 \\ 0 & 0 & 0 & 0 & f & 0 \\ 0 & 0 & 0 & 0 & 0 & f \end{bmatrix}, \qquad (5.13)$$

where

$$f = 1 + (-1/T) + (-1/T)^2 / 2! + (-1/T)^3 / 3! + ...$$

$$B = [0] \quad \text{(No control input)} \qquad (5.14),$$

$$X_k = \begin{bmatrix} x(k) & y(k) & v_x(k) & v_y(k) & a_x(k) & a_y(k) \end{bmatrix}^T \qquad (5.15)$$

$$Z_k = \begin{bmatrix} x(k) & y(k) \end{bmatrix}^T \quad \text{(Only x, y coordinators are determined from Radar image)} \quad (5.16)$$

Therefore, observation matrix is

$$H = \begin{bmatrix} 1 & 0 & 0 & 0 & 0 & 0 \\ 0 & 1 & 0 & 0 & 0 & 0 \end{bmatrix} \qquad (5.17)$$

Covariance matrices R, Q, and initial covariance matrix of P (i.e. P_0) are formed as followings

$$R = R\_val \times \begin{bmatrix} 1 & 0 \\ 0 & 1 \end{bmatrix} \qquad (5.18)$$

$$Q = Q\_val \times \begin{bmatrix} 0 & 0 & 0 & 0 & 0 & 0 \\ 0 & 0 & 0 & 0 & 0 & 0 \\ 0 & 0 & 0 & 0 & 0 & 0 \\ 0 & 0 & 0 & 0 & 0 & 0 \\ 0 & 0 & 0 & 0 & 1 & 0 \\ 0 & 0 & 0 & 0 & 0 & 1 \end{bmatrix} \qquad (5.19)$$

$$P_0 = P\_val \times \begin{bmatrix} 1 & 0 & 0 & 0 & 0 & 0 \\ 0 & 1 & 0 & 0 & 0 & 0 \\ 0 & 0 & 1 & 0 & 0 & 0 \\ 0 & 0 & 0 & 1 & 0 & 0 \\ 0 & 0 & 0 & 0 & 1 & 0 \\ 0 & 0 & 0 & 0 & 0 & 1 \end{bmatrix} \qquad (5.20)$$

Q_val, P_val, R_val and T are scalar values and taken as designing parameters, which will be determined by experiment on simulation in the following section.

Algorithms (5.6)-(5.10) are applied recursively, with the system dynamic matrices defined by (5.13)-(5.20), producing the state estimation of the moving target.

5.3 Determine Designing Parameters by Simulation Experiment

To determine the suitable values for designing parameter Q_val, P_val, R_val and T in section (5.2), experiments have been done with an MMG computer model of a training ship. The model ship was first handled to follow a prefixed track, including the course changing and speed changing maneuver. During the track, ship's positions and speeds data were saved for later reference, when calculating the filter performance indices.

To simulate the data as those received by tracking the ship on Radar Screen, the real ship positions were intentionally deviated by adding a random white noise. Amplitude of the noise is chosen to be 3 pixels, basing on the observation. The result track, which is called noise track, is used later as system output measurement for the Kalman Filter designed in section (5.2).

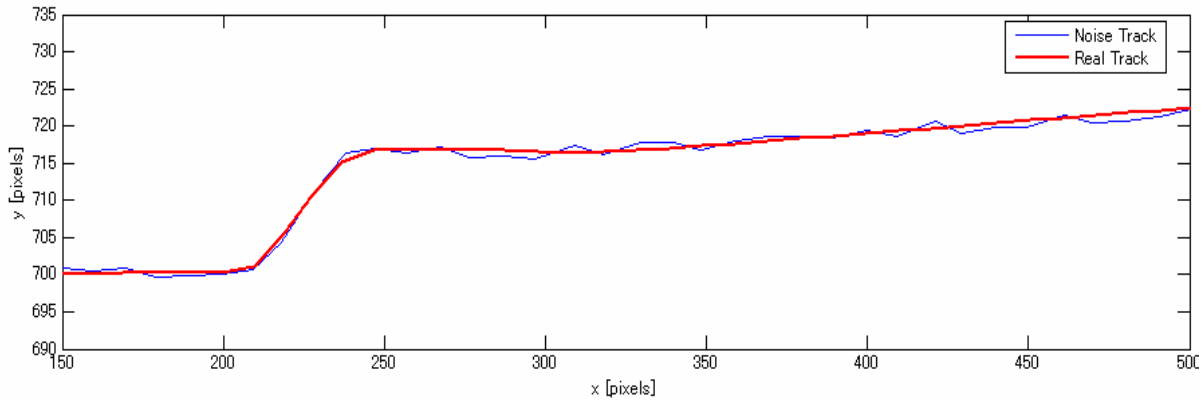

Fig.5.2 Real and observed tracks of Model Ship in simulation

Performance indices used in this study are the followings:

$$PER = \frac{\sum \Delta d_f^2(i)}{\sum \Delta d_a^2(i)} \qquad \Delta d_a, \Delta d_f \ \textit{absolute position error and postion error after filtering}$$

$$SER = \frac{\sum \Delta V_f^2(i)}{\sum \Delta V_a^2(i)} \qquad \Delta V_a, \Delta V_f \ \textit{absolute speed error and speed error after filtering}$$

$$MPE = \max\{\Delta d_f(i)\}$$

$$MSE = \max\{\Delta V_f(i)\}$$

$$i = 1 : N \ (\textit{number of sampling data})$$

From the choice of performance indices, it can be seen that apart from the error reduction effects, absolute errors of position and speed are also taken into account. This is to ensure that in all cases, the filter shall not degrade position accuracy beyond the expected level.

With T = 3 and R = 2, these indices have been calculated for different value of P_val and Q_val in (5.20, 5.21), for model's course changing and speed changing tracks. The results are shown in Fig. 5.3 and Fig.5.4.

From Fig.5.3 and Fig.5.4, it can be seen that initial value of P (P_0) does not affect the filter performance very much, as long as it is given a rather large value, representing the uncertainty of initial state of the model. Q_val, however, is an important factor. Its effects are different for different indices, and also, for Position Error Reduction, it is different between turning and straight running case. Value of Q_val to be 0.3 seems to best match all requirements.

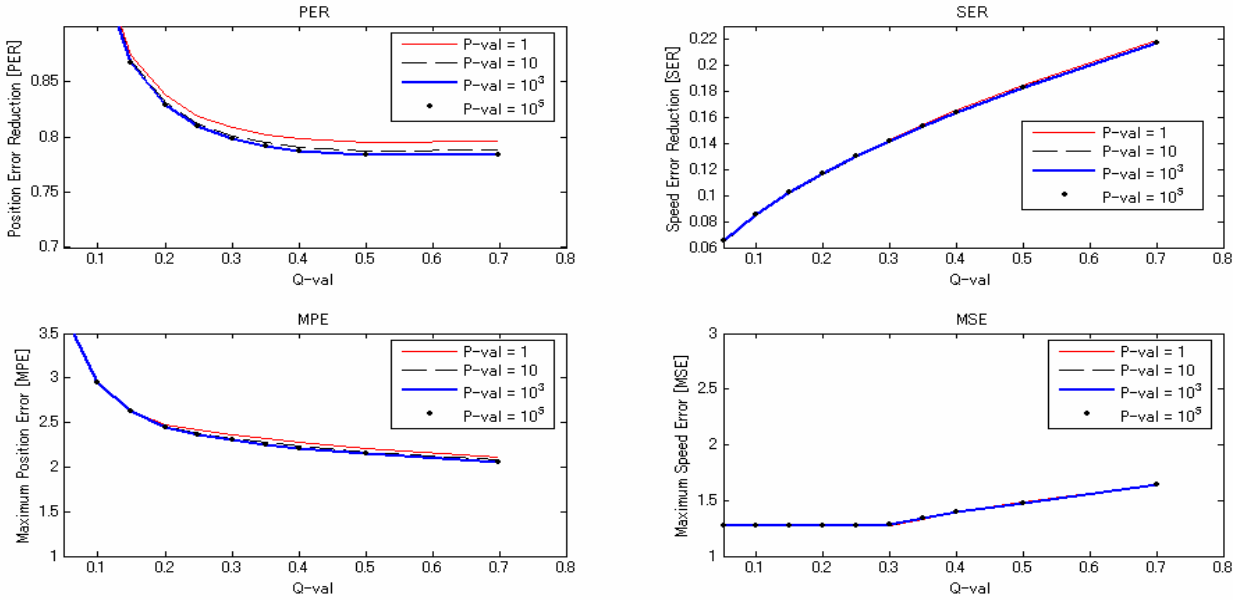

Fig.5.3 Performance indices as function of P_val and Q_val in turning maneuver

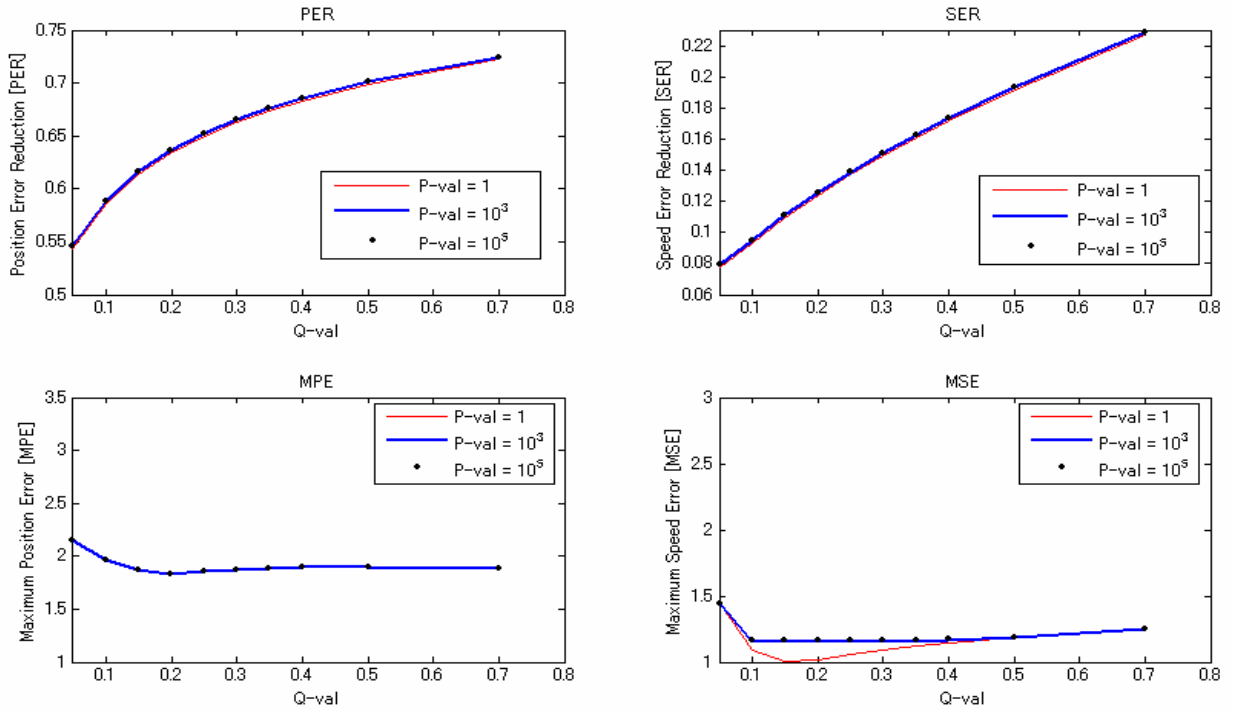

Fig.5.4 Performance indices as function of P_val and Q_val in speed changing maneuver

In a similar manner, performance indices are calculated for different values of R_val with other parameters kept constant: P_val = 1000, Q_val = 0.3, T = 3. Results are shown in Fig. 5.5 for turning track. Value of R_val around 2.0 appears to be suitable.

Value of T is chosen more or less randomly. A smaller value of T results in smaller cutting frequency and therefore may remove the working frequency of the system. T = 3 is used in this study and seems to satisfy the performance indices, as can be seen in figures 5.3, 5.4, 5.5.

Filtering results for the model used in experiments, with designing parameters' values defined above, are shown in Fig. 5.6 and Fig. 5.7.

Average values of performance indices, in this case, are:

PER = 0.72; SER = 0.16; MPE = 2.1; MSE =1.3

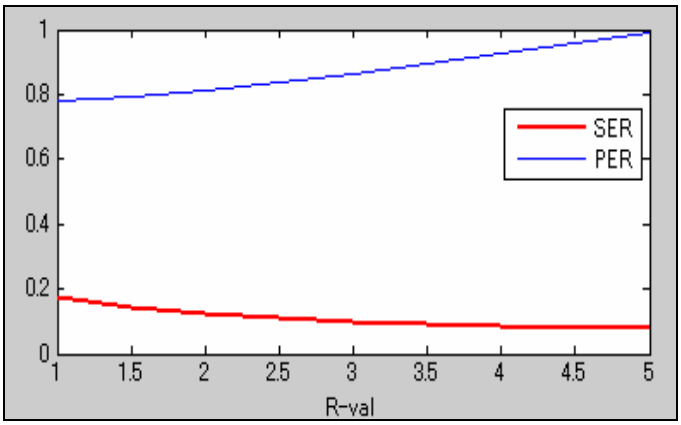

Fig.5.5 Performance indices as function of R_val

With the values assigned above, speed and course of Model Ship during the simulation track can be reconstructed from noisy positions. Filtering result is shown in figures 5.5 and 5.6, in which, it can clearly be seen that effects of noise is considerably reduced, for both speed and course parameters.

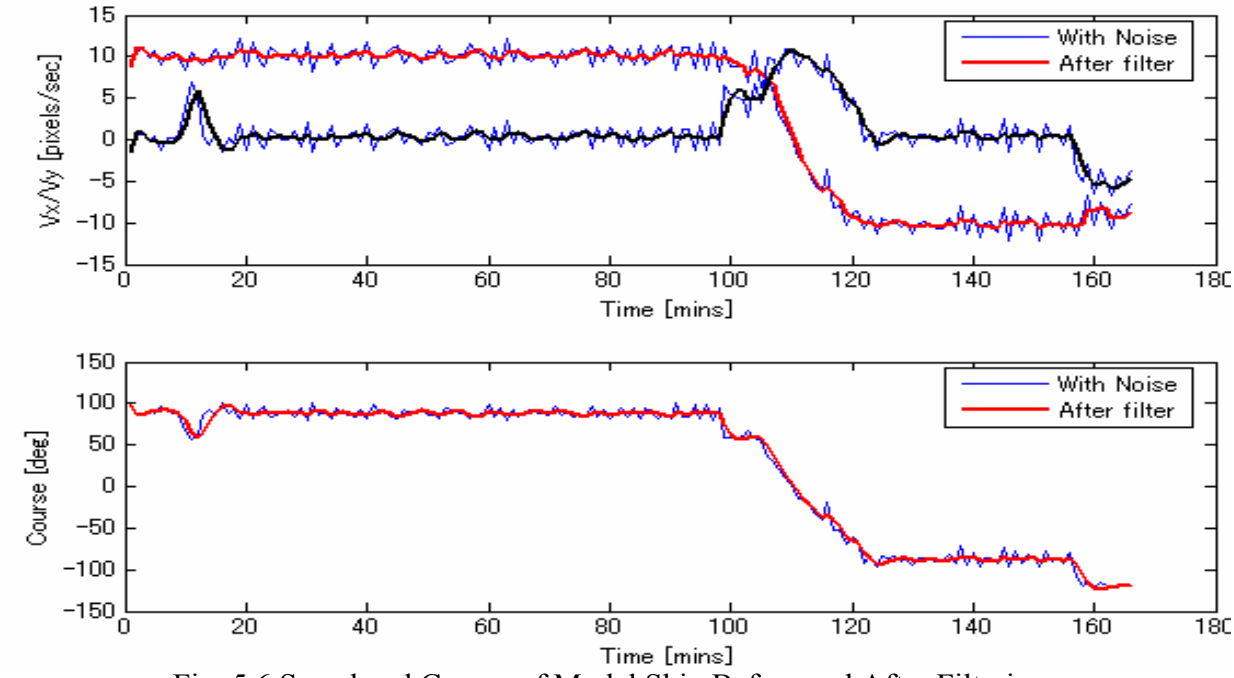

Fig. 5.6 Speed and Course of Model Ship Before and After Filtering

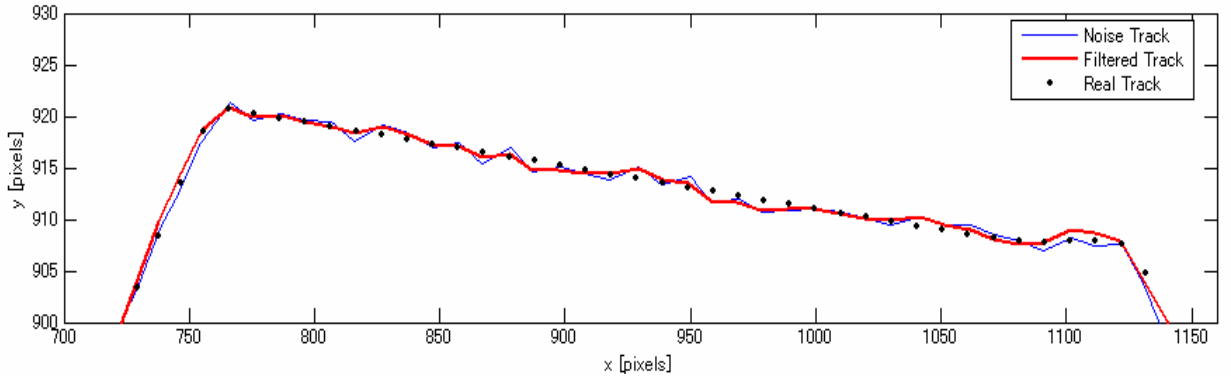

Fig.5.7 Track of Model Ship Before and After Filtering

5.4 Application in Estimation of Target Motion in Tokyo Bay

The Kalman Filter, as designed above is used to reconstruct the course and speed of targets moving in Tokyo Bay from their every one minute positions on radar pictures. Shown below in Fig. 5.8a and Fig. 5.8b are filtering results for 2 radar targets, where, the one in Fig. 5.8b has a clear speed changing during the tracked course. In both cases, the filter works as expected, producing the more reliable speed and course.

Difference in observed and filtered tracks is not very clear due to scale limitation, but it can still be seen that the filtered track is smooth and less affected by noise. When the change in course is large and abrupt, position provided by the filter is not really reliable due to the phase lag phenomenon of the filter. Therefore, Kalman Filter should be reset if there is a large change in target course over ground.

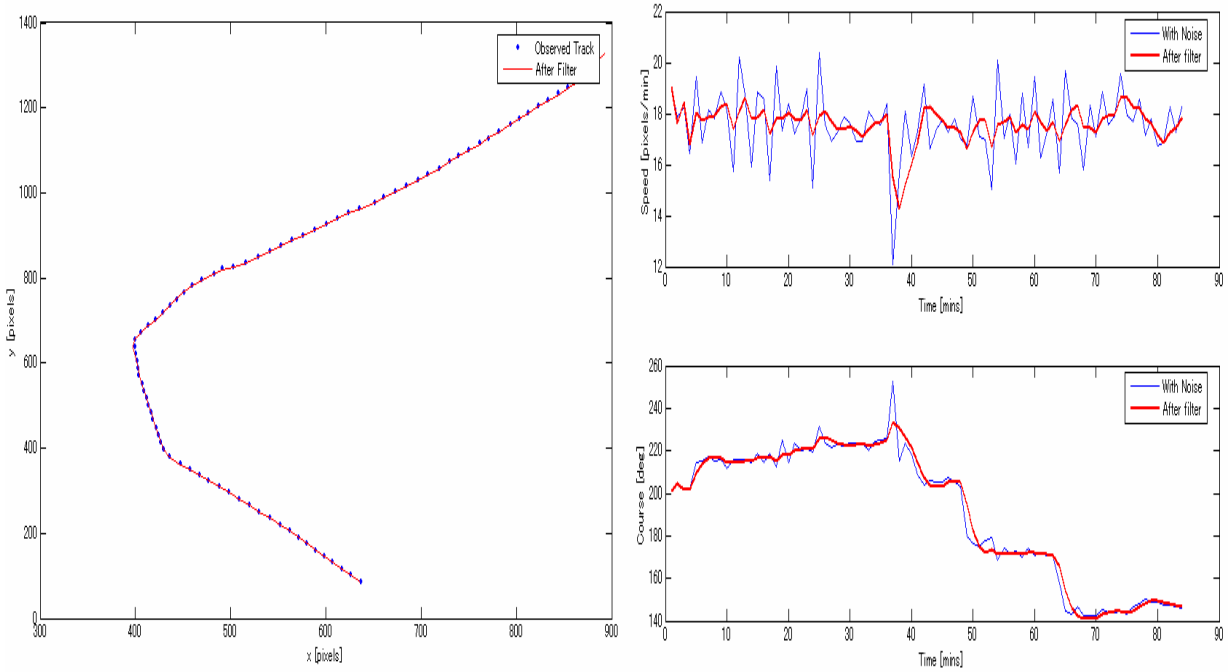

Fig. 5.8a Filtering result

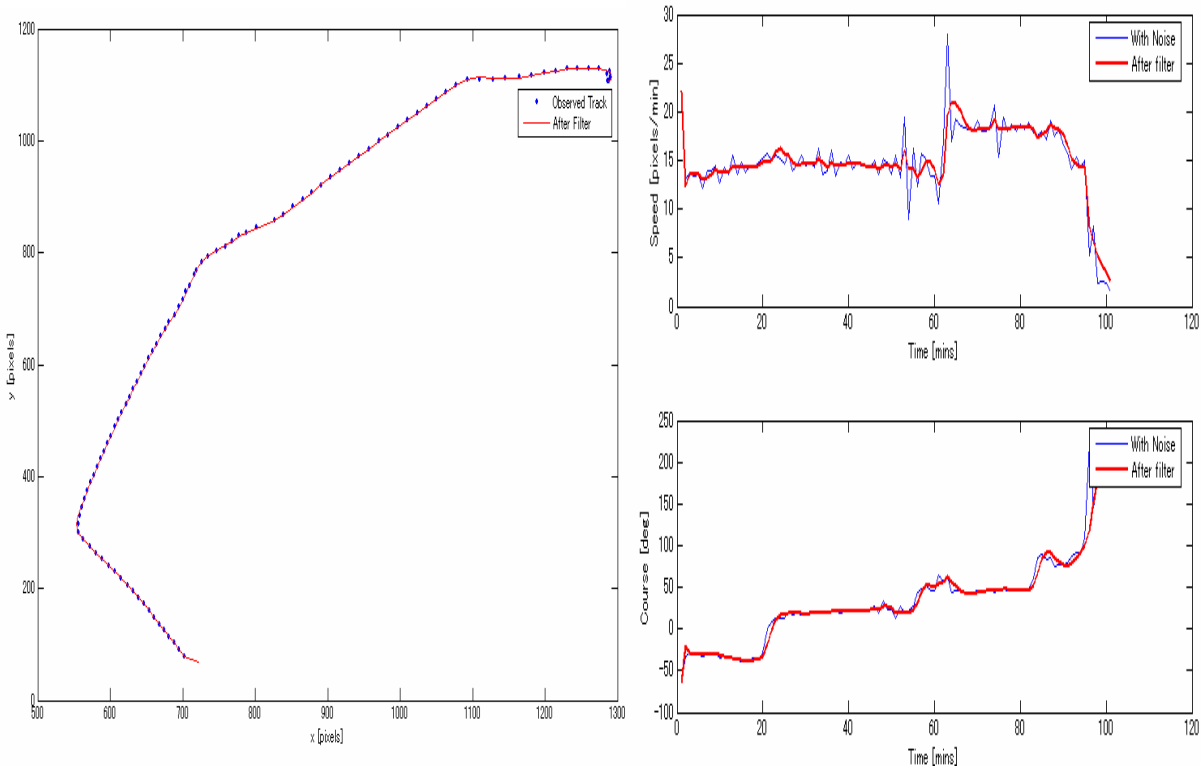

Fig. 5.8b Filtering result

5.5 Application of Kalman Filter in Target Following

Kalman Filter can be applied for target following as mentioned in chapter 2 of this study. To take also number of pixel in image position (image position size) in searching and matching algorithms, dynamics of the system need slightly modifying, where the size of target's image on radar screen is assumed to be constant from one picture to another.

Following matrices are used in designing the Kalman Filter:

State vector:

$$X_k = \begin{bmatrix} x(k) & y(k) & v_x(k) & v_y(k) & a_x(k) & a_y(k) & S(k) & \dot{S}(k) \end{bmatrix}^T \qquad (5.21)$$

State transition matrix:

$$A = \begin{bmatrix} 1 & 0 & 1 & 0 & 0.5 & 0 & 0 & 0 \\ 0 & 1 & 0 & 1 & 0 & 0.5 & 0 & 0 \\ 0 & 0 & 1 & 0 & 1 & 0 & 0 & 0 \\ 0 & 0 & 0 & 1 & 0 & 1 & 0 & 0 \\ 0 & 0 & 0 & 0 & f & 0 & 0 & 0 \\ 0 & 0 & 0 & 0 & 0 & f & 0 & 0 \\ 0 & 0 & 0 & 0 & 0 & 0 & 1 & 1 \\ 0 & 0 & 0 & 0 & 0 & 0 & 0 & 1 \end{bmatrix}, \qquad (5.22)$$

where

$$f = 1 + (-1/T) + (-1/T)^2/2! + (-1/T)^3/3! + \ldots \qquad (5.23)$$

Control input matrix:

$B = [0]$ (No control input) (5.24),

Vector of measurement:

$$Z_k = [x(k) \quad y(k) \quad S(k)]^T \qquad (5.25)$$

(x, y coordinators and target size are determined from Radar image)

Observation matrix:

$$H = \begin{bmatrix} 1 & 0 & 0 & 0 & 0 & 0 & 0 & 0 \\ 0 & 1 & 0 & 0 & 0 & 0 & 0 & 0 \\ 0 & 0 & 0 & 0 & 0 & 0 & 1 & 0 \end{bmatrix} \qquad (5.26)$$

In comparison with matrices in 5.12 to 5.17, number of pixel in target's image S(k) and its derivative are included in state vector X. Matrix A is modified accordingly. As pixel number (or image size) is also a parameter to be measured, the respective component is added to vector of measurement Z_k, and modification to observation matrix H is made.

Here, as target's image size is assumed to be constant, equation of its derivative is simply:

$\dot{S}(k) = 0$

Covariance matrices of the Kalman Filter for the application are the chosen as followings.

$$R = R\_val \times \begin{bmatrix} 1 & 0 & 0 \\ 0 & 1 & 0 \\ 0 & 0 & c1 \end{bmatrix} \qquad (5.27)$$

$$Q = Q\_val \times \begin{bmatrix} 0 & 0 & 0 & 0 & 0 & 0 & 0 & 0 \\ 0 & 0 & 0 & 0 & 0 & 0 & 0 & 0 \\ 0 & 0 & 0 & 0 & 0 & 0 & 0 & 0 \\ 0 & 0 & 0 & 0 & 1 & 0 & 0 & 0 \\ 0 & 0 & 0 & 0 & 0 & 1 & 0 & 0 \\ 0 & 0 & 0 & 0 & 0 & 0 & 0 & 0 \\ 0 & 0 & 0 & 0 & 0 & 0 & 0 & c2 \end{bmatrix} \qquad (5.28)$$

$$P_0 = P\_val \times \begin{bmatrix} 1 & 0 & 0 & 0 & 0 & 0 & 0 & 0 \\ 0 & 1 & 0 & 0 & 0 & 0 & 0 & 0 \\ 0 & 0 & 1 & 0 & 0 & 0 & 0 & 0 \\ 0 & 0 & 0 & 1 & 0 & 0 & 0 & 0 \\ 0 & 0 & 0 & 0 & 1 & 0 & 0 & 0 \\ 0 & 0 & 0 & 0 & 0 & 1 & 0 & 0 \\ 0 & 0 & 0 & 0 & 0 & 0 & 1 & 0 \\ 0 & 0 & 0 & 0 & 0 & 0 & 0 & 1 \end{bmatrix} \quad (5.29)$$

In 5.27-5.29, R_val, Q_val, and P_val are the same as those defined in section (5.3). Values of c1 and c2 represent the measurement and modeling errors of image size (in pixels).

With these arrangements, target following can be carried out using the combined procedure of prediction, matching and updating.

Prediction (Kalman Filter Time Updating): Generate the predicted state vector of the target ($\hat{X}^{-}(k+1)$) from current state vector ($\hat{X}(k)$). Note that current state vector $\hat{X}(k)$ is the target's state after being corrected by measurement values of image position and size. Algorithms for state vector and covariance matrix generating (time updating) are 5.6, 5.7 and are rewritten here.

$$\hat{X}_k^- = A \times \hat{X}_{k-1} + B \times U_k$$
$$P_k^- = A \times P_{k-1} \times A^T + Q$$

Image Position Searching and Matching: Searching area is defined around the predicted position and all image positions inside the area are possible image positions of the target.

Then, Relating-Function is used for matching (looking for the most suitable position of the target). In comparison with that defined in chapter 3, Relating-Function is slightly modified to utilize model's speed and size

$$R = d_{mdf} + f \times S_{mdf} - \cos(\psi)$$

$$d_{mdf} = \frac{d}{\sqrt{v_x^2(k) + v_y^2(k)}} - 1, \quad if\ d_{mdf} < 0 \Rightarrow d_{mdf} = \frac{\sqrt{v_x^2(k) + v_y^2(k)}}{d} - 1 \quad (5.30)$$

$$S_{mdf} = \frac{S}{S(k)} - 1, \quad if\ S_{mdf} < 0 \Rightarrow S_{mdf} = \frac{S(k)}{S} - 1$$

In (5.30), d is the distance between the position derived from current state vector and the image position in consideration. S is this image position's size and ψ is defined in the same manner as in chapter 3.

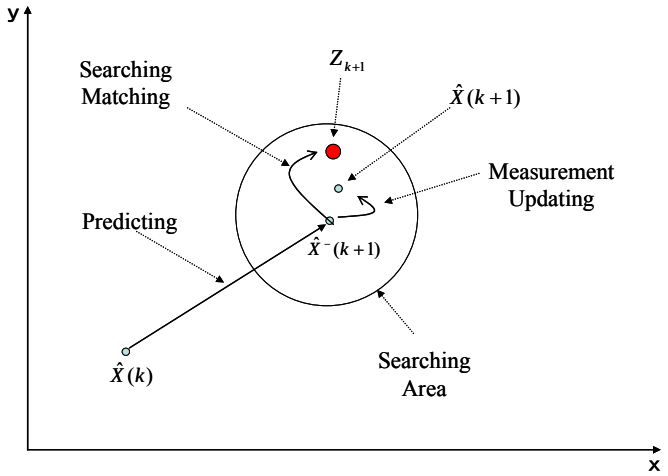

Fig. 5.9 Target Following by Kalman Filter

Correction (Kalman Filter Measurement Updating): Once the image position of the target has been found, this image position is taken as measurement (Z_{k+1}), where components of this observation vector are the position's coordination (x and y) and size (S, pixel number).

Algorithms for model updating are those in 5.8 to 5.10.

The overall procedure is illustrated in Fig. 5.9, in which the searching area is a circle centered at predicted position.

5.6. Conclusion

In this chapter, a Kalman filter is used to rebuild the movement of targets tracked from radar screen. To decide the suitable values of designing parameters of the Kalman filter, the performance indices have been chosen and experiments have been carried out with data of a model ship. Then, these values are chosen as followings:

- R_val = 2 (covariance of error of position measurement)
- Q_val = 0.3 (covariance of error of modeling)
- P_val = 1000 (initial covariance of state error)
- T = 3

The values above can be used to rebuild movement once targets have been tracked to give speed and course information less affected by noise.

Kalman filter, on the other hand, can also be used for target following. In later part of the chapter, Kalman filter is modified for the purpose of both target following and motion reconstructing simultaneously.

For this purpose, the above parameter can still be used, together with additional parameter for filtering the image size. A suggestion for this value choice is:

- c1 = 3 (equivalent to covariance error of image size measurement to be 6)
- c2 = 0.2 (target size should be more stable than its speed and course)

Chapter 6. Tokyo Bay Marine Traffic Analysis

6.1 Evaluation of Collision Risk by SJ Value

6.1.1 Definition

Subjective Judgment (SJ) value has long been used as a criterion of collision risk assessment, representing the pressure of surrounding vessel on officer of watch. It is a model for collision avoidance basing on a value of safety as recognized by ship's officer. SJ value is calculated for 3 cases of encounter:

Crossing encounter:

Own ship is give-way: $SJ=6.00\Omega + 0.09\ Rp - 2.32$ (6.1)

Own ship is stand-on: $SJ=7.01\Omega + 0.08\ Rp - 1.53$ (6.2)

Head-on encounter: $SJ=6.00\ \Omega + 0.09\ Rp - 2.32$ (6.3)

Overtaking encounter: $SJ=54.43\ \Omega + 0.24\ Rp + 2.77\ dRp/dt - 0.784$ (6.4)

where:

$\Omega = |d\theta/dt|\ Lo/Vo$: non-dimensional change rate of target ship direction

$Rp = R/\{(Lo + Lt)/2\}$: non-dimensional distance between own ship and target ship

$dRp/dt = Vr / Vo$: non-dimensional relative speed between own ship and target ship

$d\theta/dt$: change rate of target ship direction (rad/min)

Lo : length of own ship (m)

Lt : length of target ship (m)

Vo : speed of own ship (m/min)

Vr : relative speed between own ship and target ship (m/min)

R : distance between own ship and target ship (m)

It is obvious that parameters used in formulae of SJ are those that can be perceived by officer of watch visually or by available equipments such as RADAR/ARPA, AIS. These parameters are also taken into account by experienced navigators intentionally or unintentionally when considering risk of collision.

Values of factors and constants in the formulae are reasoned from simulation experiments. Values defined above have been generally accepted and are now in common use.

Simulation has proved that value of SJ is in close relation with the risk of collision. The risk of collision can be assessed basing on SJ value of own ship as followings:

a. $SJ > 0$: Encounter is "Safe".

b. $0 \geq SJ > -1$: Encounter is "Cautious" and needs following.

c. $-1 \geq SJ > -2$: Encounter is "Dangerous".

d. $-2 \geq SJ$: Encounter is "Very Dangerous".

6.1.2 SJ value calculation

The first step in SJ value calculation is determining encounter case. The case is decided basing on the heading difference and aspect of own ship and target ship. This is illustrated in Fig. 6.1.

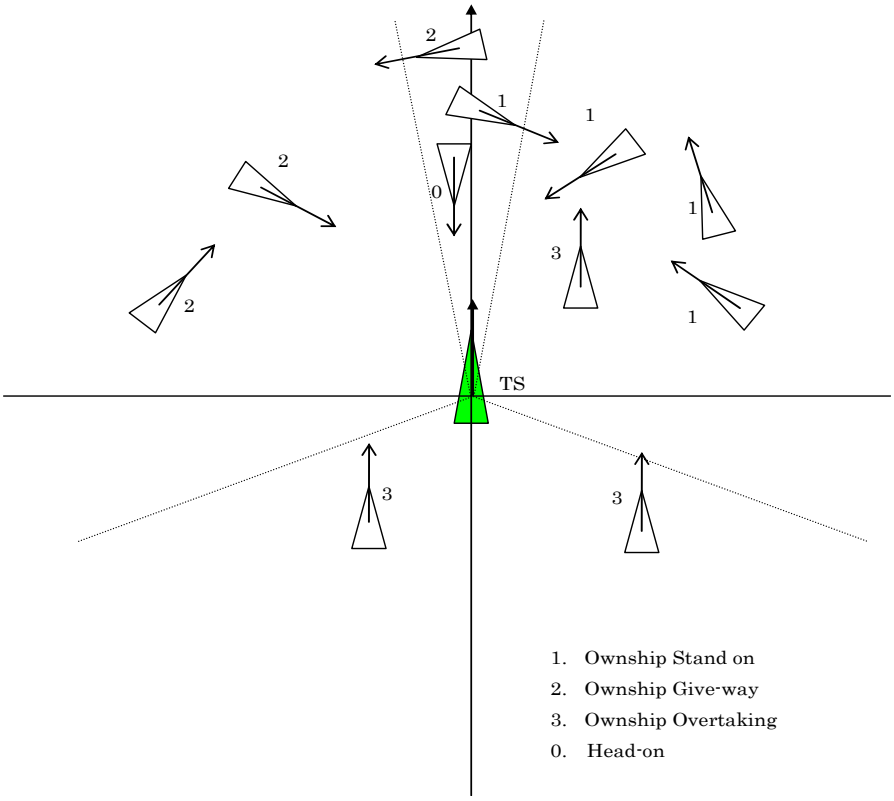

Fig.6.1 Own Ship and Target Ship Relation

Once encounter case has been decided, the appropriate formula among (6.1) to (6.4) is applied. Parameters used in the formula can be calculated easily from knowledge of own ship and target ship positions, courses, speeds etc. and therefore not mentioned here.

Evolution of the SJ value during the passage of 2 ships is illustrated in figures 6.2 to 6.4.

In Fig. 6.2, 2 cases of Head-On encounter are shown. In the first case, tracks of 2 ships coincide. For second case, 2 ships are passing at a distance of 100m but still considered to be in head-on situation as relative bearing of both ships from the other is less than 10 degree. Lengths and speeds of 2 ships are also shown in the figure. As expected, SJ values of 2 ships decrease rapidly while the distance between them keeps on decreasing or the perception of danger is increasing. When the value reaches the proximity of -2, two ships are in very dangerous situation. However, a limitation of adjusting collision risk basing uniquely on SJ value can also be noticed. When distance between ships is small, the rate of change of target bearing may be very large, causing large, positive value of SJ. The case seems to be ridiculous, keeping in mind the extremely dangerous situation. It can be seen in second case of head-on encounter in Fig. 6.2, where SJ values of both ships increase rapidly when distance between ships drops under 350m and due to their geometry, targets bearing's change rate is large.

The case, although happens sometimes, is rare because 2 ships have to take maneuver action before they are actually in the “too close” situation.

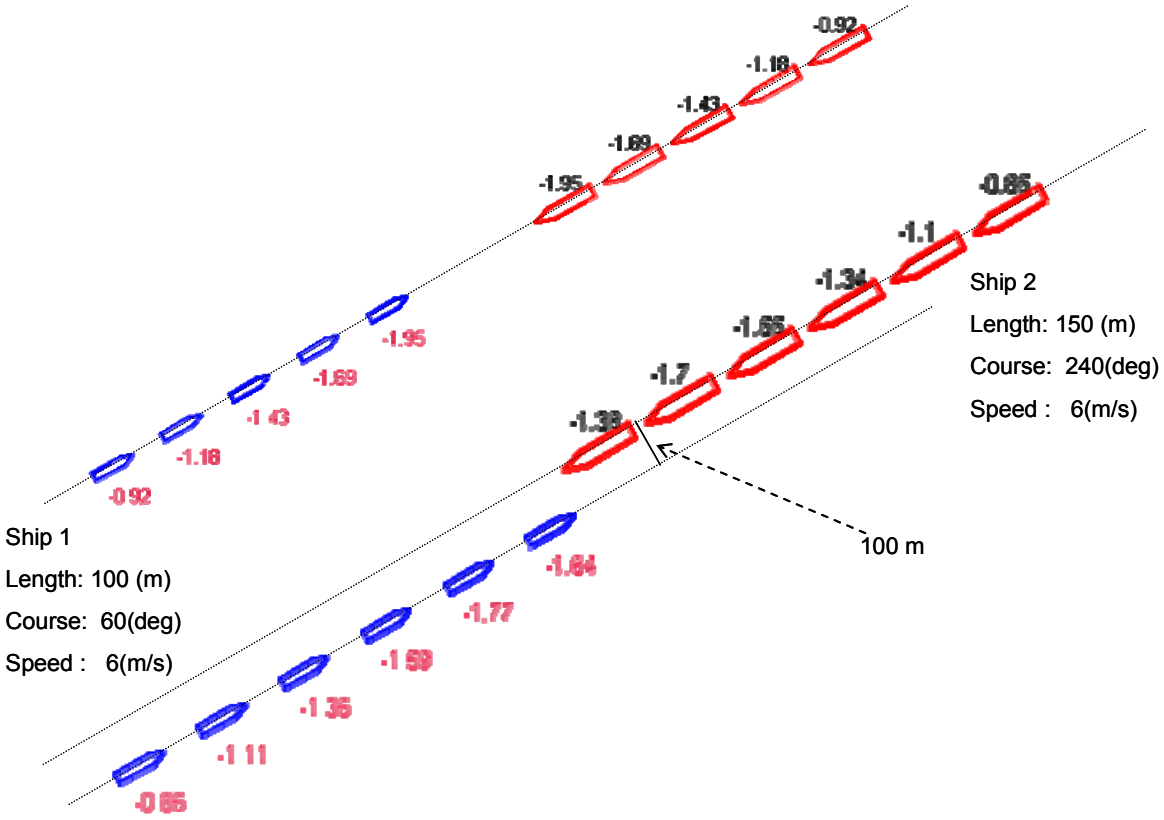

Fig.6.2 Variation of SJ Value in Head-on Encounter

Fig. 6.3 illustrates a crossing encounter. In this case, Ship 1 is give-way as it has Ship 2 on the starboard side. Ship 2, on the other hand, is a stand-on vessel. SJ values of both ships decrease consistently as they are reaching the closest point of approach (CPA). As ship 1 is supposed to take collision avoiding action, officer in watch of this ship is under the stress of having to change course in time.

When ships have passed CPA, although caution is still important, the most dangerous moment of encountering has already been over and SJ value should be set to positive.

Overtaking encounter is shown in Fig. 6.4, where a 100m length ship (Ship 1) is overtaking a 150m target ship (Ship 2) at traverse distances of 200m and 100m respectively.

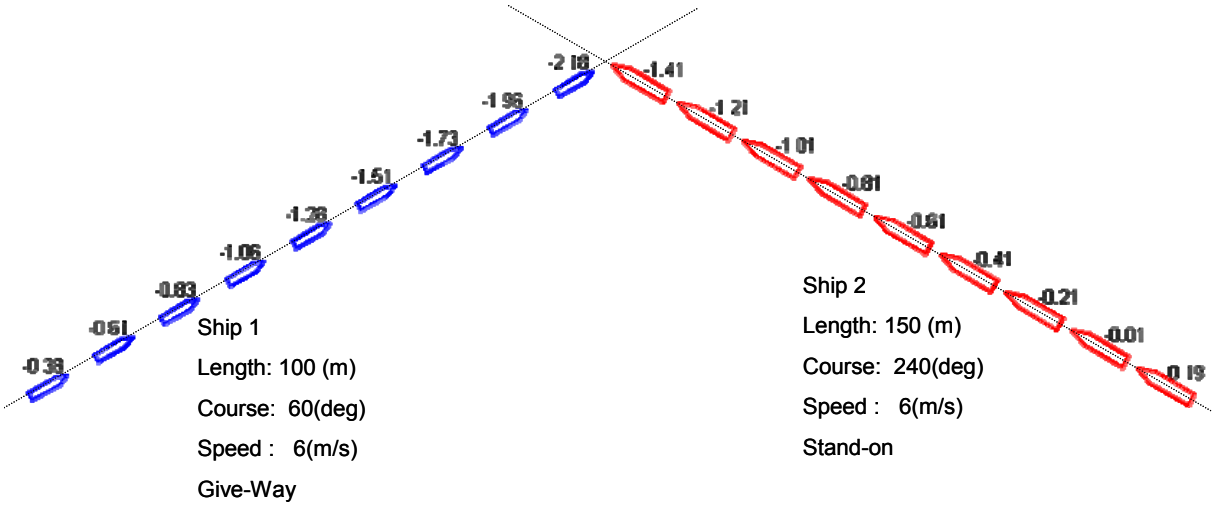

Fig.6.3 Variation of SJ Value in Crossing Encounter

The overtaking ship (Ship 1), with higher speed and activeness in the situation, has rather large value of SJ. In this case, due to the large difference in speeds, changing rate of target bearing is considerable, resulting in positive SJ value in all cases. Then, SJ value of overtaking ship should be used with care.

The overtaken ship (Ship 2), in spite of being stand-on vessel, is in "cautious" situation as overtaking ship is approaching, partly because of the passiveness and speed limitation. SJ value of this ship drops below safety threshold when the overtaking ship is approaching a too close situation.

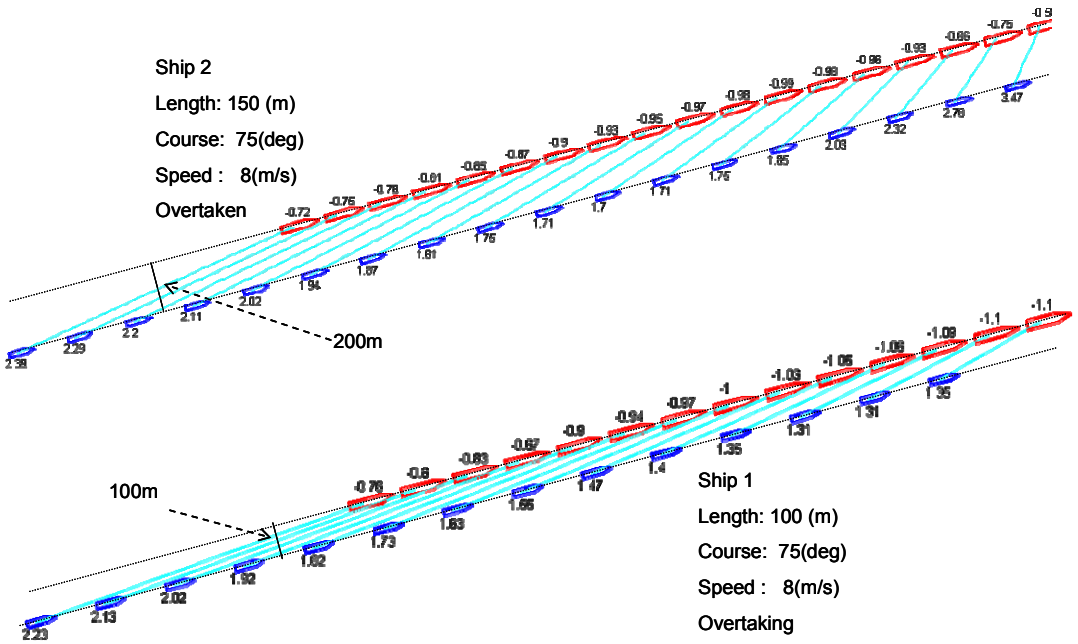

Fig.6.4 Variation of SJ Value in Overtaking Encounter

From these illustrations of SJ value evolution in approaching, it can clearly be seen that SJ value is an appropriate criterion for assessing risk of collision in ship-ship encounter. However,

as mentioned above, there are still cases where SJ value lacks the ability of representing the situation. A possible solution is to use in combination with SJ value other risk assessing criteria. Bumper Model, for example, can fulfill this shortage.

Attention should be paid in determining encountering situation that status of 2 ships in concern must strictly follow regulations defined in International Regulation On Collision Avoidance At Sea (Colreg 72).

6.1.3 Distribution of Dangerous Encounter basing on SJ value

Position, speed and course of targets tracked from Radar images have been used to assess the risk of collision between ships navigating inside Tokyo Bay. As mentioned in chapter 5, accuracy of positions tracked from radar pictures is seriously degraded by noise. The effects are worse for speed and course indirectly calculated from consecutive positions. Therefore, Kalman Filter is used to rebuild movement of targets before these data can be used.

6.1.3.1 Time Distribution of Dangerous Encounter

Time distributions of dangerous encounter assessed by SJ value criterion for 10 days of radar data are shown in figures 6.5 to 6.8 for different values of SJ.

The number of “Very Dangerous” encounters, as expected, is very small. These encounters are normally just the approaching of escorting ship or tug boat to the large vessel. The time distributions, however, still reveal the tendency that there are peaks at dawn (around 06:00) and sunset (around 18:00).

This tendency repeats also in other figures of time distributions. It agrees with the large number of ships entering the bay port system early in the morning (04:00-08:00) and ships leaving the bay late in the afternoon.

The number of cautious encounter is large, for all time during the day (Fig. 6.8). It is because of the famous congested condition of marine traffic in Tokyo bay. It requires that ships need to be fully aware of the condition while navigating in the bay.

It should also be noticed that the number of dangerous encounters (SJ < -1) or quite dangerous encounters (SJ < -1.5) is rather large. The problem should be taken into consideration in traffic managing and route designing, especially for the time where the peaks occur.

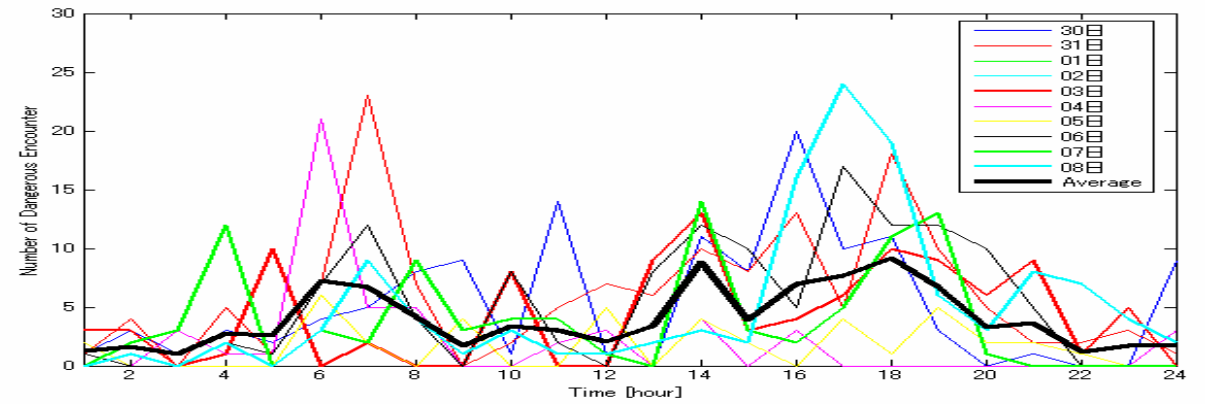

Fig.6.5 Number of Encounter in which SJ < -2

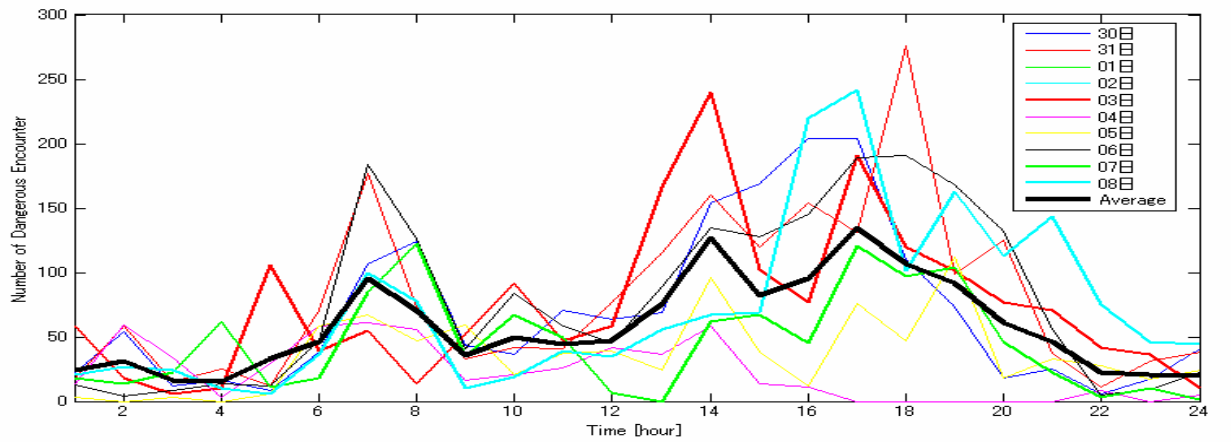

Fig.6.6 Number of Encounter in which SJ < -1.5

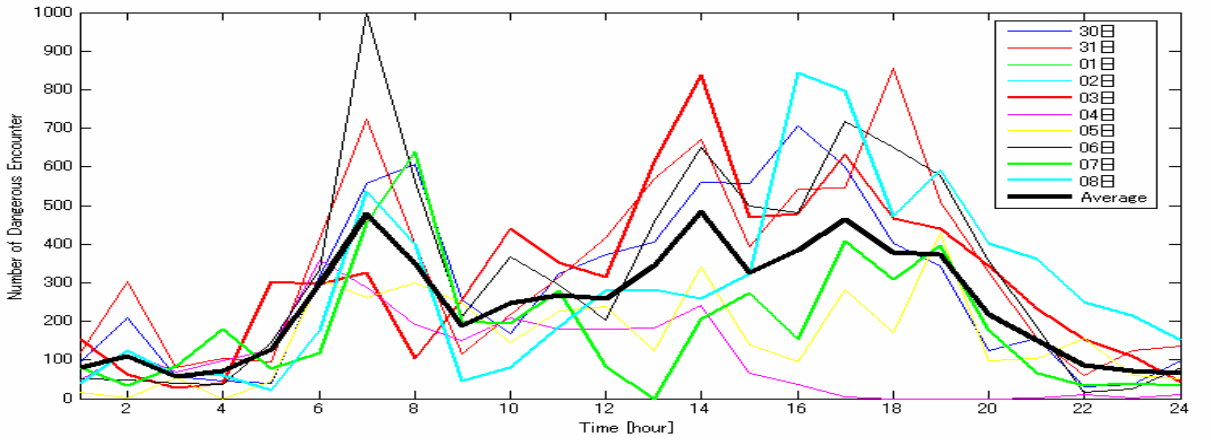

Fig.6.7 Number of Encounter in which SJ < -1

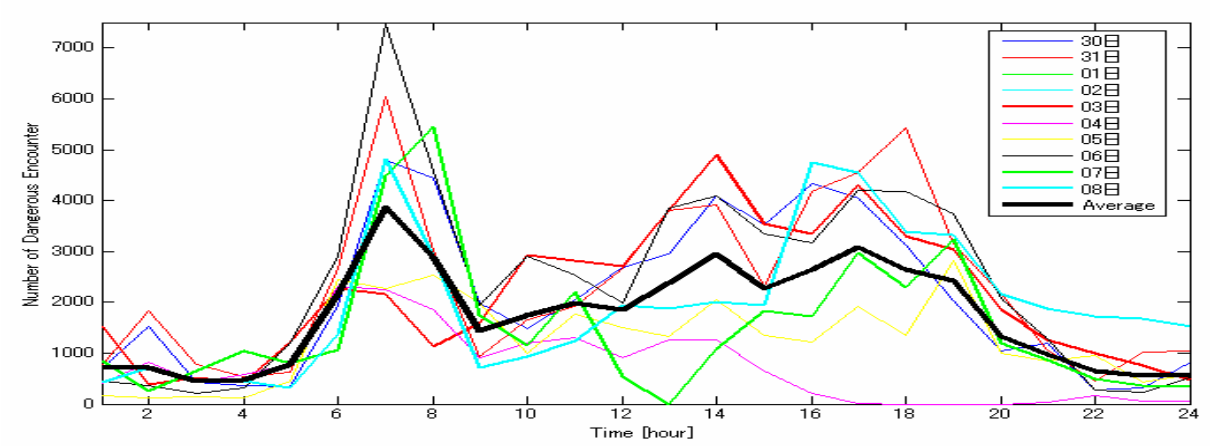

Fig.6.8 Number of Encounter in which SJ < 0

6.1.3.2 Spatial Distribution of Dangerous Encounter

To investigate the areas where frequency of dangerous encounter is higher, dangerous encounter have been plotted on the chart of Tokyo bay. Distribution results are shown in Fig. 6.9 to 6.12. The number of "Very Dangerous" encounters, as mentioned in previous section, is very small and mostly be the case involving service ship, therefore provide little information about the area that attention has to be paid. Shown in Fig. 6.9 is the whole day distribution of "very dangerous" encounters for 4 days. Due to the distribution similarity, 4 days data out of 10 days of continuous observation are shown.

Spatial distributions of dangerous encounters are shown in Fig. 6.10 for whole day data. For the same reason as mentioned above, 4 days data are used. It can clearly be seen that the dangerous encounter densely distributed along the main traffic flows of the bay. It is the northbound flow from northbound part Uraga Suido traffic route, via Nakano traffic route then through the east fairway to enter port of Tokyo and port of Chiba. The south bound flow, conversely, is via west fairway, clear from the shallow water region on the west of Nakano traffic route and enters south bound part of Uraga Suido.

Attention needs to be paid for areas on the entrances, exits of port of Yokohama and port of Kawasaki. Reason is simply be the large number of ships entering and leaving these important ports during the day.

The density of dangerous encounters is also high for east and west fairways region because many ships are crossing the main traffic flow to reach their destination ports. The dangerous crossing encounters can also be seen for ships leaving the northbound traffic flow to enter port of Kawasaki.

Spatial distribution, however, depends on time of the day and the time dependence is not proportional for different areas in the bay. Therefore, spatial distribution is plotted independently

for these 2 periods of time in which the peaks occur in Fig. 6.5 to 6.8. Distribution results are shown in Fig. 6.11 and Fig. 6.12.

In these 2 figures, the clear difference can be seen for north bound and south bound flows of traffic. In the morning time, peak of number of dangerous encounters occurs due to the large number of dangerous encounters in northbound traffic flow, while the dangerous encounters in south bound lane is very limited.

Between 16:00 and 22:00 period, difference is even clearer, but in the opposite way. Most dangerous encounter occurrences are in the southbound flow, especially at the entrance of and inside the south bound lane of Uraga Suido.

The fact can be kept in mind if virtual aid of navigation is applied to realize the concept of reversible traffic route in Uraga Suido.

a. “Very Dangerous” Encounters

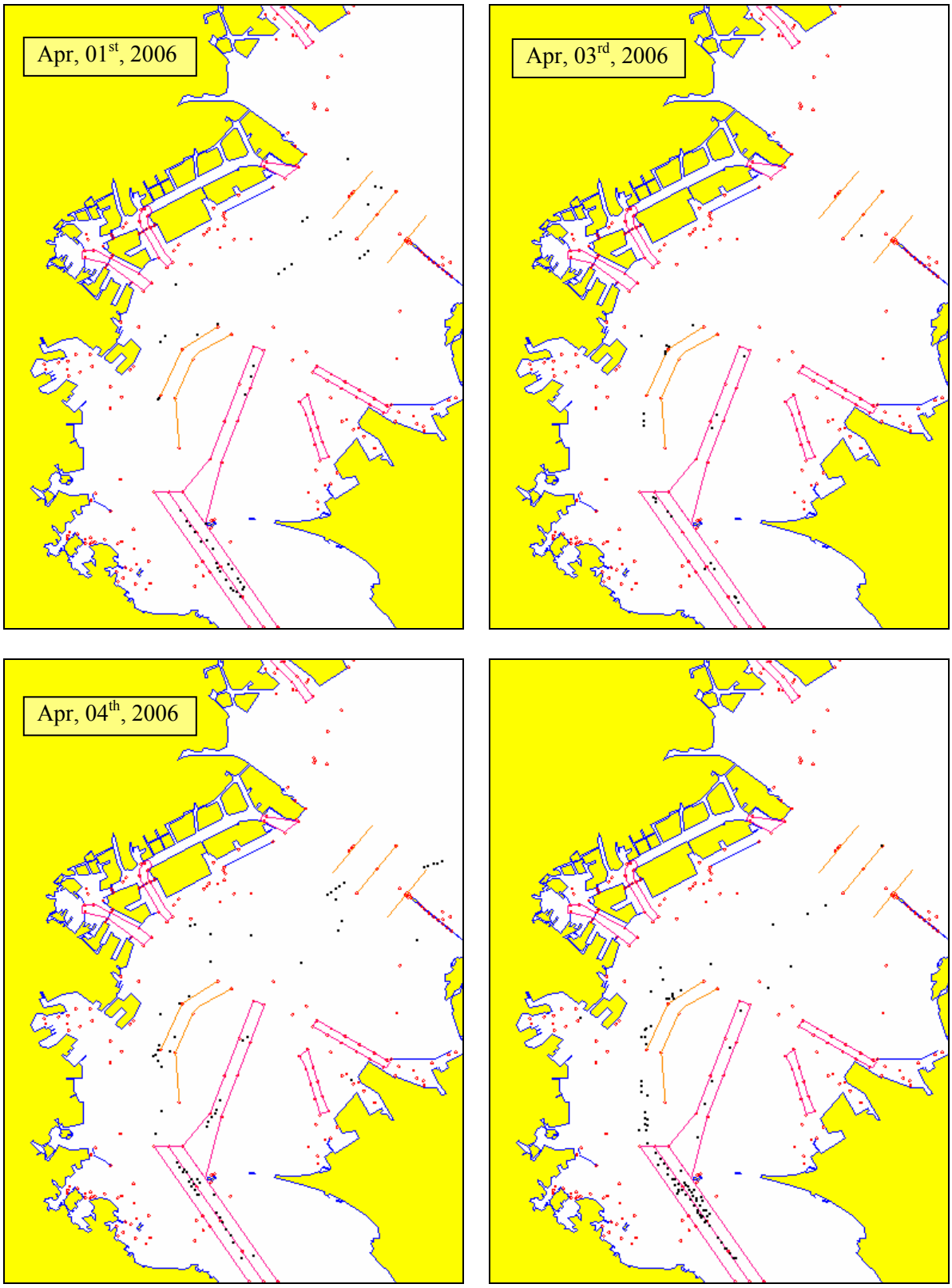

Fig. 6.9 Whole day “Very Dangerous” Encounters (SJ<-2)

b. “Dangerous” Encounters

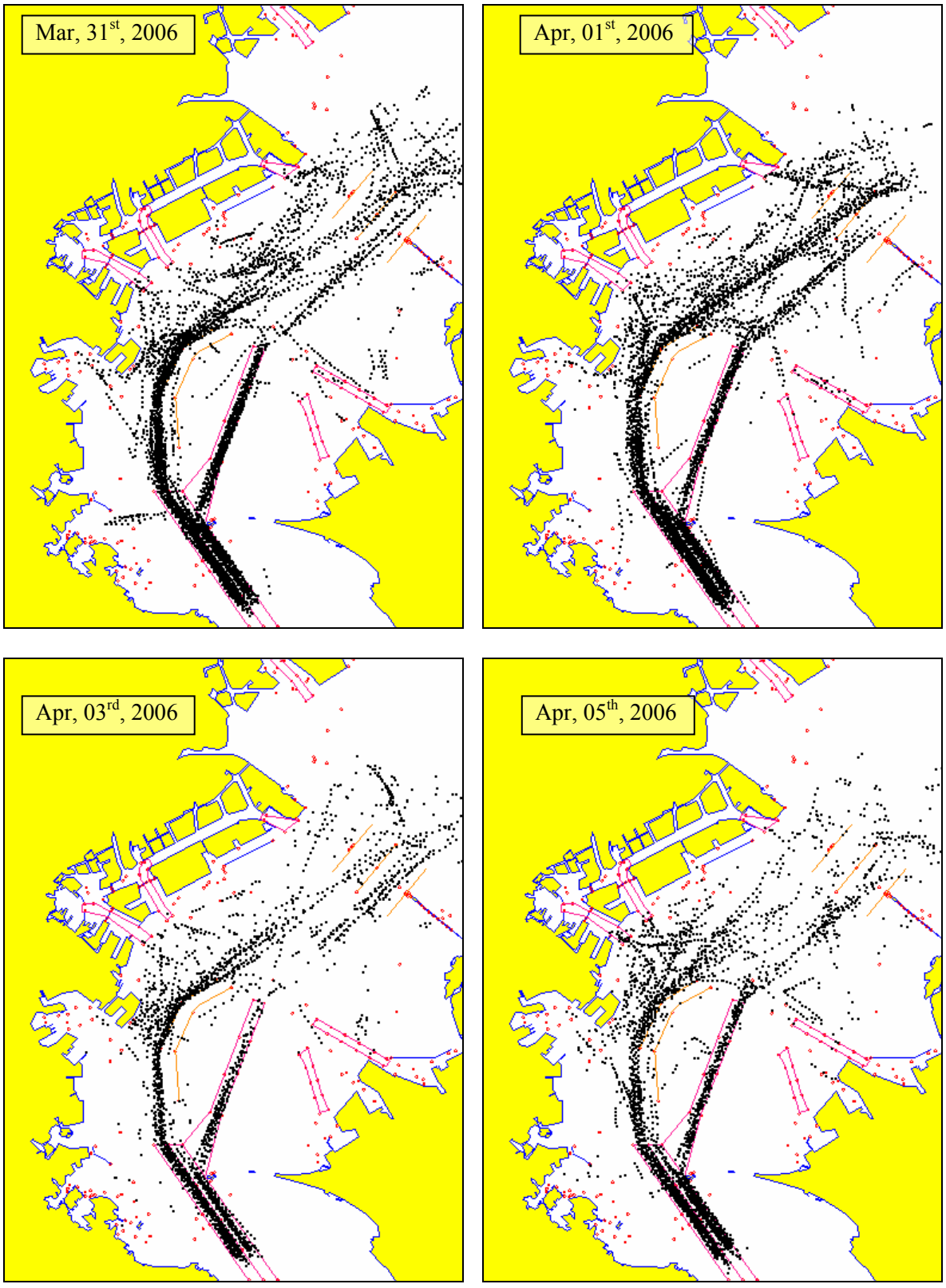

Fig. 6.10 Whole day Dangerous Encounter Distribution (SJ<-1)

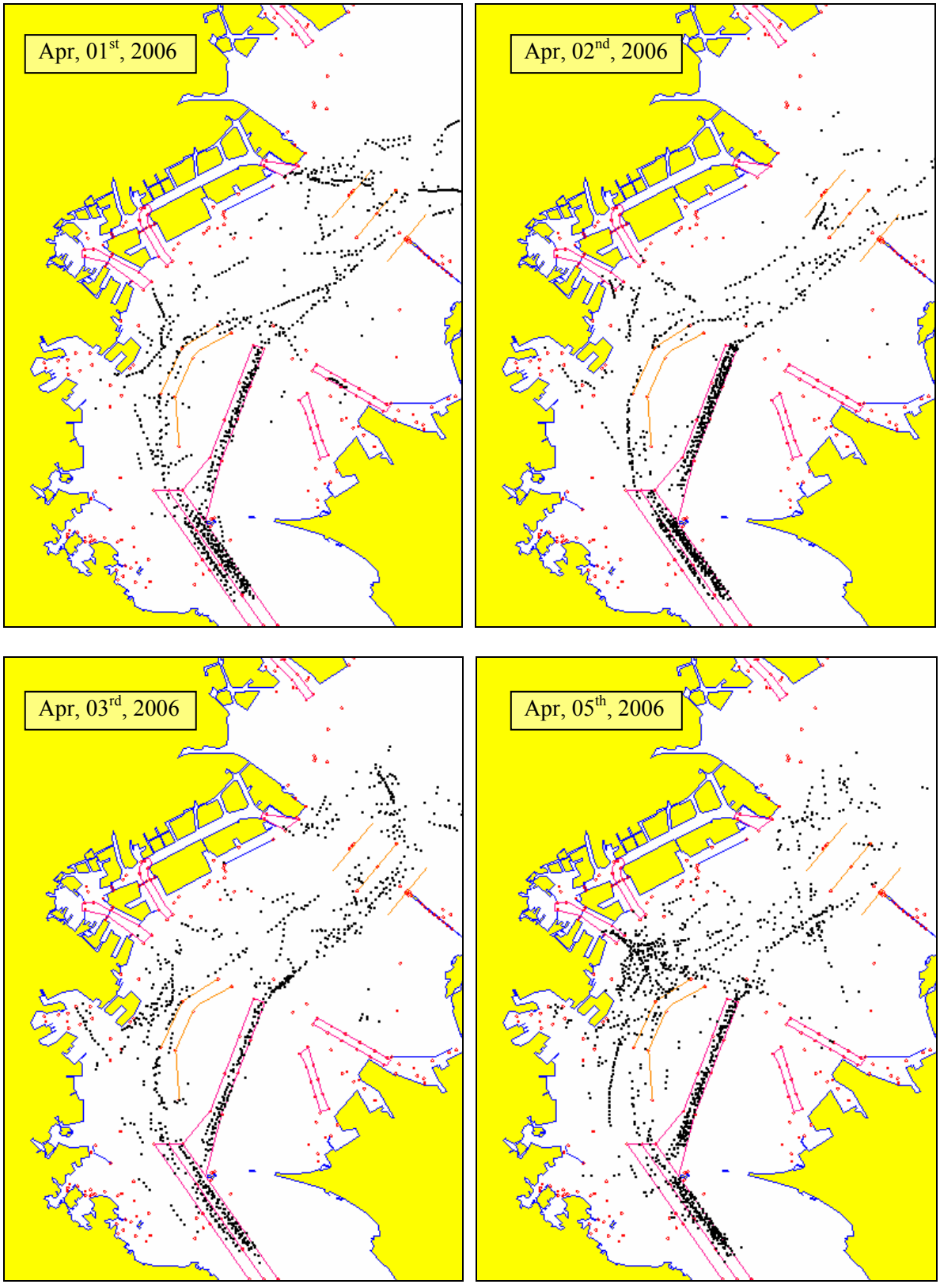

Fig. 6.11 Dangerous Encounter Distribution during 04:00 to 08:00 Period (SJ<-1)

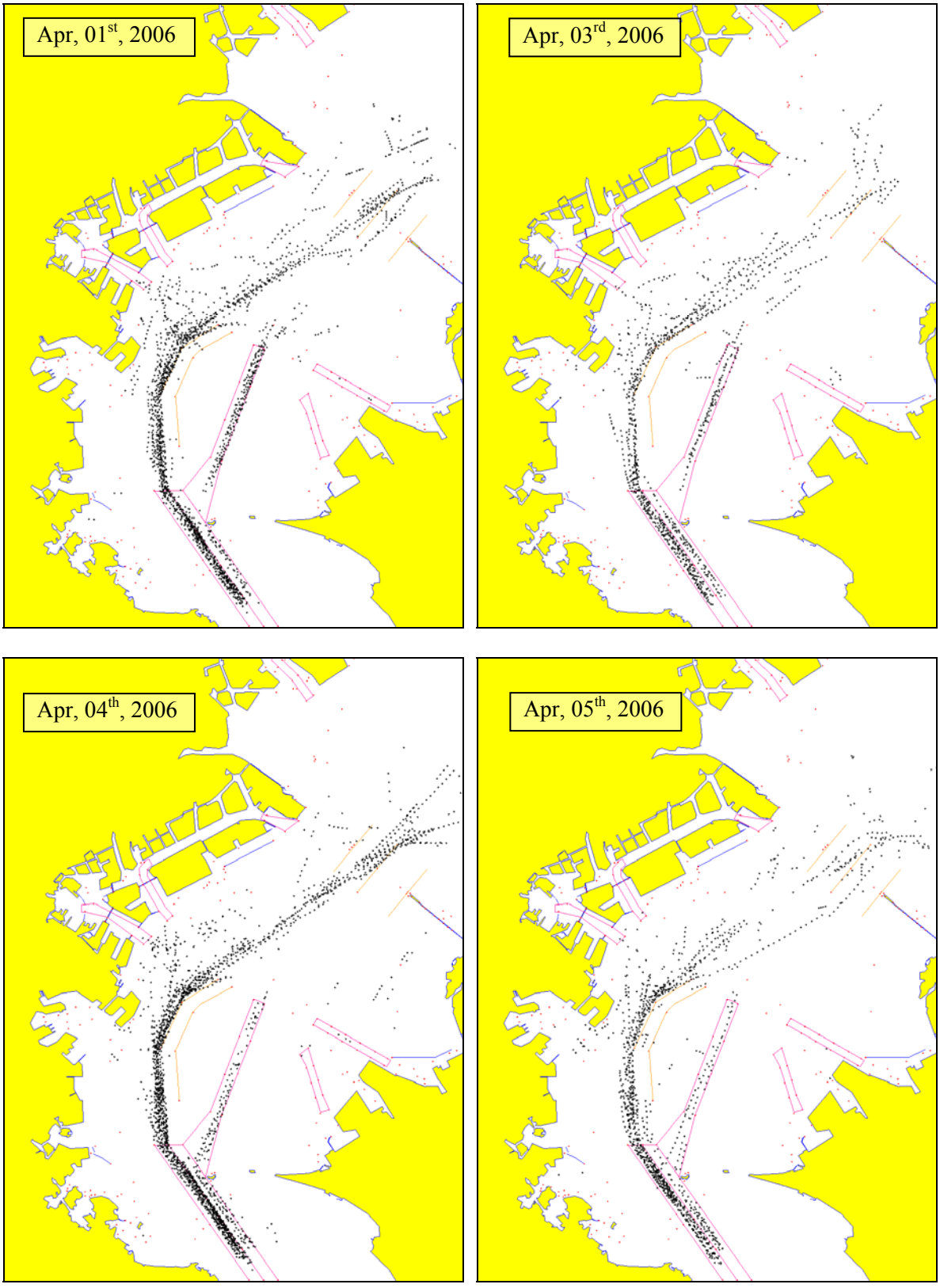

Fig. 6.12 Dangerous Encounter Distribution during 16:00 to 22:00 Period (SJ<-1)

6.2 Evaluation of Collision Risk by Bumper Model

6.2.1 Definition

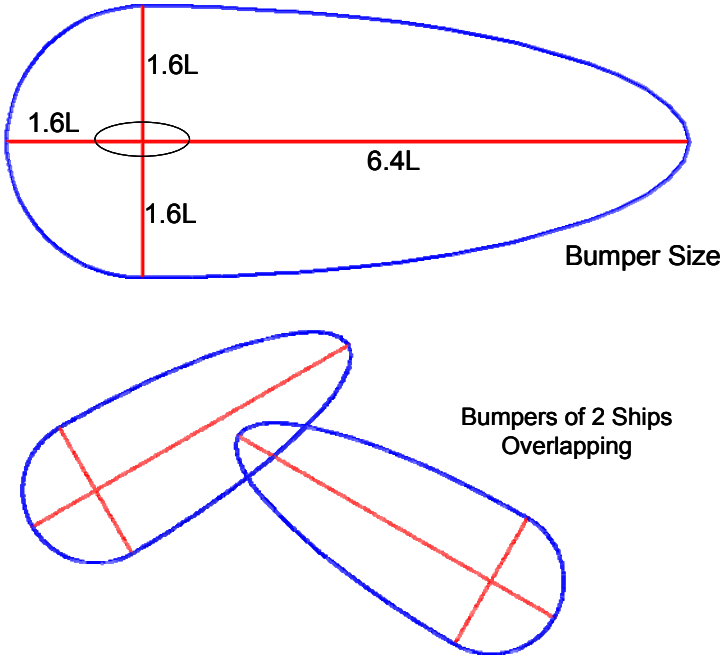

Fig. 6.13 Bumper Model and Bumper Overlap

For simple checking and assessing risk of collision, Bumper Model has long been suggested and in use. Using the model, watching region for safe navigation of a ship is assumed to be the "Bumper" defined in Fig. 6.13. The bumper consists of 2 parts separated by the ship's traverse axis. The bow part is a half of an ellipse along its major axis. Size of the ellipse is 6.4L for the semi-major axis and 1.6L for semi-minor axis. Stern part of the bumper is a half of the circle of 1.6L in radius. Here, L is length of the ship in concern.

As the name itself has implied, bumpers of 2 ships should not overlap each other. When it is the case (see Fig. 6.13), the 2 ships are considered to be in risk of collision and avoiding action should be taken as quickly as possible.

A part of the watching region inside Tokyo Bay is shown in Fig. 6.14, where the Bumper Model is used for collision risk assessment. Positions of ships, of which the bumpers overlap, are marked with a red circle for easy recognition.

It is obvious that in risk assessing using Bumper Model, the ship's speed is not taken into account. It is actually a limitation of the approach because even if the bumpers are overlapping, risk of collision still has a wide range, depending on the time left for maneuver.

Another deterrence of bumper shape above is that collision risk for the 2 ships is the same, regardless of its status (overtaking, give-way, stand-on, etc.) according to Colreg.

Therefore, Bumper Model should be used in combination with other available criteria for the best result.

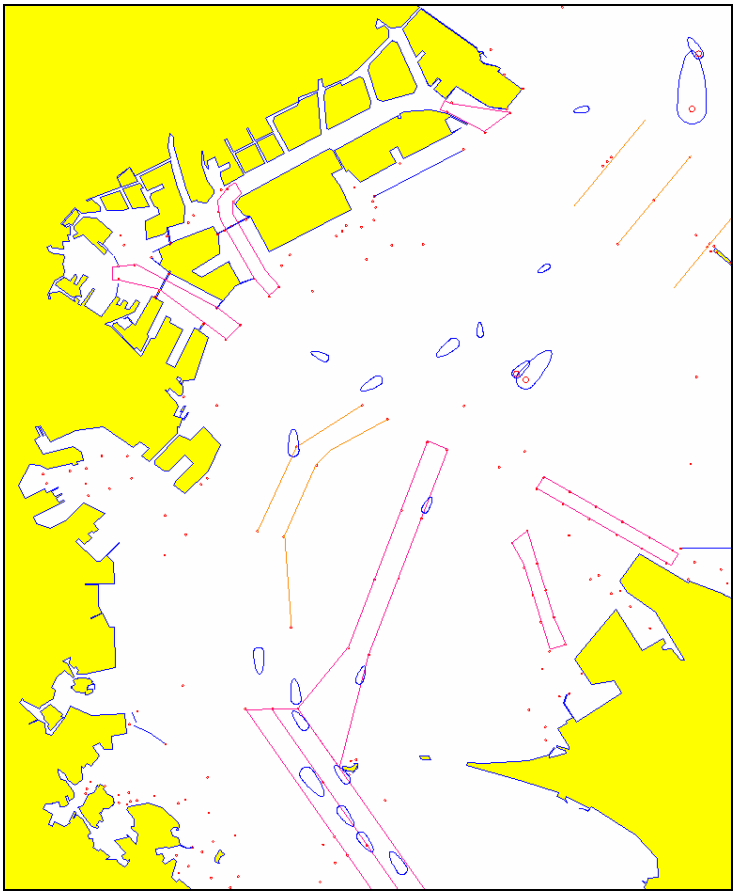

Fig. 6.14 Bumper Model in Use

6.2.2 Distribution of Bumper Overlapping Target

6.2.2.1 Time Distribution of Bumper Overlapping

Shown in Fig. 6.15 is the time distribution of bumper overlapping encounters for 10 days data that have been used for risk assessment basing on SJ criterion (section 6.1) and the average value of these 10 days.

Using bumper criterion, tendency of dangerous encounters variation is also revealed. The number of dangerous encounter considerably increases for the 04:00 to 08:00 period. Another increase, though not very clear, is in existence for late afternoon time till 22:00 in the evening.

The number of overlapping encounter is quite large, causing the concern of ensuring safe navigation in the bay, especially for these “rush hour”. The risk estimation, using Bumper model agree well with the SJ value criterion as shown in figures 6.5 to 6.8. Bumper value can be used together with SJ to produce the full assessment of collision risk as it compensates for the shortage of SJ value criterion as mentioned in the section relating to SJ.

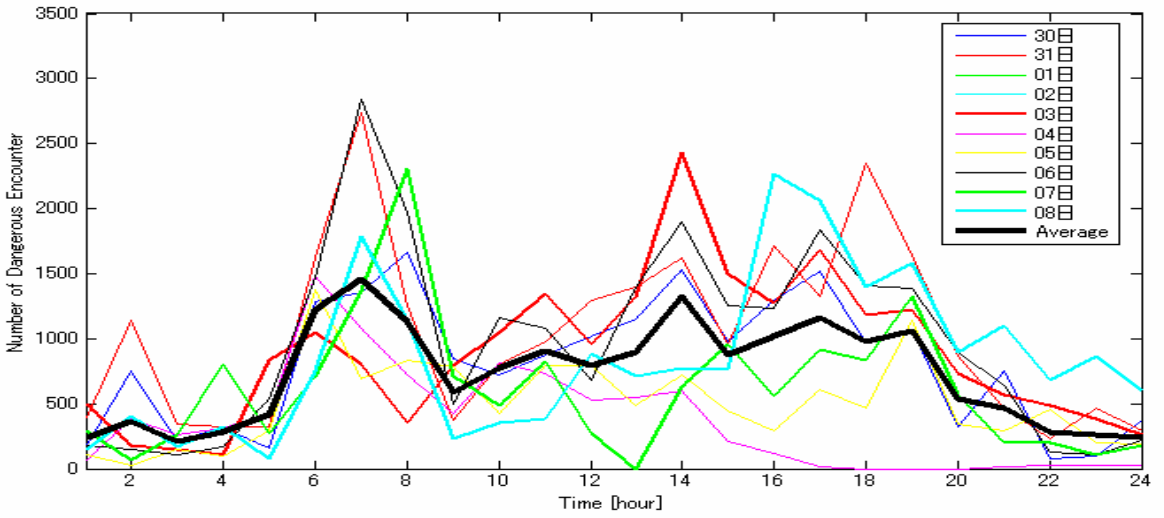

Fig.6.15 Time Distribution of Bumper Overlapping Encounter

6.2.2.2 Spatial Distribution of Bumper Overlapping

Bumper Overlapping encounters are plotted on the chart of the bay to distinguish the waters on which marine safety needs more attention.

Spatial distributions of dangerous encounters have shown regions where the number of dangerous encounter is high, including the traffic main flows, entrances of ports of Yokohama, Kawasaki, Kisarazu and east and west fairways area.

Using Bumper Model for risk of collision assessment, the clear difference can also be seen in the distribution of dangerous encounters for the north bound and south bound traffic flows in morning and late afternoon rush hours. Tendency of distribution changing is similar to those got from previous section, using SJ value. In the morning (04:00 to 08:00), dangerous encounter density is very high for north bound traffic flow, especially in the north bound lane of Uraga Suido while the density is much lower for the south bound lane. In the early evening (16:00 to 22:00), dangerous encounter density in south bound flow is much higher than that in the north bound traffic.

Difference of the 2 approaches of risk assessment is noticeable if attention is paid to the distribution of dangerous encounters in the traffic flow. It is because of the limitation of SJ value when used for the overtaking encounters. The Bumper Model, however, has its limitation as the speeds of 2 ships are not taken into account, so, it is difficult to differentiate risk of collisions between ships approaching at different speeds. Therefore, Bumper Model should be used together with other criteria for adequate risk assessment.

In comparison with Bumper Model, SJ value has the advantage that tendency of changing of SJ value is also available and can be used as the first clue of coming dangerous encounters (i.e. if SJ value is decreasing steadily, target ships should be carefully followed).

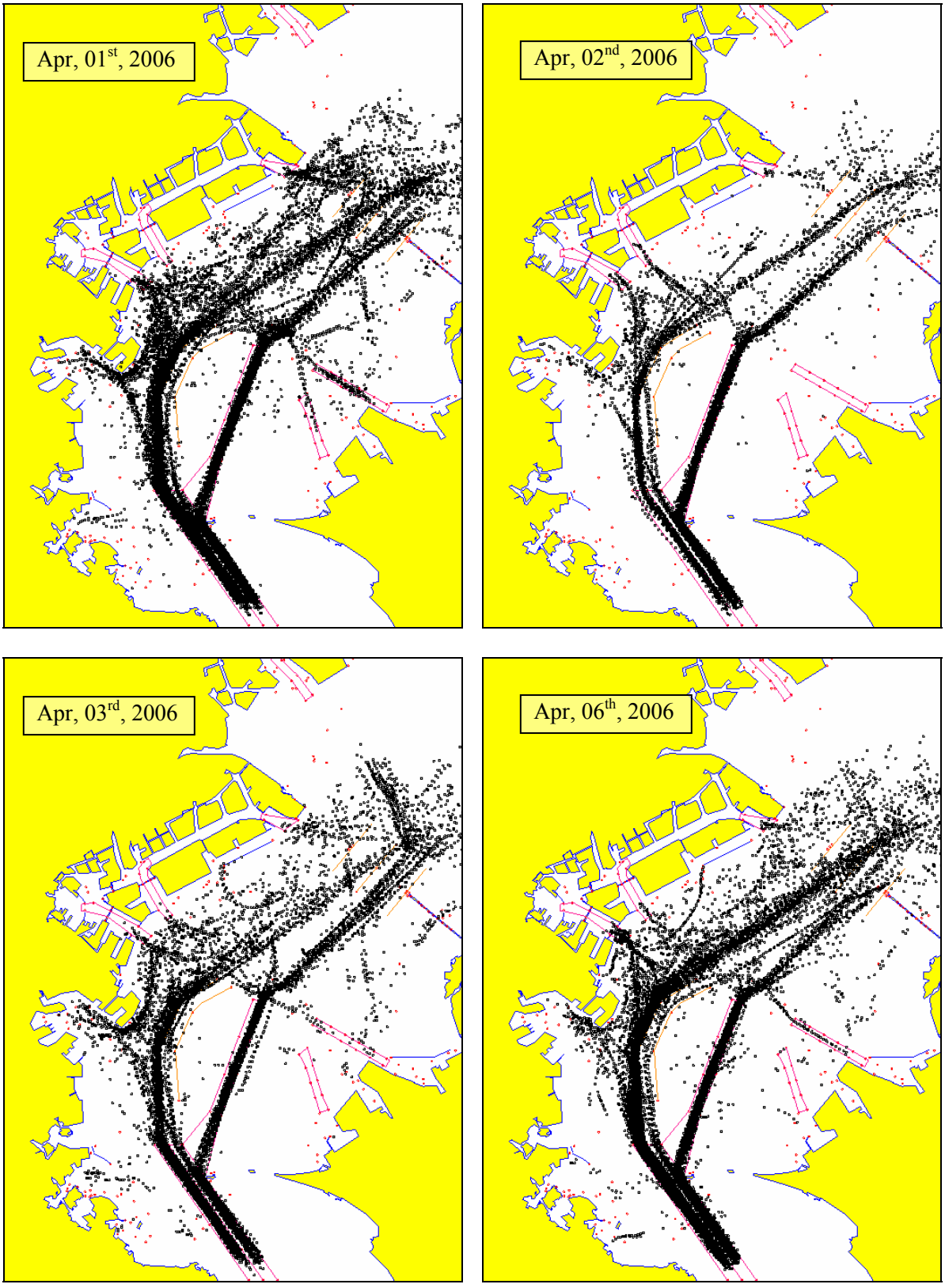

Fig. 6.16 Whole day Bumper Overlap Distribution

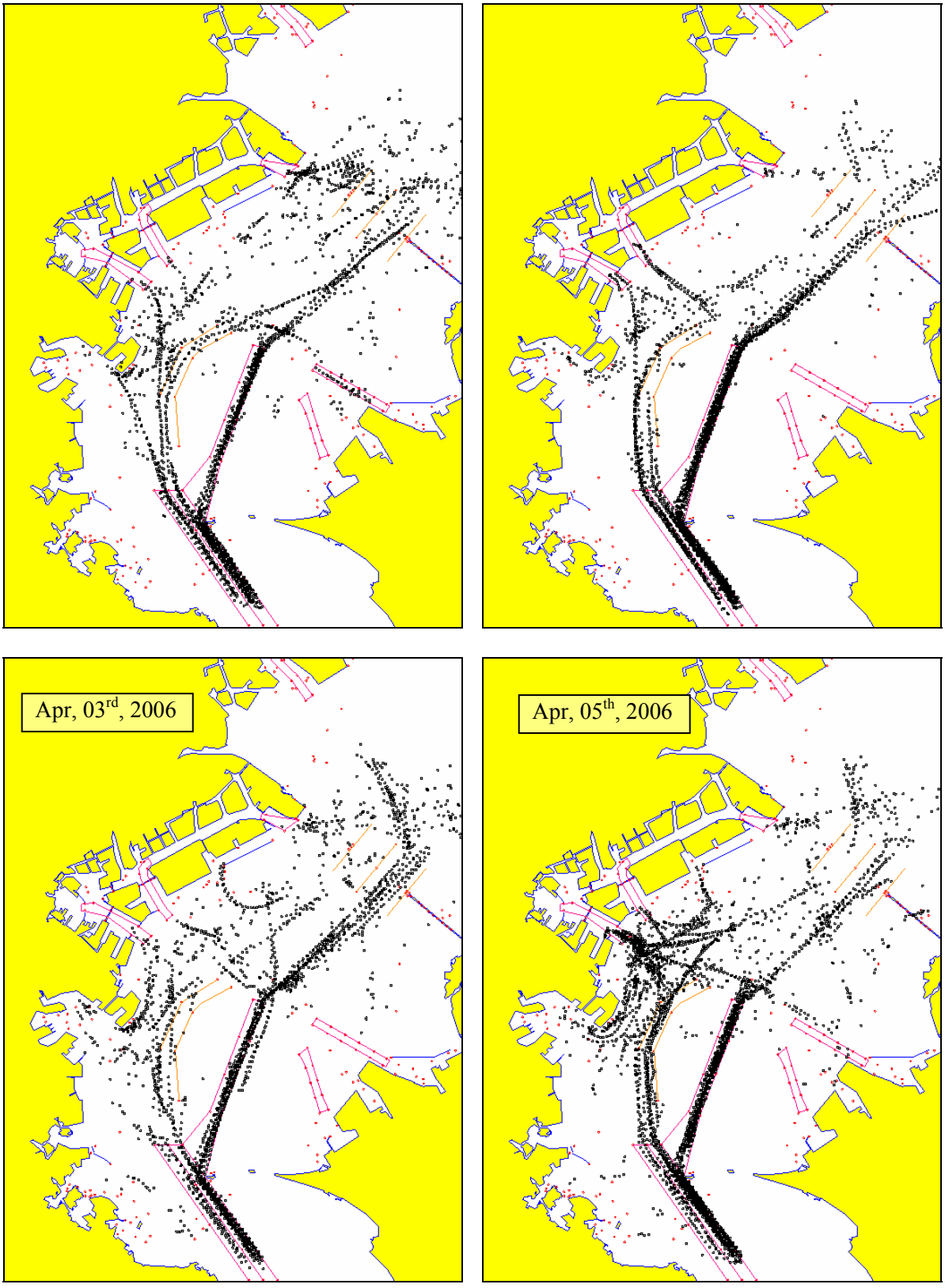

Fig. 6.17 Bumper Overlap Distribution during 04:00 to 08:00 period

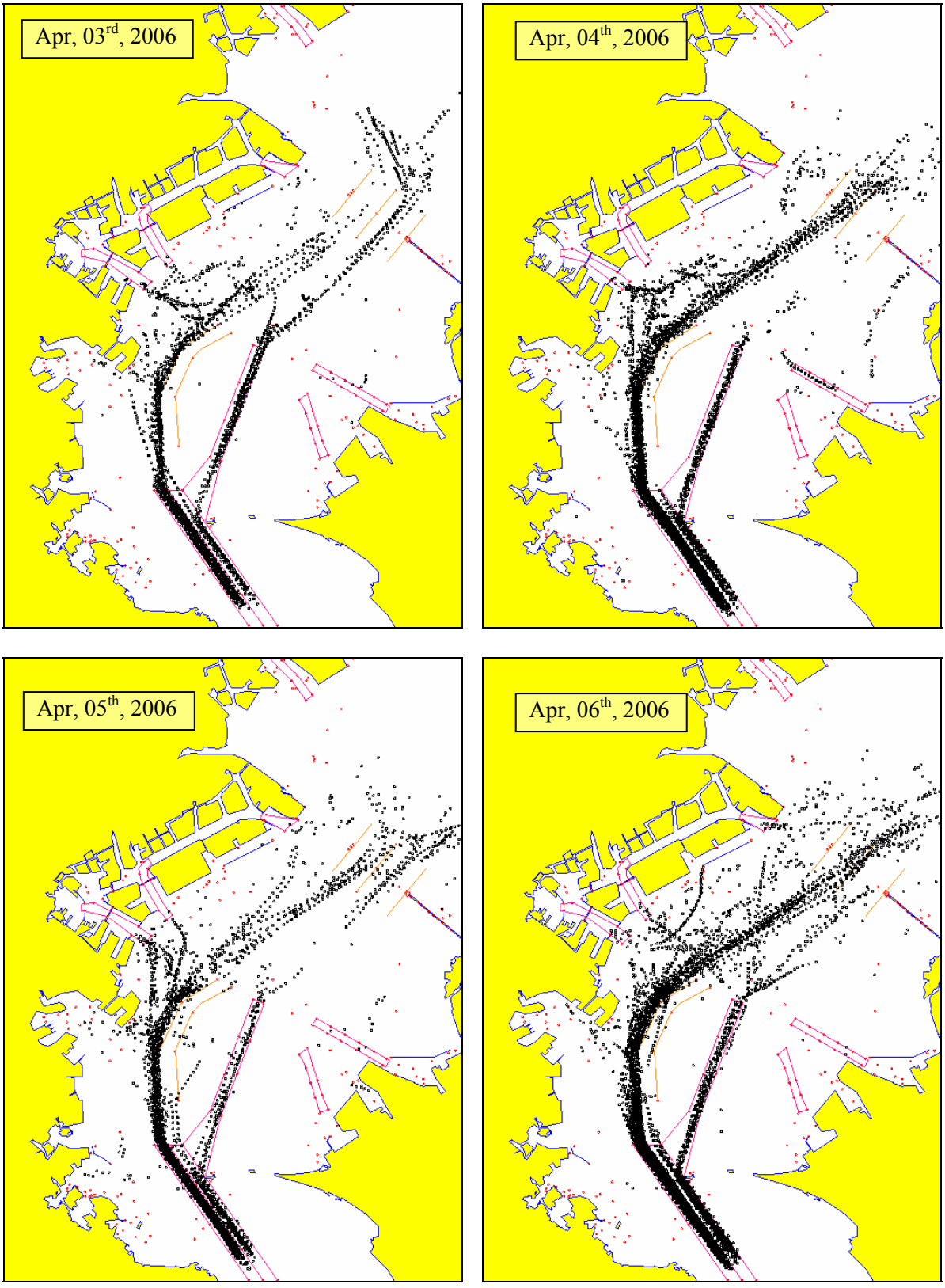

Fig. 6.18 Bumper Overlap Distribution during 16:00 to 22:00 period

6.3 Evaluation of Collision Risk by DCPA and TCPA

6.3.1 Definition

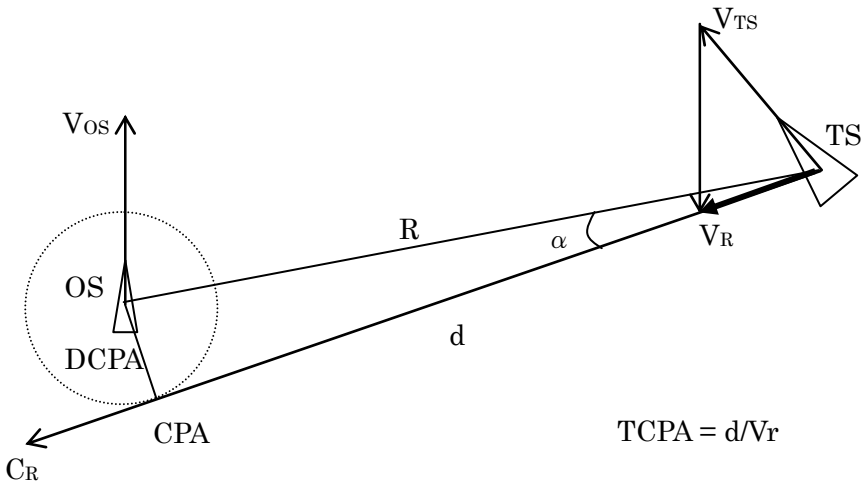

Fig. 6.19 DCPA, TCPA Calculation

DCPA/TCPA criterion may be the most popular method used by navigators while considering risk of collision between the own ship and a target ship. The core of the criterion is to ensure that the two ships will pass each other at a "Safe Distance". When the distance is less than a certain value, collision avoiding action must be made. In this case, the action should be taken a period of time before 2 ships reach the closet point of approach. There arises the name of criterion.

DCPA = Distance to the Closet Point of Approach

TCPA = Time to the Closet Point of Approach

Principle of calculation of TCPA, DCPA is illustrated in Fig. 6.19, where vector of relative velocity between 2 ships are calculated from velocity vectors of these 2 ships. DCPA is then normalized with the ship's length to get the non-dimensional DCPA.

If R is distance between own ship and the target ship and α is the angle between vector of relative speed and two ship's bearing (as shown in Fig. 6.19), then DCPA, TCPA can be calculated as followings:

DCPA = R x Sin(α)

TCPA = R x Cos(α)/Vr

Normalized DCPA ($DCPA^*$) = DCPA/{(L_OS+L_TS)/2}

where L_OS, L_TS are lengths of own ship and target ship respectively.

Two ships are considered to be in risk of collision if $DCPA^* < 3.2$ and TCPA <= 5 minutes. The criterion is usually used by navigators in collision risk assessment and calculation of avoiding action (course and/or speed change).

DCPA/TCPA criterion has, however, the limitation that the relative bearing of CPA is not taken into account. This disagrees with the common knowledge of navigators that risk of collision, as perceived by officer of watch, depends also on relative bearing of approaching.

6.3.2 Distribution of Dangerous Encounter, Basing on DCPA and DCPA

Spatial distributions of dangerous encounters, using DCPA, TCPA as assessment criterion are shown in Fig. 6.20. Due to the consistency with the dangerous distributions when SJ value and Bumper Model are used, data of 1 day is shown for the different time periods. Higher density of dangerous encounters distribution can clearly be seen along the main traffic flows of the bay. In morning rush hour, the northbound flow from northbound part Uraga Suido traffic route, via Nakano traffic route then through the east fairway to enter port of Tokyo and port of Chiba, experiences congested traffic condition, representing in the large number of dangerous encounter. The distribution is, conversely, high in late afternoon rush hour for the south bound flow via west fairway, clear from the shallow water region on the west of Nakano traffic route and entering the south bound part of Uraga Suido.

As mentioned earlier in this section, limitation of the DCPA, TCPA criterion is that the aspect of own ship and target ship is not taken into consideration. Therefore, the criterion is less suitable for the purpose of traffic analyzing in congested waters. However, due to the easy in calculation and application, DCPA, TCPA is still commonly used by officer of watch as reference for ship maneuvering decisions.

In comparison with DCPA, TCPA criterion, SJ value has another advantage that the tendency of changing of SJ value is also available and can be used as the first clue of coming dangerous encounters. Therefore, rather than being used alone, DCPA, TCPA should be used as a complementary criterion that fulfills the limitation of SJ value or Bumper Model criteria to ensure the absolute safety of navigation.

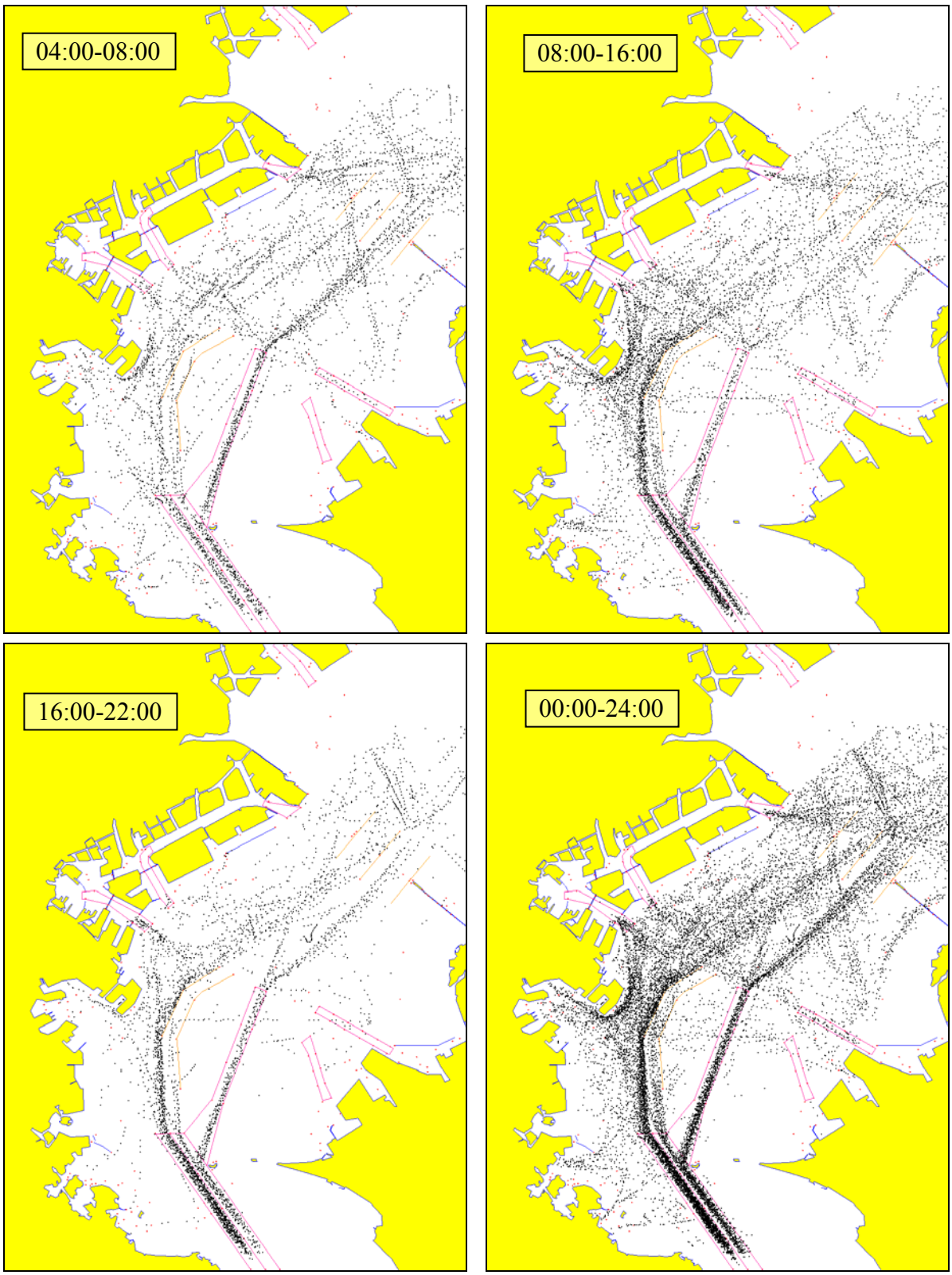

Fig. 6.20 TCPA/DCPA Dangerous Encounter Distribution

6.4 Other Characteristics of Marine Traffic in Tokyo Bay

6.4.1 Route-Use-Ratio of the Traffic Separation Scheme

Route-Use-Ratio is the ratio of total area covered by the bumpers (bumper form and size is discussed in section 6.2) of ships navigating in a route at a certain time and the area of the route itself. From the Route-Use-Ratio, a clear picture of the "busy" of route can be seen. As defined earlier, formula for route use ratio calculation is:

$$UR = \frac{\sum_{1}^{n} 6.4\pi L_i^2}{A}$$

where

A: the area of the route

Li: Length of ship number i navigating in the route

Area of a bumper can be calculated from the ship length as followings:

$$\begin{aligned} S_i &= 0.5 \times AreaOfEcllipse + 0.5 \times AreaOfCirle \\ &= 0.5 \times \pi \times 1.6 \times L_i \times 6.4 \times L_i + 0.5 \times \pi \times (1.6 \times L_i)^2 \\ &= 6.4 \times \pi \times L_i^2 \end{aligned}$$

Route-Use-Ratios of north, south bound lanes of Uraga Suido traffic route and Nakano traffic route have been calculated and the results are shown in figures 6.21 to 6.23 for 10 days data and average Route-Use-Ratio of those 10 days.

From Fig. 6.21 and Fig. 6.23, it is obvious that there is a peak at the period from 04:00 to 08:00. During this period, Route-Use-Ratio of North Bound Lane of Uraga Suido can be as high as 0.53, which means that the area left for maneuver is dangerously restricted. The fact, as explained earlier, is due to the large number of ship entering the bay ports early in the morning. For Nakano traffic route, the ratio can be up to 0.48. In comparison with Uraga Suido, Nakano traffic route seems to be less congested because just around 70% of the ships entering Nakano traffic route from the north bound lane of Uraga Suido. After this period, Route-Use-Ratio decreases gradually. In the late afternoon and during night time, Route-Use-Ratio is around 0.1 or less. Therefore, pressure of traffic density to navigators is considerably reduced.

For the south bound lane of Uraga Suido, the highest Route-Use-Ratio occurs late in the afternoon due to the large number of ships leaving ports in the bay through the lane. The period lasts form around 16:00 to 22:00. In this period, the highest ratio can be witnessed to be well over 0.5 and the route, as a result, is congested. The density reduces at midnight onward before gradually increases again around noon the following day. During this period, average route use ratio is less than 0.2 and the highest ratio is commonly less than 0.3.

Contrary tendencies of Route-Use-Ratio in north bound and south bound lanes of Uraga Suido traffic route makes it possible for the application of reversible route concept where the width of each lane is changed in a time base to fit the actual traffic conditions.

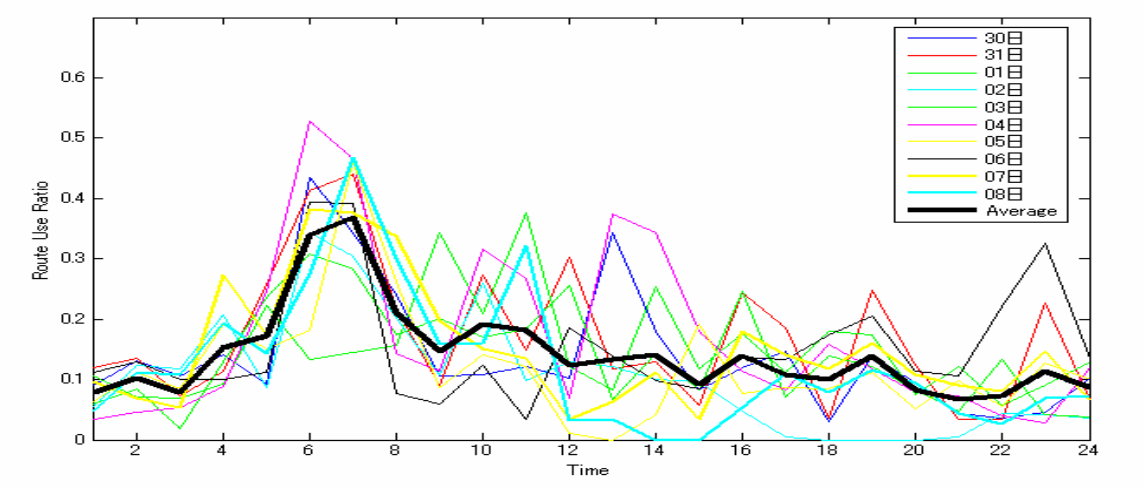

Fig. 6.21 Route Use Ratio of North-Bound Lane of Uraga Suido

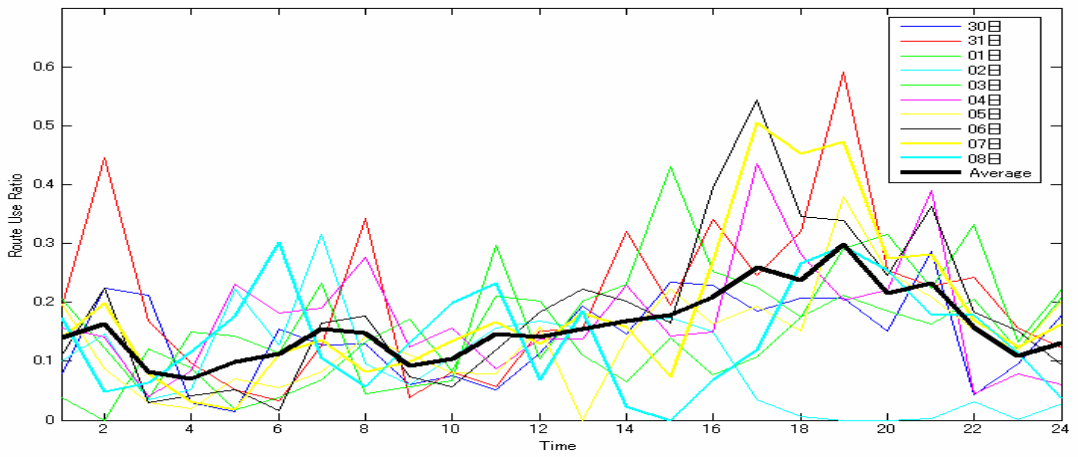

Fig. 6.22 Route Use Ratio of South-Bound Lane of Uraga Suido

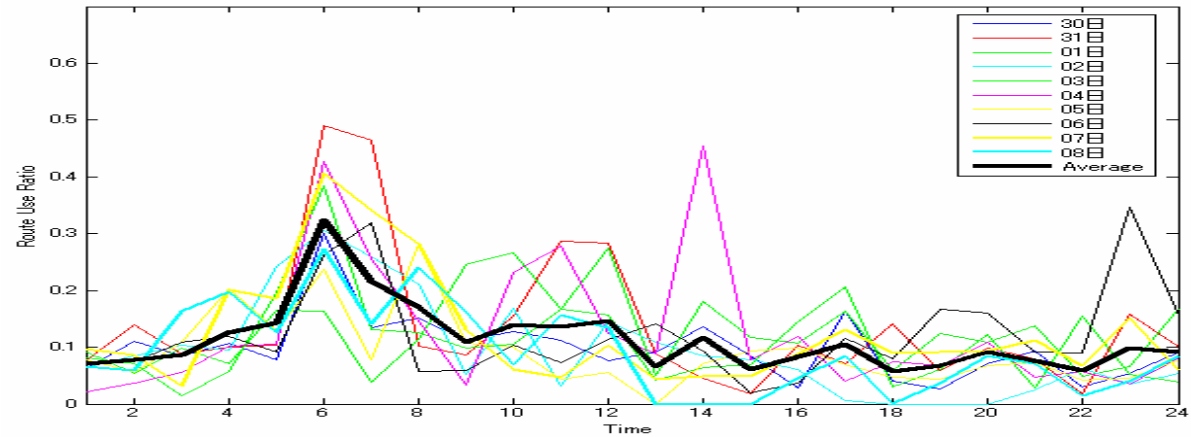

Fig. 6.23 Route Use Ratio of Nakano Traffic Route

6.4.2 Speed Distribution for Different Length Ships

Fig. 6.24 shows the distribution of speed of ships navigating in the bay. Different graphs have been drawn for different ship length. Most of the ships navigate at the speed from 8kts to 14kts. Keeping in mind the limit speed in Uraga Suido and Nakano traffic to be 12 kts, it is seen that some ships actually navigate at higher speed than that allowed. Speed over 15 kts is also seen for ship in south bound traffic flow before entering Uraga Suido.

From the Fig., it can be seen that there is almost no difference in speed distribution of ships of over 100m length. Average speed of ship from 50 to 100 meter is a little smaller, with most ships navigating at around 11kts.

The lowest average speed is for ships less than 50 meter in length. However, some ships of this type may sail at the speed over 20kts. These may be the service high speed motor vessel or high speed crafts.

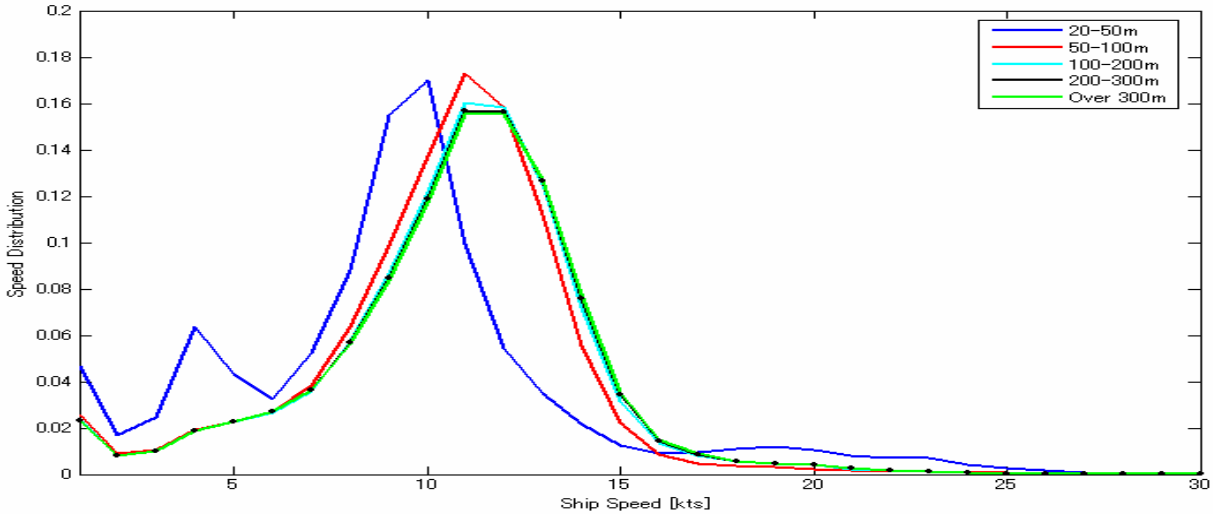

Fig.6.24 Speed Distribution

6.5 Conclusion

The chapter is an investigation in detail of the collision risk of marine traffic in Tokyo Bay. For risk assessment, different criteria have been used, including the SJ value, Bumper Model and DCPA/TCPA criteria.

Study result has shown areas of high risk of collision in the bay and time of high number of dangerous encounters in a day. Appropriate look out should be taken by the navigators while navigating in or crossing the traffic flow.

It is obvious from the figures that the time distributions of dangerous encounters, as well as available space for maneuver are inversely proportional. The highest density of dangerous encounter is from 04:00 to 08:00 for north bound traffic flow and 16:00 to 22:00 for south bound traffic flow. The fact should be taken in mind for route designing or carrying out traffic management (application of revertible traffic route, for example).

Each risk assessment criterion has its own advantages and disadvantages. Therefore, they should be used in combination to ensure the absolutely safe navigation.

Later in the chapter, Route-Use-Ratio for the important traffic routes in the bay and speed distribution of the ships navigating in the bay are taken into consideration for the same purpose. The peaks of route use ratio for the northbound lane and south bound lane of Uraga Suido traffic route can be witnessed in morning rush hour and late afternoon rush hour respectively. The Route Use Ratio difference between the 2 lanes is also most noticeable in these two rush hour period. The fact can be thought of as a motivation for applying a dynamic traffic separation scheme for the area.

Chapter 7. Conclusion and subjects for future study

This master thesis is a study on the efficiency enhancement of automatic radar tracking of targets navigating inside Tokyo Bay. Then, the targets' movement data is used for analyzing bay marine traffic. Focus of the study is on the radar and AIS based automatic traffic observing system having been applied and put into operation for visualizing the marine traffic in the bay. Using the observing results, some aspects of marine traffic flows are analyzed with the aim of estimating the critically congested areas of navigation and producing suggestions for traffic route designing as well as traffic management.

7.1 Conclusions

In the study, an approach for automatic tracking has been suggested and applied to track targets from sequential radar pictures. Using the approach, searching area is defined basing on common knowledge of ship's movements, including the normal speed and course changing in the time interval between radar pictures. Then, for matching, the Relating-Function is used as a matching criterion. This function takes into account the heading difference, size ratio and distance ratio of image positions in concern. From observation, threshold values of the Relating-Function have been decided as followings:

- For target acquisition: -0.85
- For target following: -0.6

In order to track targets in overlapping, a simple algorithm is used, in which the overlapping position is shared between 2 targets if overlapping case has been confirmed.

When AIS data is available, a method of using available AIS data to increase the automatic tracking efficiency for target equipped with AIS has been introduced. A matching algorithm has been suggested and used to match AIS data of ships equipped with AIS to radar targets tracked from Radar screen. A Relating-Function is used for this task with the threshold value decided to be 1.5. Then, the Relating-Function for 3 image positions relationship is slightly modified to take the advantages of the course and speed over ground as provided by AIS. Using this formula, Relating-Value becomes more converged (more reliable), then, the threshold value to be -0.8 can be chosen for target following. Using this approach, more than 80% of ships equipped with AIS can be tracked accurately.

Later, comparison is made between AIS provided position and position on radar image of AIS-Radar target to estimate the effect of ships' aspect to their deviation on the Radar screen.

Targets' movements tracked from radar pictures are, however, seriously affected by noise. Therefore, a Kalman Filter is used to rebuild the motion of targets tracked from radar screen. To decide the suitable values of designing parameters of the Kalman filter, the performance indices

have been chosen and experiments have been carried out with data of a model ship. Then, these values are chosen as followings:

- R_val = 2 (covariance of error of position measurement)
- Q_val = 0.3 (covariance of error of modeling)
- P_val = 1000 (initial covariance of error)
- T = 3

The values above can be used to rebuild motion once targets have been tracked to give speed and course information less affected by noise.

Kalman Filter, with some modification, can also be used for target following. For this purpose, the above parameter can still be used, together with additional parameter for filtering the image size (represented by the number of pixel in the image).

The last chapter is an investigation in detail the of collision risk of marine traffic in Tokyo Bay. For risk assessment, different criteria have been used, including the SJ value, Bumper Model and DCPA/TCPA criteria. Calculation results have shown areas of high risk of collision in the bay and time of high number of dangerous encounters in a day. Proper look out should be taken by the navigators while navigating in or crossing the traffic flow. The highest density of dangerous encounter is from 04:00 to 08:00 for north bound traffic flow and 16:00 to 22:00 for south bound traffic flow. The fact should be taken in mind for route designing or carrying out traffic management (application of revertible traffic route, for example).

Each risk assessment criterion has its own advantages and disadvantages. Therefore, they should be used in combination to ensure the absolutely safe navigation.

Later in the chapter, route use ratio for the important traffic routes in the bay and speed distribution of the ships navigating in the bay are taken into consideration for the same purpose.

7.2 Subjects for Future Study

Basing on the observation and simulation results, a boundary for safe passage of ships should be recommended. These boundary may be in the form of threshold value of SJ Value, Size of Bumper Model or limit DCPA, TCPA that are suitable for the actual marine traffic condition in congested waters, especially in Tokyo Bay.

When these threshold values have been decided, it might be possible for the optimal route calculation for vessels navigating in the bay, with real time knowledge of available traffic condition. This is the base for a system of automatic collision avoiding, which can be the subject to study next.

The realization of the automatic collision avoiding system, however, depends on the uncertainties of surrounding targets' movement. The uncertainties, therefore, requires more tedious research to be carried out, basing on theories of probability.

References

(1) Arnfinn Hammer, Kiyoshi Hara (1990) Knowledge Acquisition for Collision Avoidance Maneuver by Ship Handling Simulator

(2) GREG Welch, Gary Bishop (2001): An Introduction to the Kalman Filter.

(3) HAGIWARA Hideki, SHOJI Ruri, TAMARU Hitoi, LIU Shun, OKANO Tadashi, Development of Remote Radar/AIS Network System for Observing and Analyzing Vessel Traffic in Tokyo Bay. Proceedings of Asia Navigation Conference (Kobe), pp.67-74, Sep. 2003.

(4) HAGIWARA Hideki, OHTSU Kohei, SHOJI Ruri, TAMARU Hitoi, etc. "New Traffic Management System Based on AIS and Planned Route Information", 11th IAIN World Congress, Berlin, Oct.21st-24th,2003.

(5) HARA Kiyoshi, "Proposal of Maneuvering Standard to Avoid Collision in Congested Sea Area", "The Journal of Japan Institute of Navigation", Vol.85, pp.33-40, 1991.

(6) IALA Technical clarification on ITU Recommendation ITU-R M.1371

(7) IALA Guidelines on The Automatic Identification (AIS) Volume 1, Part 1 Operational Issues

(8) IALA Guidelines on The Automatic Identification (AIS) Volume 1, Part II Technical Issues

(9) International Maritime Organization (Model Course: 1.07, 1999): Radar Navigation, Radar Plotting and Use of ARPA: Radar Navigation at the Operational Level

(10) ITU-R M.1371: Technical characteristic for an automatic identification system using time division multiple access in VHF maritime mobile band

(11) Leow Wee Kheng (Department of Computer Science, National University of Singapore): Online Lecture on Motion Tracking (http://www.comp.nus.edu.sg/~cs6240/lecture/tracking.pdf)

(12) LIU Shun, HAGIWARA Hideki, SHOJI Ruri, TAMARU Hitoi, "New Method for Analyzing Traffic Flow Using Integrated Radar Network System and AIS in Tokyo Bay", "The Journal of Japan Institute of Navigation" , VOL.113, pp.69-76, Sep. 2005.

(13) LIU Shun, HAGIWARA Hideki, SHOJI Ruri, TAMARU Hitoi, OKANO Tadashi, "Radar Network System to Observe & Analyze Tokyo Bay Vessel Traffic" IEEE Aerospace & Electronic System Magazine, November 2004, ISSN 0885-8985, PP.3-11.

(14) LIU Shun, HAGAWARA Hideki, SHOJI Ruri, TAMARU Hitoi and OKANO Tadashi: "Observation and Analysis with Integrated Radar and AIS Network System in Tokyo Bay", International Radar Symposium, Berlin, Sep.2005.

(15) LIU Shun (2006) Study on Marine Traffic Observation and Analysis Using Radar Network

System and AIS in Tokyo Bay.

(16) Maria Isabel Ribeiro (2004): Kalman and Extended Kalman Filters: Concept, Derivation and Properties

(17) Online Lecture on Motion Tracking (www.cs.man.ac.uk/~tmorris/ct312/lecture_8.ppt)

(18) Roger Lownsborough, David Calcutt (Edward Arnold, 1993): Electronic aids to Navigation: Radar and ARPA

(19) Richard G Wiley (Artech House, 1993): Electronic Intelligence: The Analysis of Radar Signal

(20) TAMARU Hitoi (1999): Research on Ship automatic control system (in Japanese).

(21) Thor I. Fossen (2002): Marine Control System, 172-200.

(22) TRAN Viet Hung, HAGIWARA Hideki, TAMARU Hitoi, OHTSU Kohei, SHOJI RURI (Journal of Japan Institute of Navigation 2005): Strategic Collision Avoidance Based on Planned Route and Navigational Information Transmitted by AIS

(23) Tadashi OKANO (岡野 匡). レーダ観測による船舶交通データの解析手法に関する研究. (March 2007)

(24) Zoran Zivkovi (PhD thesis, ASCI graduate school. University of Twente, AE Enschede, The Netherlands 2003): Motion Detection and Object Tracking in Image Sequences.

(25) Web-page Internet Source on Raster Image:

http://graphicssoft.about.com/od/aboutgraphics/a/bitmapvector.htm

http://en.wikipedia.org/wiki/BMP_file_format

Appendix 1 Class B AIS Specifications

Specific issues for Class B Ship-borne Mobile AIS stations

Class B operation is identified in ITU Recommendation ITU-R M.1371-1 by defined message types and reporting rates. In the absence of mandatory regulations, carriage of Class B by leisure craft and other non-SOLAS vessels will be influenced largely by the perceived advantages as seen by each vessel's owner. However, carriage may be mandated in those waterways where competent authorities require AIS for this category of ships. Class B can be a standalone unit, interfaced with existing equipment (e.g. ECS or radar), or an integrated unit. During the July 2002 session of IMO's Sub-committee on Safety of Navigation a draft performance standard on Class B was created which stated in particular that Class B should not impair the use of the VDL.

There is an ongoing development by IEC for an international standard of Class B stations (future IEC 62287). This development takes into consideration the above IMO performance standard.

The minimum keyboard and display unit, as on Class A stations, is not required on pleasure craft. They may use the Class B station as a black box (to be seen) or connected to a display (e.g. ECS/ECDIS) to see and present other AIS stations and own position in relation to the environment. However, there must be at least one means to configure the station with static data during installation.

Reporting intervals for equipment other than Class A ship-borne mobile equipment

Platform's Condition	***Nominal Reporting Interval*** [(1)]
Class B Ship-borne Mobile Equipment not moving faster than 2 knots	3 minutes
Class B Ship-borne Mobile Equipment moving 2-14 knots	30 seconds
Class B Ship-borne Mobile Equipment moving 14-23 knots	15 seconds
Class B Ship-borne Mobile Equipment moving > 23 knots	5 seconds
Search and Rescue aircraft (airborne mobile equipment)	10 seconds
Aids to Navigation	3 minutes
AIS base station[(2)]	10 seconds

(1) In certain technical conditions related to synchronization, a mobile station's reporting rat

may increase to once every 2 seconds.

(2) The Base Station rate increases to once every $3^{1/3}$ seconds if the station detects that one or more stations are synchronizing to it (the base station).

Message 18: Standard Class B Equipment Position Report

The Standard Class B Equipment Position Report should be output periodically and autonomously instead of Messages 1, 2, or 3 by Class B Ship-borne Mobile Equipment, only. The reporting interval should default to the values given in Table 1B, unless otherwise specified by the competent authority, depending on the current SOG, the current Navigational status flag setting.

Parameter	**Number of bits**	**Description**
Message ID	6	Identifier for this message
Repeat Indicator	2	Indicate how many times a message has been repeated
User ID	30	MMSI Number
Reserved for regional or local applications	8	Reserved for definition by a competent regional or local authority. Should be set to zero, if not used for any regional or local application. Regional applications should not use zero.
SOG	10	Speed over ground in 0.1 knot step
Position accuracy	1	1 = high; 0 = low
Longitude	28	Longitude in 1/10000 min (negative for West)
Latitude	27	Latitude in 1/10000 min (negative for South)
COG	12	Course over ground in 1/10 degrees
True Heading	9	Degree (0-359)
Time stamp	6	UTC second when the report was generated
Reserved for regional application	4	
Spare	4	Not used. Should be set to zero
RAIM_Flag	1	Receiver Autonomous Integrity Monitoring flag of Electronic Position Fixing Device
Communication State Selector Flag	1	0 = SOTDMA Communication State follows 1 = ITDMA Communication State follows
Communication State	19	
Total number of bits	**168**	**Occupies one slot**

Message 19: Extended Class B Equipment Position Report

This message should be used by Class B Ship-borne Mobile Equipment. This message should be transmitted once every 6 minutes in two slots allocated by the use of Message 18 in the

ITDMA Communication State. This message should be transmitted immediately after the following parameter values change: Dimension of Ship/Reference for Position or Type of Electronic Position Fixing Device.

Parameter	**Number of bits**	**Description**
Message ID	6	Identifier for this message
Repeat Indicator	2	Indicate how many times a message has been repeated
User ID	30	MMSI Number
Reserved for regional or local applications	8	Reserved for definition by a competent regional or local authority. Should be set to zero, if not used for any regional or local application. Regional applications should not use zero.
SOG	10	Speed over ground in 0.1 knot step
Position accuracy	1	1 = high; 0 = low
Longitude	28	Longitude in 1/10000 min (negative for West)
Latitude	27	Latitude in 1/10000 min (negative for South)
COG	12	Course over ground in 1/10 degrees
True Heading	9	Degree (0-359)
Time stamp	6	UTC second when the report was generated
Reserved for regional application	4	
Name	120	Maximum 20 characters 6 bit ASCII
Type of ship and cargo type	8	
Dimension of Ship/Reference for Position	30	Dimensions of Ship in meters and Reference point for reported position
Type of Electronic Position Fixing Device	4	Not used. Should be set to zero
RAIM_Flag	1	Receiver Autonomous Integrity Monitoring flag of Electronic Position Fixing Device
DTE	1	Data terminal ready
Assigned Mode Flag	1	0 = Station operating in autonomous and continuous mode 1 = Station operating in assigned mode
Spare	4	Not used. Should be set to zero
Total number of bits	**312**	**Occupies two slots**

Appendix 2 AIS Message Decoding Program

1. NMEA Checksum and Parity Check

AIS messages are divided into sentences which are fit for transferring in 1 time slot. Apart from the part containing information, additional characters are suffixed for ensuring the accuracy of data encoding and transferring process. Given a sentence as in the following example, the part “0*01” is used for checking. Of which, the 1 numerical character (0) before asterisk symbol (*) is for parity checking and 2 additional characters (01) after this symbol are for Checksum.

!AIVDM,1,1,,A,1P000Oh1IT1svTP2r:43grwb0Eq4,0*01

The following 2 Visual Basic functions are used for producing Checksum and parity check characters.

```
Public Function GetChecksum(ByVal NMEA_sentence As String) As String
        Dim Character As Char
        Dim Checksum As Integer = 0
        For Each Character In NMEA_sentence
            If Character <> "!" Then
                If Character <> "*" Then
                    If Checksum = 0 Then
                        Checksum = Convert.ToByte(Character)
                    Else
                        Checksum = Checksum Xor Convert.ToByte(Character)
                    End If
                Else
                    Exit For
                End If
            End If
        Next
        Return Checksum.ToString("X2")
    End Function

    Public Function check_parity(ByVal DataStream As String)
        Dim k As Integer = 0
        Dim arr_char() As Char = DataStream.ToCharArray
        For i As Integer = 0 To DataStream.Length - 1
            If arr_char(i) = "1" Then k = k + 1
        Next
```

```
    k = k Mod 6
    If k = 6 Then k = 0
    Return k
End Function
```

2. Converting AIS Message into Binary String

In AIS messages, information is encoded in the form of consecutive bit (bits) in a binary string. The binary string is then converted into the NMEA format for external data transferring between equipments. Therefore, the first task to solve in decoding AIS data is to converting NMEA sentences into original binary string. It should be borne in mind that characters in NMEA sentence are representations of every 6 bits binary string.

```
Public Function MesToBitString(ByVal msgArr As String) As String
    Dim c() As Char
    c = msgArr.ToCharArray
    Dim ans As String = ""
    For i As Byte = 0 To c.Length() - 1
        ans = ans & CharacterToBitArray(c(i))
    Next
    MesToBitString = ans
End Function

Public Function CharacterToBitArray(ByVal Cval As Char) As String
    Dim ArrCval() As Char = {"0", "1", "2", "3", "4", "5", "6", "7", "8", "9", ":", ";",_
    "<", "=", ">", "?", "@", "A", "B", "C", "D", "E", "F", "G", "H", "I", "J", "K", "L",_
    "M", "N", "O", "P", "Q", "R", "S", "T", "U", "V", "W", "`", "a", "b", "c", "d", "e",_
    "f", "g", "h", "i", "j", "k", "l", "m", "n", "o", "p", "q", "r", "s", "t", "u", "v","w"}
    Dim ans As String = ""
    For count As Byte = 0 To ArrCval.Length - 1
        If Cval = ArrCval(count) Then
            ans = ByteTo6bitsArray(count)
            Exit For
        End If
    Next
    CharacterToBitArray = ans
End Function

Public Function ByteTo6bitsArray(ByVal ByteVal As Byte) As String
    Dim b As Byte
```

```
    Dim ans As String = ""
    Dim count As Byte = 0
    Do while count <= 5
       b = ByteVal Mod 2
       ByteVal = ByteVal ¥ 2
       ans = b & ans
       count += 1
    Next
    Return ans
End Function
```

3. Converting Binary String into Numerical or Alphabetical Information

AIS data may be in the form of numerical and/or alphabetical strings (ship name, type, call sign, etc.) or real values (latitude, longitude, rate of turn, etc.). Attention should be paid in extracting numerical and/or alphabetical string data due to the special 6 bits format of AIS data messages.

```
Public Function _6bitsArray_2_Character(ByVal binval6 As String) As Char
    Dim ans As Char
    Dim char_arr() As Char = {"@", "A", "B", "C", "D", "E", "F", "G", "H", "I", "J", "K",_ ,
    "L","M", "N", "O", "P", "Q", "R", "S", "T", "U", "V", "W", "X", "Y", "Z", "[", "", "]",_
    "^", "-", " ", "!", "`", "#", "$", "%", "&", "'", "(", ")", "*", "+", ",", "_", ".",_
    "/", "0", "1", "2", "3", "4", "5", "6", "7", "8", "9", ":", ";", "<", "=", ">", "?"}
    Dim count As Integer = BitsArrayToDecimal(binval6)
    ans = char_arr(count)
    Return ans
End Function

Public Function BitsArrayToDecimal (ByVal BitArray As String) As Integer
    Dim v() As Char
    v = BitArray.ToCharArray
    Dim ans As Integer = 0
    For count As Integer = 0 To v.Length() - 1
        ans = 2 * ans + Val(v(count))
    Next
    BitsArrayToDecimal = ans
End Function
```